DEVELOPMENT AND CHARACTERIZATION OF INDUCED PLURIPOTENT STEM CELLS (IPSCS) DERIVED FROM HUMAN ORAL SQUAMOUS CARCINOMA CELL (OSCC)

By

NALINI DEVI VERUSINGAM

A dissertation submitted to the Department of Pre-Clinical Science,

Faculty of Medicine and Health Sciences,

Universiti Tunku Abdul Rahman,

in partial fulfilment of the requirements for the degree of

Master of Medical Sciences

April 2016

ABSTRACT

DEVELOPMENT AND CHARACTERIZATION OF INDUCED PLURIPOTENT STEM CELLS (IPSCS) DERIVED FROM HUMAN ORAL SQUAMOUS CARCINOMA CELL (OSCC)

Nalini Devi Verusingam

Induced pluripotent stem cells (iPSCs) technology pioneered by Yamanaka and group had offered a new insight to study the pathophysiology of cancer. Cancer cells can be reprogrammed into iPSCs by forced expressions of pluripotency vectors (Oct4, Sox2, Klf4 and c-Myc). To date, reprogramming of OSCC remained unexplored. We attempted to transduce OSKM into H103-STNMP Stage 1 and H376-STNMP Stage III cell lines by retroviral mediated method and characterize its pluripotency properties. Reprogrammed cells were characterized for their ESC-like morphology, pluripotent gene expression via quantitative real-time polymerase chain reaction (RT-qPCR), and immunofluorescence staining, as well as their ability to form embryoid bodies (EBs) and to differentiate into three germ layers. Microsatellite instability analysis and global methylation were also assessed between parental and the reprogrammed counterpart to determine the presence of allelic imbalance and global methylation status. Embryonic Stem Cells (ESCs) like colonies with flatten clear borders on

feeder layer showing high nucleus to cytoplasm ratio morphology appeared at day 15 in reprogrammed H103 and were distinct from that of the parental cancer cells. H376 cell line failed to retain ESCs like features and exhibited disorganized morphology indicating reprogramming resistance. Stable up-regulation of core pluripotency genes Oct4, Sox2 and Nanog expressions were detected in H103 colonies. Down-regulation of Nanog expression was detected in H376 at passage 5. An increase was observed again at passage 10 but the level of expression was much lower than that of H103. Significant down-regulation of oncogenic Klf4 and c-Myc were observed in both reprogrammed cell lines. Subsequent characterizations were focused on reprogrammed H103 as this cells showed more pluripotent stem cells like properties. Reprogrammed H103 exhibited positive antibody signals for the pluripotency markers (Oct4, Sox2, Nanog and Tra-1-60) and exhibited Embryoid Bodies (EB) formation with the presence of markers representing the three germ layer. Reprogrammed H103 was shown to differentiate into adipocytes and osteocytes as indicated by Oil-Red-O and Alizarin Red S. Loss of heterozygosity (LOH) was detected at (D3S1228) in reprogrammed H103 which suggest possible correlation with the common activation of tumor suppressor gene (FHIT) found in OSCC. Increase in hypermethylated genes in reprogrammed H103 indicates epigenetic remodelling was involved in the reprogramming process. In conclusion, reprogramming was only successful in H103 cell line, which exhibited ESCs-like characteristics based on cell morphology, pluripotency expression and are distinct from that of reprogrammed

H376. Differences in the inherent genetic constituents between H103 and H376 cell lines determine their capacity to be reprogrammed into iPSCs. Our study showed the vital roles of Oct4, Sox2 and Nanog, towards successful reprogramming of reprogrammed H103. Suppression of oncogenes c-Myc and Klf4 observed in reprogrammed cells denotes reprogramming may reverse the oncogenic properties epigenetically. Differentiation capacity in reprogrammed H103 suggests that reprogramming enabled restoration of existing terminal state of cancer cells to early pluripotency. Reprogrammed H103 cells shall be further explored its potential as a model to study cancer progression in OSCC, which may give rise to novel therapeutic intervention.

ACKNOWLEDGEMENTS

APPROVAL SHEET

This dissertation entitled "**DEVELOPMENT AND CHARACTERIZATION OF INDUCED PLURIPOTENT STEM CELLS (IPSCS) DERIVED FROM HUMAN ORAL SQUAMOUS CARCINOMA CELL (OSCC)"** was prepared by NALINI DEVI VERUSINGAM and submitted as partial fulfillment of the requirements for the degree of Master of Medical Sciences at Universiti Tunku Abdul Rahman.

Approved by:

_____

(Associate Prof. Dr Alan Ong Han Kiat)

Professor/Supervisor   Date:…………………..

Department of Pre-Clinical Sciences

Faculty of Medicine and Health Sciences

Universiti Tunku Abdul Rahman

_____

(Emeritus Prof Dr. Cheong Soon Keng)

Professor/Co-supervisor   Date:…………………..

Department of Medicine

Faculty of Medicine and Health Sciences

Universiti Tunku Abdul Rahman

FACULTY OF MEDICINE AND HEALTH SCIENCES

UNIVERSITI TUNKU ABDUL RAHMAN

Date: 8th April 2016

SUBMISSION OF DISSERTATION

It is hereby certified that **Nalini Devi A/P Verusingam** (ID No: **11UMM06722**) has completed this dissertation entitled "Development and Characterization of Induced Pluripotent Stem Cells (IPSCS) Derived From Human Oral Squamous Carcinoma Cell" under the supervision of Associate Prof. Dr. Alan Ong Han Kiat (Supervisor) from the Department of Pre- Clinical Sciences, Faculty of Medicine and Health Sciences, and Emeritus Prof. Dr. Cheong Soon Keng (Co-Supervisor) from the Department of Medicine, Faculty of Medicine and Health Sciences.

I understand that University will upload softcopy of my dissertation in pdf format into UTAR Institutional Repository, which may be made accessible to UTAR community and public.

Yours truly,

_____

(Nalini Devi A/P Verusingam)

DECLARATION

I NALINI DEVI A/P VERSUSINGAM hereby declare that the dissertation is based on my original work except for quotations and citations which have been duly acknowledged. I also declare that it has not been previously or concurrently submitted for any other degree at UTAR or other institutions.

_____

NALINI DEVI A/P VERUSINGAM

Date: 8th April 2016

TABLE OF CONTENTS

LIST OF TABLES

LIST OF FIGURES

LIST OF ABBREVIATIONS

ACTB	Beta-Actin
APC	Adenomatous polyposis coli
BSA	Bovine serum albumin
cDNA	Complementry deoxyribonucleic acid
CDNK2A	Cyclin dependent kinase inhibitor 2A
CML	Chronic myeloid leukemia
c-Myc	Avian myelocytomatosis viral oncogene
CT	Co-axial tomography
DMEM	Dulbecco's modifie eagle medium
DNA	Deoxyribonucleid acid
DNMT1	DNA (cytosine-5)-methyltransferase 1
EB	Embryoid bodies
EMT	Epithelial-mesenchymal transition
ESCs	Embryonic stem cells
FHIT	Fragile histidine triad
FITC	Fluorescein isothiocyanate
GATA4	Gata binding protein 4
GFP	Green fluorescence protein
GSTP1	Gluthione S-transferase pi
hMLH1	mutL homolog 1
hMSh2	mutS homolog 2

hMSH6	mutS homolog 6
hPMS2	Postmeiotic segregation increased 2
HPV	Human papiloma virus
ICM	Inner cell mass
IL-6	Interleukin-6
iPSCs	Induced pluripotent stem cells
ISH	In situ hybridization
IVF	*In-vitro* fertilization
Klf4	Kruppel-like factor 4
LFS	Li-fraumeni syndrome
Lin28	Lin28 homolog A
LINE-1	Long interspersed elements
LOH	Loss of heterozygosity
MEF	Mouse embryonic fibroblast
MGMT	0-6-methylguanine-DNA-methyltransferase
MHC	Major histocompatibility complex
miRNA	Micro ribonucleic acid
MMR	Mismatch repair
mRNA	Messenger ribonucleic acid
MSI	Microsatellite instability
MTHFR	Methylenetetrahydrofolate reductase
OCT4	Octamer-binding protein 4
OSCC	Oral squamous cell carcinoma

PAGE	Polyacrylamide gel electrophoresis
PCR	Polymerase chain reaction
PE	Phycoerythrin
pESCs	Parthenogenetic embryonic stem cells
PGCs	Primordial germ cells
PVDF	Polyvinylidene fluoride
qPCR	Quantitative polymerase chain reaction
RARB	Retinoic acid receptor
RASSF1A	RAS association domain family 1
RPM	Revolution per minute
RT-PCR	Reverse transcriptase polymerase chain reaction
SCNT	Somatic cell nuclear transfer
SD	Standard deviation
SDS	Sodium dodecyl sulphate
SEM	Standard error mean
SOX1	Sex determining region Y – box 1
SOX2	Sex determining region Y – box 2
SOX17	Sex determining region Y – box 17
SV40	Simian virus 40
TAE	Tris-Acetate-EDTA
TGF-β	Transforming Growth Factor- Beta
TSG	Tumour suppressor gene
UV	Ultra-violet

CHAPTER I

INTRODUCTION

Oral Squamous Cell Carcinoma (OSCC) belongs to the head and neck malignancies and is known as one of the leading causes of death worldwide (Chandra et al., 2013). Although OSCC is treatable at the early stages of detection, screening and diagnosis of OSCC is still a challenging task as there are no definite symptom, suitable markers and visual diagnostic aids for early detection of OSCC (Singh and Schenberg, 2013). Available models for OSCC study were derived from xenograft of primary tumours previously and have limitations for *in-vitro* studies due to lack of cell number and continued mutations on prolonged culture. Moreover, existing human cell models of OSCC, which are based on tumour cell lines that supposedly bear a resemblance to the advanced tumour state, are unlikely to recapitulate the actual cancer pathogenesis. Hence the differences between the existing OSCC cancer model and actual human cancers call for alternative human cancer models of OSCC (Shirako et al., 2015).

Recent advancement in reprogramming technology by the introduction of pluripotent factors on cancer cells have provided a new platform to study tumour characteristics of OSCC. Previous studies have shown that the generated pluripotent stem cells from cancer cells achieved pluripotency capacity, but retain

the genetic aberrations of the cancer cells. These properties facilitate cancer oncogenesis development study not achievable with current available cancer models (Lee et al., 2015, Kim and Zaret, 2015). Reprogramming cancer cells into iPSCs provides the basis for oncogenesis modelling by demonstrating the utility of establishing patient specific cancer disease, unravelling the underlying cellular pathways in the cancer disorder, and identifying potential biomarkers which could be used for therapeutic purpose (Lang et al., 2013a). At the present time, reprogramming and subsequent characterisation have been successfully performed on lung cancer, gastrointestinal cancer, osteosarcoma, CML, skin cancer, hepatocellular carcinoma, and pancreatic adenocarcinoma (Kim and Zaret, 2015, Semi et al., 2013).

In the present study, we reprogrammed OSCC cancer cell lines H103 (derived from the tongue region) and H376 (derived from the floor of mouth region) (Prime et al., 1990) by introducing four pluripotent factors (Oct4, Sox2, c-Myc, and Klf4) via the retrovirus mediated system. Reprogrammed OSCC cell lines were then characterised for the embryonic stem cell-like morphological changes and endogenous pluripotent gene signals (Oct4, Sox2, c-Myc, Klf4 and Nanog) via mRNA expression (Glauche et al., 2010). Stable reprogramming was achieved in H103 cell line. The product was then evaluated for pluripotency characteristics through embryoid bodies (EB) formation and the capacity to differentiate. Apart from that, a set of microsatellite panel markers was used on

parental and H103 reprogrammed counterparts to determine the presence of microsatellite instability. Global methylation differences were also tested between parental H103 and its stable H103-derived iPSCs.

Reprogramming capacity in these cell lines provides an opportunity to test the hypothesis that iPSCs can be generated from OSCC cells and OSCC-derived iPSCs may serve as an oncogenesis model to study OSCC development and progression.

General Objective

To generate OSCC derived pluripotent cells that may serve as a suitable oncogenesis model.

Specific Objectives

a) To reprogramme oral squamous cell carcinoma derived from two cancer cell lines via retroviral-OSKM mediated transduction system.

b) To characterise the properties of reprogrammed oral squamous cell carcinoma for the following:

   i. To determine whether the morphological changes of the products are similar to that of Embryonic Stem Cells (ESCs).

   ii. To evaluate the expression of pluripotent genes in the reprogrammed cells compared to the parental cells.

   iii. To evaluate the differentiation capacity of the reprogrammed cells.

   iv. To detect the molecular signatures by microsatellite analysis and global methylation status in the reprogrammed cells.

CHAPTER 2

LITERATURE REVIEW

2.1   Pluripotent Stem Cells

Pluripotent stem cells are defined as cells that exhibit functional capacity to differentiate into all adult cell types in the body. They exhibit unlimited self-renewal and are capable of giving rise to three embryonic germ layers namely endoderm, ectoderm and mesoderm (Ooi and Liu, 2012, Medvedev et al., 2010b). The pluripotency state of these cells provides a valuable platform to study multiple processes that occur in the early development of humans and serves as a promising tool in understanding human diseases and their treatment (Chen and Daley, 2008, Watt and Driskell, 2010).

Previously, the most well-studied pluripotent stem cell type was embryonic stem cells (ESCs) that were developed from the inner cell mass (ICM) of developing blastocyst-stage embryo at day five after *in-vitro* fertilisation (IVF) (Lerou and Daley, 2005, Wert and Mummery, 2003). Growing ESCs in *in-vitro* culture is challenging as the cells demand specialised culture media that hold vital ingredients, which are often difficult to standardise. In fact, maintaining the culture

conditions is critical to ensure ESCs self-renewing and pluripotent properties during prolonged culture (Schwartz et al., 2011). ESCs can be cultured on mouse embryonic fibroblast (MEF) or feeder layer and also cultured indirectly on Matrigel or feeder-free culture systems. MEF feeder layer is vital to maintain the pluripotency properties of the ESCs as feeder cells secrete essential cytokines (Lin and Talbot, 2011, Lei et al., 2007).

ESCs were prominently used in early human development research involving embryonic ageing, pregnancy loss in older women (Solter, 2006, Eve et al., 2008), and also in drug screening as potential drugs on ESCs were found to be more sensitive than in somatic cells ((Pouton and Haynes, 2007). Subsequently, ESCs were investigated in cell-based therapies which include Parkinson's disease (Wijeyekoon and Barker, 2009, Correia et al., 2005, Alizadeh et al., 2014), multiple sclerosis (Ardeshiry lajimi et al., 2013), diabetes (McCall et al., 2010), spinal cord injuries (Tewarie et al., 2009) and stroke (Kalladka and Muir, 2014). However, the use of ESCs is highly contentious as they are derived from unused human pre-implantation embryos acquired from IVF donated for research. Indeed, allogeneic immune responses following transplantation due to recipient's response to donor cells also contribute to the technical constraints encountered in ESCs application (Hughes, 2004, Strauer and Kornowski, 2003).

2.2   Sources of Embryonic Stem Cells

Apart from ICM derived ESCs, there are other types of embryonic sources that have been known to provide human pluripotent stem cell lines. All the methods need viable cells from an early phase of development though the use of embryonic tissues often provokes ethical concerns (Strauer and Kornowski, 2003, Hug, 2005).

2.2.1   Human Primordial Germ Cells (PGCs)

The development of primordial germ cells (PCGs) indicates an early episode of embryogenesis. Precursors of PGCs are early committed as epiblasts before gastrulation, which further shift into an extra embryonic region where PGCs are destined to become oogonia or gonocytes within gonad (Zwaka and Thomson, 2005). These cells are called the embryonic germ cell lines, which share many properties with ESCs.

Nevertheless, PGCs present difficulties with prolonged growth in culture due to spontaneous differentiation. Therefore, potential clinical application of PGCs necessitates an extensive understanding of their derivation and maintenance *in-vitro* (Farini et al., 2005).

2.2.2 Parthenogenetic Embryonic Stem Cells (pESCs)

Parthenogenesis is a method of generating embryonic stem cells by using an oocyte without the need of fertilization, It contains genetic constituents exclusively from the oocyte donor or in other words excludes the sperm's genetic contribution (Mai et al., 2007). Embryos developed via parthenogenesis are not viable but capable of forming blastocysts that can be used to derive ESCs (Lin et al., 2007). Consequently, ESCs derived are grown on feeder cell layer to maintain pluripotency.

Parthenogenetic ESCs (pESCs) serve as a potential source for cell therapies with no or minimum allogeneic immune responses because, the presence of major histocompatibility complex (MHC) molecules in pESCs provides more efficient immune compatibility than that of conventional ESCs (Hao et al., 2009). However, it is questionable whether pESCs themselves can form all tissue types in the body, since pESCs are solely derived from the female. Generation of pESCs is laborious as this method requires expensive chemicals and instruments as well as highly trained laboratory technicians (Pennarossa et al., 2011).

2.2.3 Dead Embryos

In-vitro fertilised embryos that have stopped dividing and are considered dead can be potentially used to generate ESCs. These dead embryos will not be picked for implantation and be discarded as medical waste. ESCs generated via dead embryos whose cells remain viable in culture typically behave like pluripotent stem cells by expressing pluripotency proteins and possess differentiation capability into three germ layers. Yet, ethical contemplation and the current legislative issues prevent them being used widely (Landry and Zucker, 2004).

2.3 Issues Associated with ESCs

There are ethical concerns on the use of embryos for research (Hyun, 2010). In addition, ESCs based therapies may fail due to immune rejection when cells from one individual are transplanted into another individual. Recipient's immune system detects genetic difference and tends to destroy those foreign cells transplanted earlier. This process may also work the way round by means of transplanted immune cells recognize the new host as a foreign body causing graft-versus-host disease. This dilemma has been overcome from Somatic Cell Nuclear Transfer (SCNT) whereupon the patient's own somatic cell nucleus is inserted into an oocyte, which reverts into a pluripotent state. Nevertheless, this method solves

the immune rejection issues but pluripotent clones generated via SCNT still keep the mitochondrial DNA of the oocytes (Lo and Parham, 2009).

2.4   Generation of Induced Pluripotent Stem Cells

The induced pluripotent stem cells (iPSCs) technology has offered an alternative approach that sidesteps the need for Embryonic Stem Cells (ESCs) and created a new prospect in clinical research for different diseases, including cancer. This has caught the attention of many scientists (Stadtfeld and Hochedlinger, 2010). Hence, generation of iPSCs has brought hope towards resolving ethical and technical constraints faced in ESCs applications.

Technically, iPSCs are derived by genetically reprogramming of adult somatic cells from healthy donors or patients to an ESC- like state. Reprogramming is made possible by forced introduction of pluripotency transcription factors by means of viral or non-viral delivery system (González et al., 2011). In year 2006, Yamanaka and group, successfully reprogrammed mouse embryonic fibroblasts (MEFs) and human dermal fibroblast into iPSCs by four pluripotency factors OSKM (Oct4, Sox2, Klf4, and c-Myc) (Takahashi et al., 2007) . Subsequently, Thomson and group also successfully generated human iPSCs but they used a different pluripotency cocktail consisting of Oct4, Sox2, Nanog, and LIN28 via the lentiviral delivery system (Yu et al., 2007). At first, the

reprogramming transcription cocktail was identified by screening of 24 pre-selected panel of genes generally expressed in embryonic stem cells (ESCs) by Takahashi and Yamanaka. OSKM factors were then found to be sufficient for reprogramming. Since then, they have been extensively used as essential factors for iPSCs reprogramming. Other combinations of reprogramming factors were also reported to be successful (Takahashi and Yamanaka, 2006).

Reprogrammed adult somatic cells do resemble ESC-like cells whereby they can undergo unlimited proliferation and possess the ability to differentiate into three germ layers (ectoderm, endoderm and mesoderm). These ESCs characteristics can be defined in iPSCs via gene expressions, protein expression assays, embryoid body formation, epigenetic signatures, teratoma formation and chimerism (Han et al., 2010).

Ultimately iPSCs technology offers a novel pathway in disease modelling to understand the unique manifestation of various diseases, a therapy that avoids immune rejection following transplantation, an inexhaustible cell source which may not be easily accessible for drug screenings, and a therapeutic approach that is personalised (Medvedev et al., 2010a). Indeed, the process of cellular reprogramming that switches the cell fate from somatic cells into pluripotent stem cells, renders it an ideal model for studying cell development and differentiation (Boulting et al., 2011).

2.4.1 Types of iPSCs Technology

Successful reprogramming is highly dependent on the cell types, methods of reprogramming, and pluripotency vector delivery efficiencies (Rao and Malik, 2012). Method via viral integration still remains as a better reprogramming option with higher efficiency. However, integration free iPSCs are ultimately required for clinical application (Li et al., 2014). Thus, non-integrating lentiviral based expression of micro RNA (miRNA) to enhance the iPSCs generation without the need for Yamanaka factor had been developed recently. It can achieve up to 11.6% reprogramming efficiency by using a specific *miR302/367* cluster targeting the core pluripotent genes, Oct4 and Sox2 (Onder and Daley, 2011). Figure 2.1 describes the types of the reprogramming method used in iPSCs generation and their relative reprogramming efficiencies (Rao and Malik, 2012).

EFFICIENCY

Adenoviral

Retroviral

Lentiviral

Sendai virus

PiggyBac Transposon

Episomal

Minicircle

Protein Transduction

Lentiviral-miRNA

SAFETY
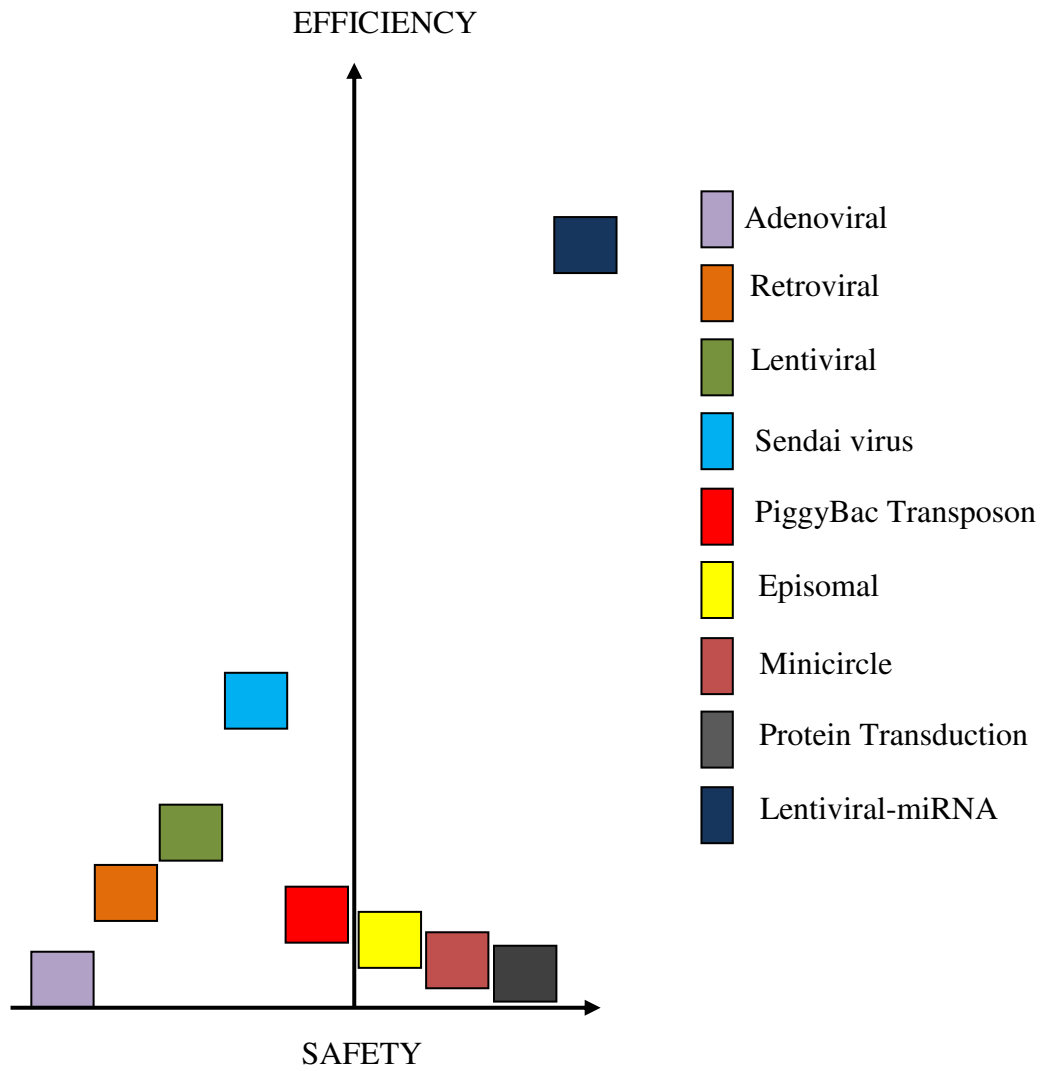
Figure 2.1 Reprogramming methods and efficiencies,

(Rao and Malik, 2012)

## 2.5	Cellular Reprogramming

Cellular reprogramming involves the switch in cell fate of one particular cell type to another. Many reprogramming techniques have been widely used in conversion of adult somatic cells into pluripotent stem cells with a combination set of pluripotency transcription factors OSKMLN (Oct4, Sox2, Klf4, c-Myc, Lin28 and Nanog) and subjected to specific culture conditions for a period of time (Rao and Malik, 2012, Buganim et al., 2013). Successful reprogramming results in colony appearance, phenotype and molecular similarities to that of ESCs colonies on a cell culture dish. Indeed among those adult somatic cells that had been successfully reprogrammed included mouse and human fibroblast (Takahashi et al., 2007, Miller and Schlaeger, 2011), keratinocytes (Aasen et al., 2008), adipose stem cells (Sugii et al., 2010), dermal fibroblast (Hayashi et al., 2012), mesenchymal stromal cells (Guzzo et al., 2013), peripheral blood cells and bone marrow cells (Chan and Yoder, 2013). However, the efficiency and kinetics in reprogramming are dependable on the cell types (Tat et al., 2011) and their specific responses towards transcription factors and the vector delivery system.

2.5.1 Vectors

Vectors are commonly used in cancer therapy (El-Aneed, 2004), cell-based therapies (Gardlik et al., 2005), vaccination (Brave et al., 2007), and cellular reprogramming (Takahashi and Yamanaka, 2006, Shao and Wu, 2010). Vector delivery systems that include both viral vectors and non-viral vectors are established in reprogramming (Rao and Malik, 2012). Viral vectors are classified into genome-integrating viruses and non-integrating viruses (Okita and Yamanaka, 2011a) whereas, non-viral vectors belong to the non-integrating vector system (O'Doherty et al., 2013). Initially, reprogramming efforts were accomplished via retroviruses and lentiviruses (integrating vectors) to generate iPSCs cells. Owing to several risks upon the integration of viral vectors, application of adenovirus, episomal vectors and sendai virus (non-integrating viruses) were then developed. Subsequently, non-viral methods such as minicircle vectors, piggyback transposon, small molecules and miRNA transient transfection were proposed to reduce possible genome integration during reprogramming (Oh et al., 2012).

2.5.1.1 Integrating Vector System

Integrating system in cellular reprogramming involves the delivery of pluripotent transcription factors and vectors are stably integrated within the genome of the target cells. Though integrating viruses ensure the stability of

reprogramming and confer higher efficiencies, these system limit the types of cells that can be reprogrammed because the infectivity is confined to dividing cells only. Furthermore, these approaches were found to be risky due to their insertional propensity. Genome integration leaves permanent hoofmarks through insertional mutagenesis and triggers off abnormal tumourigenicity that potentially impinges the gene expression and biological properties of the derived iPSCs (Han and Yoon, 2011).

2.5.1.2 Non-Integrating Vector System

Non-integrating vector system was then developed to resolve the existing drawback from integrated system and still pluripotency could certainly be achieved. Studies have shown that iPSCs generated via non-viral method expressed ESCs markers and are capable of forming chimeric mice, a gold standard for indicating pluripotency. In fact no integration of vectors was identified in the genome of target cells. Yet, successful reprogramming was achieved with lower efficiencies and required manifold of transfection compared to integration methods (Zhou and Zeng, 2013). Since then, much progress was made to sustain the efficient production of high-quality iPSCs (Deng et al., 2015).

2.6   Applications of iPSCs

Application of iPSC technology has shown remarkable promises, since year 2006 due to the flexibility of these pluripotent cell types. IPSCs are extensively applied as a tool in disease modelling, drug screening, regenerative tissue engineering and gene therapy, which paves the way for future clinical applications (Lu and Zhao, 2013, Nelson et al., 2010).

2.6.1   Disease Modeling

iPSCs serve as a replenishable source for disease models *in-vitro* (O'Neill and Ricardo, 2013). Earlier, mouse was used as a tool or model system to investigate the functional properties of specific genetic mutations that occur in patients with inherited disease. Unfortunately, mouse models were unable to display similar phenotypes as those found in humans (Marian, 2011). On the other hand, iPSCs offer a disease model where a particular genetic mutation of a disease detected in patient's cells is carried though upon reprogramming; iPSCs derived from a disease cell retain its genetic mutation and exhibit its phenotypic expression, though the cellular morphology has been altered (Unternaehrer and Daley, 2011). In recent years, numerous iPSCs have been successfully derived, including liver diseases (Soto-Gutierrez et al., 2011), cardiovascular disorders

(Sinnecker et al., 2012), blood disorders (Adams et al., 2013, Focosi et al., 2014), and neurological diseases (Chen et al., 2011b, Wan et al., 2015).

2.6.2 Drug Screening

Drug screening is usually carried out using immortal cancer cells lines that exhibit traits such as chromosomal aberrations and mimic the disease condition *in-vivo*. Unfortunately, presence of heterogeneity amongst cell line cultures often leads to contradictory results and lack of reproducibility during drug toxicity testing (Deshmukh et al., 2012). In fact, drug toxicity testing in an animal model does not reflect the actual human condition (Wilding and Bodmer, 2014).

The resemblance of iPSCs to conditions in human diseases, enables them to be used as disease models for drug screening. Besides, iPSCs have relatively low heterogeneity and give consistency for drug screening efforts. Therefore, patient-specific iPSCs had been used for screening therapeutic agent as well as validating its pharmacokinetics and safety properties (Ko and Gelb, 2014). Applications of iPSCs as a disease model for drug screening were previously highlighted in neuronal and cardiac diseases where the process yielded efficacious drug candidates. Seeing the benefits, this method for drug screening is now extended to other diseases. (Singh, 2015).

2.6.3   Gene Therapy

Patient-specific iPSCs can be utilised to uncover the pathogenesis of various diseases. In general, gene defects carried upon reprogramming into iPSCs may be repaired, and potentially differentiated into normal counterpart of its cell types. As a result, iPSCs are deemed ideal as patient-tailored therapy to reinstate those damaged cells prior to the disease. Gene therapy also serves, as a complementary therapeutic option particularly when pharmacological and surgical approaches do not provide beneficial results. Up to now, the use of iPSCs had been explored in genetic diseases such as spinal muscular atrophy (Ebert et al., 2009), abnormal genitalia (Tchieu et al., 2010), thalassemia (Tolar et al., 2011a), Hurler syndrome (Tolar et al., 2011a), skin disorder epidermolysis bullosa (Tolar et al., 2011b) and Parkinson's disease (Alizadeh et al., 2014). Continuous efforts are being made to improve the methods of generating iPSCs for gene therapy in order to make them more effective and safe for patients (Pawitan, 2012).

2.7   Potential Application of iPSCs in Cancer Research

Cancer is an aggressive disease known for its high mortality globally. This disease are triggered by multiple genetic and epigenetic aberrations that resulted in uncontrolled defective clonal expansion forming tumours (Hanahan and Weinberg, 2011). Much research is carried out to understand the possible pathogenesis behind

cancer progressions and identify biomarkers for diagnosis and development of specific therapeutic drugs. Different approaches were used to describe cancer pathogenesis via cell lines and animal models. Most of the available information on cancer progressions was developed from cancer cell lines. As a matter of fact, primary patient samples were known as the best model for cancer research, but inadequate number of cells readily obtainable often limits in-depth downstream analysis and *in-vitro* studies (Begley and Ellis, 2012) (Cekanova and Rathore, 2014). IPSC technology promises a substantial tool to investigate progress of multiple cancer stages that could provide potential dynamic networks of cancer pathology and biomarkers of early stages.

IPSCs generated from cancer cells showed pluripotent characteristics including expression of pluripotent markers and differentiation potentiality. These cells acquired dominance over the cancer phenotypes that allowed the study of cancer pathophysiology. Generally, loss of tumourigenecity denoted by increased tumour suppressor gene expressions, decreased aggressive proliferation and reduction in tumour formation were observed in reprogrammed cancer cells (Zhang et al., 2013). Studies have also portrayed the abilities of certain reprogrammed cancer cells, showing early-stage phenotypes with merely partial expression of the cancer genome (Kim et al., 2013). IPSC cells derived from cancer cells acquired sensitivity to chemotherapeutic drugs upon differentiation (Carette et al., 2010). Reprogramming cancer cells induces suppression of cancer

phenotypes, reinstates differentiation capacity, and modulates cancer specific gene expression. Reprogrammed cancer cells also retained the similar genomic aberrations prior to reprogramming and yet capable of differentiating into various lineages (Kim and Zaret, 2015).

IPSCs derivation from cancer cells suggests reprogramming process influences tumorigenesis in cancer cells by reversible epigenetic changes and irreversible mutations within oncogenes and tumour suppressor genes. The ability of reprogrammed cells to show reverse malignant specific expressions via epigenetics modification provides a novel strategy in drug screening (Kim and Zaret, 2015, Ramos-Mejia et al., 2012). Hence, iPSCs can be generated from the same cancer from different stages of development and the products facilitate the understanding of the evolution (development and progression) of the disease. Such an understanding would further allow manipulation of the cancer-specific iPSCs during differentiation to validate the processes of carcinogenesis (Kim et al., 2013). This technology provides a platform to determine the impaired regulation of the imprinted cancer genes which may serve as therapeutic targets for treatment of cancer (Lee et al., 2015).   IPSCs from cancer cells can be applied for immunotherapy of cancer which may lead to personalized cell based therapies and a suitable disease model.

IPSCs have previously been successfully established from various reprogramming methods from a few cancer types including skin cancer, prostate cancer (Lin et al., 2008), gastrointestinal cancer, colorectal cancer, esophageal cancer, hepatocellular cancer, pancreatic cancer (Miyoshia et al., 2009), chronic myeloid leukemia (Carette et al., 2010), lung cancer (Mahalingam et al., 2012), juvenile myelomonocytic leukemia (JMML) (Gandre-Babbe et al., 2013), glioblastoma multiforme (GBM) (Stricker et al., 2013), pancreatic ductal carcinoma (Kim et al., 2013), liposarcoma, Ewing's sarcoma, osteosarcoma (Zhang et al., 2013), hepatocellular carcinoma (Koga et al., 2014), myelodysplastic syndromes (MDS) (Kotini et al., 2015) and Li Fraumeni syndrome (Lee et al., 2015).

2.8   Reprogramming Cancer Cells to Pluripotent State

Reprogramming induced pluripotency in cancer cells into iPSCs enable differentiation into a specific cell type of the cancer type. Many different groups have successfully generated and characterized iPSCs, but due to different techniques, different methods of calculating efficiency of reprogramming were used.

Viral vectors including retrovirus, lentivirus, sendai virus and viral episomes have been used to transfer pluripotent transcription factors (Oct4, Sox2,

c-myc, Klf4, Nanog, Lin28, SV40 LT) into various cancer cell types to generate iPSCs (Miyoshia et al., 2009, Lin et al., 2008, Hu and Slukvin, 2013). Virus mediated reprogramming methods are preferred in for its ability to efficiently induce pluripotency. The reprogramming technology established by Yamanaka and team employed retroviral-OSKM vectors to generate iPSCs from somatic cells and this viral transduction method is conveniently implemented in most studies (Takahashi et al., 2007).

OSKM transcription factors commonly induced up-regulation of the crucial endogenous pluripotency mRNAs indicating pluripotency capacity and successful reprogramming are achieved. Among those established endogenous markers up-regulated after reprogramming are Oct4, Sox2, and Nanog. Extensive findings revealed that the expression of these core endogenous markers control the pluripotency network upon reprogramming (Johansson and Simonsson, 2010). These core pluripotency genes represent the stemness in ESCs but are also found in cancer stem cells (CSCs) population. Many findings have shown the relationship between reprogramming factors and carcinogenesis. Susceptibility towards reprogramming was demonstrated in existing studies by Li et al in which c-Met signalling, a CSC marker associated with Oct4, Sox2 and Nanog, enhanced reprogramming capacity (Li et al., 2011b). Noguchi et al then identified that high expression levels of Oct4, Sox2, Klf4, c-Myc and Nanog in c-Met population and these population showed higher reprogramming efficiency compared to low c-Met

population (Noguchi et al., 2015). Reprogramming factor c-Myc which is also crucial in inducing pluripotency poses a threat to the safety of medical application of iPSCs as overexpression of c-Myc, a known oncogene could result in neoplasm formation (Li et al., 2011a). However, the mechanisms involved in successful reprogramming are still unknown.

However, resistance towards reprogramming were reported previously in few reprogrammed cancer cells. Breast cancer cell line (MCF-7) was reprogrammed via retroviral-OSKM method and ended up being partially reprogrammed with over-expression of Sox2 and detection of CSC markers (CD44 and ALDH) instead (Corominas-Faja et al., 2013). Moreover, three cell lines (MIAPaCa, PSN-1 and AsPC-1) of pancreatic cancer reprogrammed via Sendai virus-OSKM were also reported to resist reprogramming (Dewi et al., 2012). These findings indicated that TGF-β triggered epithelial-mesenchymal transition (EMT) which then affected reprogramming efficiency (Ebrahimi, 2015). EMT signalling is a crucial process in tissue regeneration as it engages tissue repair such as wound healing and inflammatory process due to its ability to switch between epithelial and mesenchymal states. Contrast to its role in tissue regeneration, EMT was found to initiate metastatic activities (Huang et al., 2015). Therefore, reversion of EMT signalling to mesenchymal-epithelial transition state and suppression of TGF-β improves reprogramming efforts (Chen et al., 2011a). Additionally, signal transduction of TGF-β may involve the p53 tumour suppressor gene. Evidence

suggested that dysregulation of TGF-β in cancerous epithelial cells induce p53 mutations (Elston and Inman, 2012). Previous study has demonstrated that the presence of p53 tumour suppressor gene safeguarded the genomic integrity of pluripotent cells which eventually blocked reprogramming and influenced the stepwise process (Spike and Wahl, 2011a).

Complexity in reprogramming cancer cells were not caused by technical barriers but instead due to biological barriers. Existing DNA damage in cancer cells engaged by genetic mutations, epigenetic remodeling halts the reprogramming process in human cancer cells (Ramos-Mejia et al., 2012). In addition, presence of diverged cellular hierarchy in a cancer cell also leads to differences in reprogramming efficiencies. Reprogramming in cancer cells were shown to be more difficult than from normal somatic cells due to the genetic and epigenetic constituents of these cells (Lang et al., 2013b). Recent studies demonstrated possible cell fate upon reprogramming from cancer cell types that are amenable to reprogramming and the resistant group.

2.9   Oral Cancer: Overview

Cancer cases was reported to reach 14.1 million worldwide in 2014 (Roshandel et al., 2014) with 8.2 millions of deaths. Among all the cancers, oral malignancies were ranked the 6th position as one of the most common cancer with

approximately 300,400 new cases diagnosed and 145,400 deaths worldwide in 2012 (Torre et al., 2015). Oral cancers contributed to high incidence in recent years and reported to be the highest in South and Southeast Asia, Eastern Europe, Latin America and Pacific regions (Warnakulasuriya, 2009). High prevalence oral cancer was observed in developed countries and to be increasing among developing countries (de Camargo Cancela et al., 2010). It remains as a deadly disease for above 50% of diagnosed cases were known to be in advanced stages at the time of detection (Shin et al., 2010).

Among the important etiological factors attributing to oral cancer are excessive consumption of alcohol, smoking, betel quid and a small proportion of Human Papilloma Infection (HPV). These factors may act individually or synergistically (Ram et al., 2011). These were all alluded to the multi-factorial risks factor involving lifestyle and environmental conditions. As reported by the World Health Organization (WHO), oral cancer is a global burden as it results in high degree of mortality as well as morbidity.

2.9.1. Risk Factors

Multiple risks factors contributed towards the development of oral squamous cell carcinoma. Among risk factors associated with OSCC pathogenesis

are alcohol consumption, tobacco smoking and Human Papilloma Virus (HPV) infection (McDowell, 2006).

Alcohol impairs DNA via oxidative stress subsequently giving rise to OSCC (Kandi et al., 2014, Feller et al., 2013). Besides, consumption of alcohol interrupts cellular metabolism such as DNA synthesis and repair by inducing mineral deficiencies such as folate (Mason and Choi, 2005). Alcohol enhances the excretion and inhibits the absorption of folate in the body by affecting its enzymes (Methylenetrahydrofolatereductase, MTHFR) involved in folate metabolism (Supic et al., 2011). Therefore, folate deficiency is an important component contributing to pathogenesis of OSCC.

Carcinogenic components from cigarette smoking especially N-Nitrosamines were known to cause DNA aberrations by alterations in bases, adducts, and disruption in DNA structure. Those cancer causing components also impair the DNA structure by affecting the pairing and synthesis of DNA. In addition, DNA adducts or specific regions in DNA that bind to the carcinogen were found to be increased in heavy smokers when compared to in non-smoker patients (Weber et al., 2011).

Human Papilloma Infection (HPV) originally acknowledged as sexually transmitted infection (STI), is known to cause cervical cancer. Deregulation of

cell cycle controled by E6 binding and degradation of tumour suppressor gene, p53 as well as inhibition of retinoblastoma protein by E7 increases the over expression of E6 and E7 proteins that induce tumourigenesis (Ganguly and Parihar, 2009). Numerous studies had demonstrated the over expression of E6 and E7 in OSCC (Wong et al., 2014). OSCC being associated with HPV infection had been documented a decade ago (Termine et al., 2008, Kelesidis et al., 2011).

2.9.2   Development Stages of Oral Cavity

The oral mucosal epithelium develops mainly from the ectoderm (lips, cheeks, vestibule, palate, gingivae, floor of mouth) and also from the endoderm (tongue). Histologically oral mucosa consists of an outer layer of stratified squamous epithelium and an underlying layer of dense connective tissues or lamina propria. Presence of both epithelial and connective tissues in the different regions of the oral cavity provides recognizable histological types that corresponded to the function of the tissues from lining mucosa in floor of mouth, inferior surface of the tongue, and mucosa distributed on the dorsum of the tongue (Winning and Townsend, 2000).

Histopathologic variants of OSCC are categorised as well differentiated disease with greater than 75– 100% of keratinisation, moderately differentiated with 50-75% of keratinisation, poorly differentiated with less than 25-50% of

keratinisation, and anaplastic tumour with less than 0-25% of keratinisation. In male, OSSC were in the form of poorly and moderately differentiated tumours while in female were frequently diagnosed as well and moderately differentiated tumours (Pires et al., 2013). Subsequently, other grading systems (Broder's classification 1920, Anneroth's multifactorial grading system 1987, Bryne's deep invasive cell grading system 1992) were developed in order to facilitate clinical classification (Doshi Neena et al., 2011). The degree of differentiation displayed by cells measures how closely tumour cells resemble the normal tissue structure. The keratin proteins distributed among the layers of epithelium indicates a disease process manifested in OSCC (Shetty and Gokul, 2012) which often correlates to epithelial-mesenchymal transition (EMT) (Krisanaprakornkit and Iamaroon, 2012).

2.9.3   Oral Squamous Cell Carcinoma (OSCC)

Typically oral cancers occur in the oral cavity and oropharyngeal cancers originate from the head and neck regions (Majchrzak et al., 2014). Most of the oral cancers developed in this region with more than 90% of the cases classified as Oral Squamous Cell Carcinoma (OSCC) and known as the prevalent malignant neoplasm with poor survival rate (Markopoulos, 2012). Generally, OSCC begins via regulation of EMT when the flat mucosal epithelium of oral cavity cell lining turns into an invasive epithelial neoplasm (Colley et al., 2011) with certain degree

of squamous differentiation. This occurs in lip, floor or roof of the mouth, tongue, soft palate, gingiva, and other areas of the oral cavity (Omar, 2013).

Regulation of EMT sets of metastasis and invasion which indicates poor prognostic and high risk of survival rate in OSCC patients (da Silva et al., 2015). TGF-β, a tumour suppressor gene identified in normal oral epithelial lineage transformed into oncogenic activator which activates EMT most likely due to pathological stress (Krisanaprakornkit and Iamaroon, 2012). Malignant transformation in human oral keratinocytes can be characterized by altered expressions of TGF- β and changing patterns of multiple oncogenic expressions including mutant P53. OSCC cell lines used in this study are well-differentiated cell types (H103-STNMP Grade 1 and H376-STNMP Grade III). Both cell lines expressed TGF- β and contain mutant P53 (Prime et al., 1994, Prime et al., 1990) but study conducted by Yeudall et al, showed that H376 carried nonsense mutation of P53 that caused truncated protein (Yeudall et al., 1995). Whilst H103 cell line expresses mutant P53 in missense form. Previously Paterson et al demonstrated the effect of TGF- β in OSCC H-Series cell lines and found H376 cell line highly responsive towards TGF- β compared to H103 cell line. (Paterson et al., 1995).

2.9.4   Genomic Alterations

Tumourigenesis in cancer initiated through the accumulation of numerous genetics alteration specifically through loss or gain of DNA sequences in tumour

suppressor genes and oncogenes. In addition, involvement of microsatellite instability (MSI) and loss of heterezygosity (LOH) had also been identified in cancerous cells (Kamat et al., 2012).

2.9.4.1 Microsatellite Instability (MSI)

Study of MSI was initially established in colorectal cancer and subsequently in other types of cancer. Microsatellite instability (MSI) is consequential from gene mutations as in insertion and deletion of one or more short tandem DNA repeat sequences or replication error phenotype in tumour suppressor gene and oncogenes. MSI is characterized by the loss of DNA mismatch repair (MMR) genes. MMR genes are responsible for fixing those replication errors occurring in the sequence. Presence of faulty mismatch repair genes results in genomic instability. In fact, the increase of MSI frequency in the absence of MMR proteins further kick starts the tumourigenesis process (Vaish and Mittal, 2002, Shilpa and and Lakshmi, 2014). Among those well observed DNA mismatch repair (MMR) genes frequently screened in tumours including OSCC are hPMS2, hMSH2, hMLH1 and hMSH6 (Jessri et al., 2015). Besides, potential microsatellite markers (D3S192, D3S966, D3S647, D3S1228 and D3S659) have been identified on chromosome 3p from the head and neck squamous cell carcinomas and showed high frequency of alterations (Ashazila et al., 2011).

2.9.4.2 Loss of Heterozygosity (LOH)

Loss of heterozygosity (LOH) strikes when there is a loss of functional allele in a gene where the other allele is already been inactivated. The pattern of LOH can be detected by observing for polymorphism between the normal and also the tumour cells as a pair of alleles present in normal cells while tumours has only one allele due to the loss of another one. Tumour progression begins when LOH takes place at a tumour suppressor genes or oncogenes (Yamamoto et al., 2015).

Over the years, LOH have been known as an important chromosomal event that results in OSCC progression. Studies have shown chromosomal deletion in OSCC often involves chromosomes from 3p, 5q, 9p, 11p, 11q, 13q and 17p. Down-regulation of tumour suppressor genes CDNK2A, APC and TP73 were associated to LOH in OSCC. Similar to that of MSI, study of LOH allows researchers to map for specific DNA regions and understand the development and progression of OSCC (Kasamatsu et al., 2011).

2.9.5   Epigenetic Remodelling

Genetic alterations constitute the hallmark of cancer development and progression. However, recent studies suggest that epigenetic remodelling of DNA sequences in human may also trigger tumourigenesis. Epigenetic events occur

when changes in gene expressions take place without altering the primary DNA sequence (Handy et al., 2011). Epigenetic alterations are potentially reversible and can be restored to their normal state via epigenetic therapy (Brunet and Berger, 2014). Such criterion was not identified in genetic aberrations. In contrast, any impairment to the DNA sequence is irreversible. Generally, epigenetic modification often commences via two different processes known as histone methylation and DNA methylation. Histone methylation results in changes of chromatin structure which affects the gene expression. Whereas, DNA methylation involves alterations of genes through hypomethylation and hypermethylation of site-specific CpG island promoter. (Gasche and Goel, 2012a).

Epigenetic is crucial in the regulation of normal cells as well as in embryonic development whereby activation and silencing of particular genes are meant to control the normal cellular growth and differentiation. On the contrary, epigenetic alteration of methylation affecting the promoter regions or first exons of tumour suppressor genes or oncogenes could switch on the tumourigenesis process. Hypothetically, during methylation process, two possible outcomes are being identified such as hypomethylation of regulatory DNA sequences that turned on the transcription of oncogenes and hypermethylation of CpG island promoter causing silencing of transcriptional TSG function (Mascolo et al., 2012).

In recent times, many cancers have been reported to be affected by misdirected epigenetic including OSCC. Ascertaining epigenetic patterns in both cancerous tissues and in circulating tumour cells of OSCC, offer opportunities in clinical application as in pre-diagnostic stage, tumour examination and non-invasive testing. (Jithesh et al., 2013).

2.9.5.1 Hypermethylation

Tumour suppressor genes are meant to regulate normal cell proliferations. They induce cell apoptosis upon abnormal cell division and secrete proteins that retain suppressive properties in cancer pathogenesis. However, the abnormal hypermethylation process interrupts the binding of CpG islands in promoter regions of a tumour suppressor gene, further resulting in its loss of function (Kulis and Esteller, 2010).

This mechanism of hypermethylation that strikes on promoter genes of tumour suppressor genes in OSCC impedes its normal function and triggers malignant transformation. The key events that initiate oral tumourigenesis are influenced by multiple etiological factors such as alcohol consumption, betel-quid chewing, smoking and HPV infections. Intensive studies on methylation status in OSCC had revealed multiple cancer causing genes which are frequently hypermethylated. Among these are RAS association domain family (RASSF1A),

MGMT, P16, T73, adenomatous polyposis coli (APC), GSTP1 and RARβ (Gasche and Goel, 2012b).

2.9.5.2 Hypomethylation

Global hypomethylation is a mechanism of oncogene activation which also initiates paths for methylation alterations contributing towards tumourigenesis. Promoter hypomethylation event of transcription regulatory regions were much less reported in cancer compared to the rate of recurrence of hypermethylation activity in CpG islands. This mechanism triggered by impairment of physiological regulatory systems of DNA methyltransferase DNMT1 that further causes the loss of genomic 5-methylcytosine (Arzenani et al., 2011). DNMT1 gene is known to uphold 5-methylcytosine which is important in newly synthesised DNA. While in OSCC, cytokine IL-6 induced inflammation was found to initiate oncogenesis activity. Loss of methylation patterns in oral cancer cells via LINE -1 gene along with induced inflammation by IL-6 which increases the chromosomal instability in OSCC (Gasche et al., 2011).

2.10   Future of iPSCs from Oral Squamous Cell Carcinoma

OSCC is treatable at the early stages of detection but diagnosis of OSCC often   late.   Histopathology   based   early   diagnosis   represents

a challenge for clinicians and pathologists (Scully et al., 2008). Suitable molecular markers and visual diagnostic aids such as staining and optical techniques have yet to be successfully proven as suitable early markers of OSCC (Messadi et al., 2009). Existing biological variation in tumours restricts research for potential biomarkers in OSCC as the solid tumours are heterogeneous in nature (Li et al., 2013). The lack of OSCC *in-vitro* model to study the cancer development and progression hinders findings which are crucial for translation to the clinical application. Derivation of iPSCs from OSCC could serve as an oncogenesis model to identify the potential biomarkers in cancer development and progression. Discovery of these biomarkers via OSCC-iPSCs may facilitate future development of diagnostics and novel therapies of the disease (Ono et al., 2012).

Therefore, the development of pluripotent stem cells via reprogramming technology from OSCC specific cell lines offers a new way to understand the oncogenic development. Such knowledge in oncogenesis allows genetic or epigenetic manipulation of established iPSCs from OSCC cell lines to serve as model for early stage or terminal stage OSCC cancer cell types. These models could also be further differentiated to different entities for the elucidation of the heterogeneity of OSCC manisfestations and the clinical spectrum of the disorder (Semi et al., 2012). Finally, iPSCs derived from OSCC allows the generation of a patient specific cancer model and provides an unlimited source of cells for diagnostic, prognostication and research purposes (Kim and Zaret, 2015).

CHAPTER 3

MATERIALS AND METHODS

3.1   Overview of Methods

Two cell lines of Oral Squamous Cell Carcinoma (OSCC), H103 - Grade I and H376 - Grade III from oral keratinocytes were used in this study (Table 3.1). The OSCC cells at early passages were obtained from Prof. Ian Patterson, University Malaya, Kuala Lumpur, Malaysia. Details and purity of culture conditions for the H-series OSCC cell lines, had been described and characterised earlier. OSCC cell lines were stained for cytokeratin markers via immunohistochemistry technique to exclude the possibility of the cell lines are being fibroblasts (Prime et al., 1990, Prime et al., 1994). Commercial 293FT cell line (human embryonal kidney cells) (Thermo Fisher Scientific, USA) was used as it is commonly applied in transfection work and known for its highly transfectable properties. Embyonic Stem Cells (ESCs) were used to optimise Quantitative Real-Time PCR (qPCR) assay. The reprogrammed OSCC cells in this study were generated via retro viral transduction and co-cultured on Mouse Embryonic Fibroblast (MEF) feeder layer (GlobalStem, USA). Prior to cell transduction, supernatant containing OSKM vectors was harvested from transfected 293FT.

Transfection efficiencies were assessed in both transduced cell lines with retro virus-GFP vector. Reprogrammed cells were characterised in terms of their morphologies and gene level expression as the primary screening criteria of their pluripotency characteristics. Further, proof of concept experiments were carried out on successfully reprogrammed OSCC cell line, H103 by immuno-fluorescent staining, embryoid bodies formation and three germ layer directed differentiation. All cell lines used in this study were tested for mycoplasma via Polymerase Chain Reaction (PCR). The cultures were ensured free of mycoplasma contamination and maintained in culture for not more than 8 weeks after thawing from frozen stocks. An overview of the methods used is shown in the flow chart below (Figure 3.1).

Table 3.1: Clinicopathological characteristics of the H103 and H376 Cell Lines

Cell line	Nationality	Age	Sex	Site[a] (S)	Size (T)	Nodal metastasis (N)	Distant metastasis (M)	Pathology[b] (P)	STNMP grade[c]
H103	British	32	M	T	< 20	-	-	W	I
H376	British	40	F	FOM	20-40	+	-	W	III

[a]**Site:** T, tongue; BM, buccal mucosa; FOM, floor of mouth; AP, alveolar process.
[b]**Pathology:** W, well-differentiated; M, moderately-differentiated; P, poorly-differentiated.
[c]**STNMP grade:** prognostic indicator for OSCC with 51.5%, 40.7%, 21.6% and 8.3% 5 year survival for patients with a stage I, II, III or IV tumours, respectively.
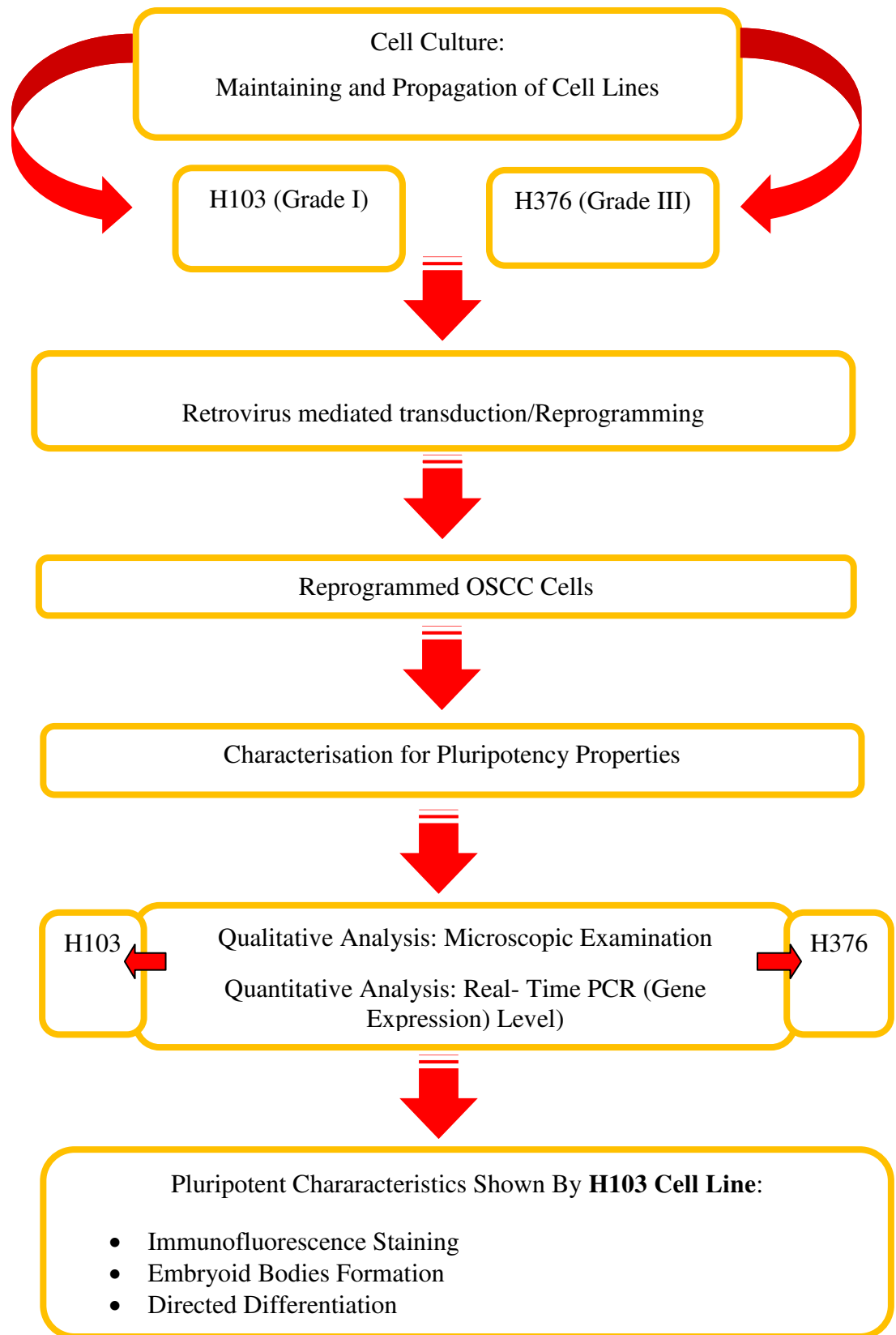
Figure 3.1 Flow chart of experimental design of the study.

3.2   Cell Culture

3.2.1   Culture of Oral Squamous Cell Carcinoma (OSCC) Cell Line

OSCC cell line vials were removed from liquid nitrogen and thawed in 37°C water bath (Memmert, Germany). Both vials were sprayed with 70% ethanol as in aseptic technique performed in a bio-safety cabinet (Esco, Singapore). Thawed cells, (approximately 1x 10^6 cells) were transferred into 15ml conical tubes with 10ml of DMEM/F12 medium supplemented with 10% FBS (Gibco, Invitrogen, USA), 1% penicillin/streptomycin (Gibco, Invitrogen, USA) and 0.5 ug/ml hydrocortisone (Sigma-Aldrich, USA). Medium composition of OSCC cell lines in 500ml is summarised in Table 3.2. Tubes containing H103 and H376 cells were centrifuged at 300 x g for 10 minutes to pellet down the cells. The medium was discarded without disturbing the pellet formed and the pellet was re-suspended in 10ml of fresh medium via gentle pipetting. OSCC cells were then sub-cultured and evenly seeded into 1:3 T75 culture flask and maintained in an incubator under 5% CO_2 atmosphere at 37°C. Cultured cell were examined daily using the Eclipse TS100 inverted microscope (Nikon, Japan) to ensure the attachment of the cells and to check for any possible contamination. The medium was changed every two days, followed by washing in 1x PBS each time, in order to remove non-adherent cells. Cells were harvested by using 3ml of 0.25% trypsin-EDTA (Sigma-Aldrich, USA) and sub-cultured every three days upon reaching 80% confluency.

Table 3.2: Medium composition of OSCC medium in 500ml

COMPOSITION	WORKING CONCENTRATION	TO PREPARE 500ML MEDIUM:
DMEM/F12	90%	450ml
Fetal Bovine Serum	10%	50ml
Penicillin-Streptomycin	1%	5ml
Hydrocortisone	250µg	0.5µg/ml

3.2.2 Culture of 293FT Cell Line

Thawed cells, approximately $1x\ 10^6$ cells were transferred into 15ml conical tubes with 10ml of DMEM high glucose medium supplemented with 10% FBS, 1% penicillin/streptomycin (Gibco, Invitrogen, USA), 1mM sodium pyruvate 100x (Gibco, Invitrogen, USA), 6mM L-glutamine 100x (Gibco, Invitrogen, USA), 0.1mM non-essential amino acid (NEAA 100x) (Gibco, Invitrogen, USA) and 50ug/ml geneticin 500x (Gibco, Invitrogen, USA). Medium composition of 293FT cell line in 500ml is summarised in Table 3.3. Tubes containing 293FT cells were centrifuged at 300 x g for 10 minutes to pellet down the cells. The medium discarded without disturbing the pellets formed and the pellet was re-suspended in 10ml of fresh medium via gentle pipetting. 293FT cells were then sub-cultured and evenly split into 1:2 T75 culture flask and maintained in an incubator under 5% CO_2 atmosphere at 37°C. Cultured cell were examined daily using the Eclipse TS100 inverted microscope (Nikon, Japan) to ensure the

attachment of the cells and to check for any possible contamination. The medium was changed every two days, followed by washing in 1x PBS each time, in order to remove non-adherent cells. Cells were harvested by using 3ml of 0.25% trypsin-EDTA (Sigma-Aldrich, USA) and sub-cultured every three day upon reaching 80% confluency.

Table 3.3: Medium composition of 293FT medium in 500ml

COMPOSITION	WORKING CONCENTRATION	TO PREPARE 500ML MEDIUM:
DMEM high glucose	90%	425ml
Fetal Bovine Serum	10%	50ml
Penicillin-Streptomycin	1%	5ml
Sodium Pyruvate 100x	1mM	5ml
L-glutamine 100x	6mM	5ml
NEAA 100x	0.1mM	5ml
Geneticin 500x	50mg/ml	5ml

3.2.3 Culture of Mouse Embryonic Fibroblast (MEF) Feeder Layers (IRRADIATED)

Cryo-vials containing 2×10^5 cells were thawed and transferred into 15ml conical tubes with 10ml of DMEM high glucose medium supplemented with 10% FBS (Gibco, Invitrogen, USA), and 1% penicillin/streptomycin (Gibco, Invitrogen, USA). Medium composition of MEF (GlobalStem, USA) in 500ml is summarised

in Table 3.4. Tubes containing MEF cells were centrifuged at 300 x g for 10 minutes to pellet down the cells. The medium was discarded without disturbing the pellets formed and the pellet was re-suspended in 10ml of fresh medium via gentle pipetting. A total of 2.5×10^5 MEF cells were plated in each well of 6-well plate and maintained in an incubator under 5% CO_2 atmosphere at 37°C. Cultured cell were examined daily using the Eclipse TS100 inverted microscope (Nikon, Japan) to ensure the attachment of the cells and to check for any possible contamination. The medium was changed every two days, followed by washing in 1x PBS each time, in order to remove non-adherent cells. Cells were sub-cultured every three day upon reaching 80% confluency.

Table 3.4: Medium composition of MEF medium in 500ml

COMPOSITION	WORKING CONCENTRATION	TO PREPARE 500ML MEDIUM:
DMEM high glucose	90%	445ml
Fetal Bovine Serum	10%	50ml
Penicillin-Streptomycin	1%	5ml

3.3   Preparation of Plasmid pMX-Retroviral Vector

3.3.1   Retrieval of Plasmids

Vectors, pMX-based retroviral h*Oct4* (Plasmid 17217) (Adgene), h*Sox2* (Plasmid 17218) (Adgene), h*Klf4* (Plasmid 17219) (Adgene), h*c-Myc* (Plasmid 17220) (Adgene), retroviral gag–pol packaging plasmid (Plasmid 8449) (Addgene), VSV-G expression plasmid (Plasmid 8454) (Addgene) and pMX-GFP (Cell Biolabs) used in this experiments were obtained from Dr. Shigeki Sugii, DUKE-NUS Graduate Medical School, Singapore. Plasmids were retrieved from the glycerol stock from -80°C freezer. Vectors from glycerol stock were streaked on LB agar plate treated with ampicillin (Sigma-Aldrich, USA) using an inoculum loop. LB-ampicillin agar plate was incubated overnight at 37°C. Streaked plates were incubated for not more than 16 hours as bacteria could possibly reach an overgrown state after 16-hours. Colonies appeared, and were picked for liquid culture. Plasmids map and other features are detailed in Appendix A-G.

3.4 Bacteria Culture Media and Antibiotic

3.4.1 Lysogeny (LB) Agar Plate

Lysogeny (LB) agar plate contained growth medium, commonly used to culture *Escherichia coli* (*E. coli*), DH5α strain. Commercial LB powder supplemented with tryptone, yeast extract and sodium chloride (Nacl) (Sigma-Aldrich, USA) were weighed at 5g into 250ml of doubled distilled water in a flask. Another 3.75g of agar (Sigma-Aldrich, USA) was added into the mixture. The medium was autoclaved at 121°C for 20 minutes and cooled to 55°C-60° in a water bath. Ampicillin was added into LB agar medium at a concentration of 50ug/ml. Next, LB agar medium was poured into sterile 100mm petri dishes and allowed to solidify. Prepared LB-Ampicillin agar plates were wrapped with aluminium foil and stored at 4°C to avoid possible degradation of antibiotics. Preparation was strictly carried out in a laminar hood.

3.4.2 Lysogeny (LB) Media

Lysogeny broth (LB) medium was used to grow *E.coli.* LB medium was prepared according to the manufacturer's protocol. To prepare the medium, 3.75 g of LB powder (Sigma-Aldrich, USA) was dissolved in 250ml of double distilled water in a 500ml flask. LB medium was autoclaved at 121°C for 20 minutes and

cooled around 55°C-60°C in a water bath. Ampicillin was added into LB the medium at a concentration of 50ug/ml and the medium was stored at room temperature (RT) prior to use.

3.4.3 Antibiotic Selective Marker

In this experiment, ampicillin was used as a selection marker. *E.coli* that had taken up and expressed the ampicillin resistance gene on plasmids was used in the growth medium and were selectively allowed it to grow. For stock preparation, 50 mg of ampicillin was dissolved in 1ml of double distilled water which was then filtered and stored at -20°C. Ampicillin working concentration used in this experiment to culture desired plasmid transformed *E.coli* was 50ug/ml.

3.5　Storage of Transformed Plasmids

A single colony of *E.coli* from the streaked selective plate was picked and cultured in 3-5ml ml LB medium containing ampicillin in a 15ml tubes at 37°C, overnight (≥ 16 hours). Tubes containing transformed *E.coli* were placed in shaking incubators (approx. 300 rpm). Stocks were made with 200µl of autoclaved glycerol and 800µl of transformed *E.coli* into the cryovials. The cryovials were vortexed vigorously to ensure homogenous mixing before freezing at -80°C.

3.6   Plasmid Extraction

One colony from the LB-Ampicillin agar plate of each plasmid was inoculated into 3ml Ampicillin treated LB Broth Media in a 15 ml tubes. A few replicates were prepared to determine the growth capacity of each colony. Bacteria cultured tubes were incubated overnight at 37°C in a shaking incubator (IKA, China). Colony that grew well in a 15 ml tube was characterised by cloudy haze LB-Ampicillin media. Approximately 250-500µl from 3ml LB-Ampicillin media containing well grown plasmid infected *E.coli* is was transferred into a 250ml LB-Ampicillin media to culture enough for plasmid extraction and the resultant soultion incubated overnight at 37°C in shaking incubator. About 250-500ml (depending on the copy numbers of plasmid) of well grown plasmid infected *E.coli* was centrifuged to pellet the bacterial cells and then subjected to Plasmid Extraction (According to Manufacturer's Protocol – PureLink® HiPure Plasmid Maxiprep Kit, Life Technologies, USA). As for high copy number plasmids, 100–200 mL of an overnight LB culture per sample was used while for low copy number plasmids approximately 250–500 mL of an overnight LB culture per sample was used. Bacterial cultures were then incubated in a shaking incubator at 37°C, overnight, with vigorous shaking ($\geq$ 16 hours). Transformed *E.coli* pellets were harvested by centrifuging the overnight LB culture at 4000 × g for 10 minutes. Excessive medium was discarded and each vector was extracted according to the manufacturer's protocol. Re-suspension Buffer (R3) with RNase

A were added to the pellets to inhibit the nucleus activity of cellular enzymes and the resultant mixture was stirred until homogenous. Lysis Buffer (L7) containing sodium dodecyl sulfate (SDS) was added into the mixture to break up the lipid structure of the bacterial cell membrane by keeping both proteins and DNA, in their denatured form. Lysis steps were carried out by inverting the capped tubes but not vortexed; subsequently incubating at room temperature for 5 minutes. The mixture was then neutralised and precipitated by adding in the Precipitation Buffer (N3) and mixing immediately by inverting the tubes until thoroughly homogeneous. The mixture was centrifuged approximately $12,000 \times g$ for 10 minutes at room temperature. The precipitation step was meant to dissolve proteins, membrane debris and associated genomic DNA aided by acidic potassium acetate. Plasmid DNA remained dissolved during this step. Supernatant collected and transferred onto the equilibrated column while the solution was allowed to drain by gravity flow through the column. The column washed with Wash Buffer (W8) and the excess flow through was discarded prior to next step. Elution Buffer (E4) was then added to the column to elute the plasmid DNA by gravity flow. The column was discarded as the elution contained purified plasmid DNA. Thereafter, isopropanol was added to the elution tube which resulted in the precipitation of the plasmid DNA which was subsequently sedimented by centrifuge at $12,000 \times g$ for 30 minutes at 4°C. DNA pellet was then re-suspended in 70% ethanol in order to remove the salt content of the preparation. The elution was centrifuged at $12,000 \times g$ for 5 minutes at 4°C and the supernatant was

removed leaving behind the pellet. The pellet was then air-dried for 10minutes before being re-suspended in 300µl of TE buffer (TE). Plasmid DNA of each vector was transferred into labelled 1.5ml tubes. Measurement of the concentration and purity was performed by using NanoPhotometer UV/Vis spectrophotometer (Implen, Germany). The ratio of A260/A280 for pure plasmid DNA was achieved in the ranged of 1.7-1.9. Plasmid concentration and purity are summarised in Appendix H.

3.7 Verification of Plasmids Extracted

3.7.1 Restriction Enzyme (RE)

Restriction enzyme method was applied to confirm the identity of the plasmids extracted. Patterns of DNA fragments produced by restriction digest serve as a fingerprint of a plasmid. Two types of restriction enzymes (RE) were used as the pattern varies according to the plasmids. Restriction enzyme reaction mixtures used were summarised in Table 3.5. Types of RE and plasmid DNA (OSKM) sizes are detailed in Appendix I. Approximately ~0.2µg of each plasmid DNA was required for restriction digestion. The master mix components were prepared according to the manufacturer's protocol (Thermo Fisher Scientific, USA) before adding into each tube containing plasmid DNA. The resultant

solution was thoroughly mixed, spun down and incubated at 37°C for 5-15 minutes to digest the DNA in a water bath.

Table 3.5: Reaction mixtures of restriction enzyme

COMPONENT	VOLUME (µL)
Water, nuclease-free	15
10X FastDigest Buffer	2
FastDigest enzyme	1
Plasmid DNA (~0.2µg)	2
Total	**20**

3.7.2   Gel Electrophoresis

Agarose gel electrophoresis was conducted to analyse the restriction enzyme product size of each vector. The 1% agarose was prepared by dissolving 1g agarose powder (SeaKem® LE, Lonza, Switzerland) in 100 mL of 1x TAE. Solution heated in the microwave for 2 minutes until the agarose gel was completely melted and then cooled down to 70°C in a water bath. Casting tray was rinsed and dried with ethanol prior to use. About 25-30 mL agarose was poured into the clean casting tray containing a comb and let to solidify about 15 minutes at room temperature. The comb was then removed slowly and carefully, without breaking the casted agarose gel and the entire gel tray was placed in an electrophoresis tank, covered with 1x TAE buffer which was diluted from 50X

TAE Buffer (Tris-acetate-EDTA) (Thermo Fisher Scientific, USA). Ten micro litres of digested DNA was mixed with 2ul of 6x loading dye and loaded into the wells created by the coomb and the digested DNA was then run on 1% agarose gel electrophoresis at 80V for 45 minutes using 1kB DNA ladders as markers. The agarose gel post-run was stained in 3 x GelRed solutions (Biotium, USA) for 15 minutes and the visualized under ultraviolet light (UVP LLC, USA). The gel image was captured using a molecular imager (BioSpectrum Imaging System).The images of are shown in Appendix J.

3.8 Reprogramming

3.8.1 Retrovirus Packaging

Retrovirus is a virus that belongs to the viral family *Retroviridae*. It consists of genetic material in the form of RNA molecules and is covered with an envelope. The envelop of the retrovirus has a viral glycoprotein that binds to cellular receptors to ensure its specific host and cell type that is being infected. Generally, retroviruses encoded three essential genes, GAG, POL, and VSV-G whereby Gag codes for structural proteins containing the matrix, capsid, and the nucleoprotein complex. Whereas, POL codes for reverse transcriptase, integrase and VSV-G codes for the proteins of the envelope. GAG-POL and VSV-G were all made into packaging cell lines (293FT) in order to produce vector particles that

provide all the viral proteins required for capsid production and the virion maturation of the vector. The 293FT cell lines (human embryonal kidney cells) were used to package retroviruses using the GFP and four Yamanaka vectors (O/S/K/M).

3.8.1.1 Transfection for Retrovirus: Green Fluorescent Protein (GFP)

Tissue culture grade petri dishes were coated with 0.1% gelatin. For optimal density, approximately 3.6×10^6 293FT cells were seeded in 100 mm petri dish the night before, to achieve 70% − 80% confluency on the day of the transfection. After 22 hours of seeding, the medium was changed to a non-FBS 293FT medium, for starvation (2hrs before transfection). In between and before transfection, the transfection reagent (Lipofectamine 2000) (Life Technologies, USA) was prepared and incubated 30 minutes prior to use. Lipofectamine components and plasmid used are summarised in Tables 3.6 and 3.7 respectively. Complete fresh 293FT growth medium was used to replace the non-FBS medium at 24 hours. GFP + Lipofectamine mixture + VSV-G + Gag-Pol were added to each petri dishes. Fresh medium was replaced the next day. Transduced cell lines were viewed under Zeiss Imager A.1 Fluorescence Microscope (Carl Zeiss, Germany) at 48 hours post transduction to determine the transduction efficiency.

3.8.1.2 Transfection Efficiency of pMX-GFP in OSCC Cell Lines

Transfection efficiencies in H103 and H376 were assessed via manual counting method of the green fluorescent protein (GFP) expressing positive cells under Zeiss Imager A.1 Fluorescence Microscope (Carl Zeiss, Germany). As for the quantification counting, at least four separate fields were counted in each transfected cell line.

3.8.1.3 Transfection with Retrovirus: Vectors (Oct4, Sox2, Klf4, c-Myc)

Tissue culture grade petri dishes were coated with 0.1% gelatin and labelled according to the vectors. For optimal density, approximately 3.6×10^6 293FT cells were seeded in each dish the night before, to achieve 70% − 80% confluency the day of the transfection. After 22 hours of seeding, the medium was changed to non-FBS 293FT medium, for starvation (2hrs before transfection). In between and before transfection, the transfection reagents (Lipofectamine 2000) (Life Technologies, USA) was prepared and incubated 30 minutes prior to use. Lipofectamine components and types of plasmid used are summarised in Tables 3.5 and 3.6 respectively. Complete fresh 293FT growth medium was used to replace the non-FBS medium at 24 hours. Respective Yamanaka factors in transfection mixture (Retro-O/S/K/M + Lipofectamine mixture + VSV-G + Gag-Pol) were added to each petri dish. Fresh medium was used to replace the next day.

The first virus collection was performed 24 hours post-transfection and briefly centrifuged at 2000 rpm for 5 minutes to remove unwanted debris. Supernatant was then filtered with 0.45μm PVDF filter unit, and 0.5μl /ml from 10mg/ml stock of Polybrene was added to the pool of supernatant. Fresh supernatant was used to transduce Oral Cancer Cell carcinoma immediately after collection.

Lipofectamine mixture + Plasmids (Vector)   Gag-Pol   V-svg
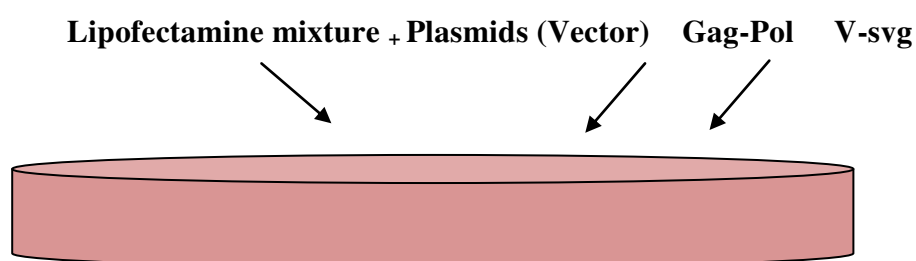
Figure 3.2 Transfection components

Table 3.6: Amount of plasmid DNA for retroviral transfection in ratio of

3:2:1

VECTORS	AMOUNT (μG)
Plasmid (O/S/K/M)/GFP	16.5
Gag-Pol	11.0
VSV-G	5.5

Table 3.7: Component A and B (Lipofection 2000 Protocol).

Component A: Dilution of lipofectamine in blank DMEM

MIXTURE	OCT4	SOX2	KLF4	C-MYC	GFP
Lipofectamine	50µl	50µl	50µl	50µl	50µl
Blank DMEM	450µl	450µl	450µl	450µl	450µl
Total	**500 µl**	**500 µl**	**500µl**	**500µl**	**500µl**

Component B: Dilution of plasmid DNA in blank DMEM

MIXTURE	OCT4	SOX2	KLF4	C-MYC	GFP
Plasmid	5.2µl	5.2µl	5µl	4.1µl	15µl
Gag-Pol	18.3µl	18.3µl	18.3µl	18.3µl	18.3µl
VSV-G	7.9µl	7.9µl	7.9µl	7.9µl	7.9µl
Blank DMEM	468.6µl	468.6µl	468.8µl	469.7µl	458.8µl
Total	**500µl**	**500µl**	**500µl**	**500µl**	**500µl**

3.8.2   Retrovirus Transduction

Oral squamous cell carcinoma (OSCC) cell lines H103 and H376 were passaged to ensure active proliferation within cells to accomplish successful reprogramming. Approximately 7×10^4 cells of H103 and H736 cell were each seeded in a six well plate and incubated overnight at 37°C in 5% CO_2 to achieve 60–70% confluency. The next day, H103 and H376 were transduced with established retroviral reprogramming factors (Oct4, Sox2, Klf4 and c-Myc, or GFP

positive control vector), collected and filtered at 48 hours post transfection. As for Yamanaka reprogramming vectors (Oct4, Sox2, Klf4 and c-Myc), the supernatants of each vector were equally mixed (0.5ml/per vector), made up to 2ml of combined retroviral supernatants before being added to each well of both OSCC cell lines. Six-well plates of H103 and H376 cell lines were then centrifuged (known as 'spin-fection') with viral supernatants at 800 xg, 90 minutes at 32°C for 50 minutes. This procedure was used to increase transduction efficiencies. Soon after the spin-fection procedure, the plates were returned back into the hypoxic incubator (37°C, 5% O_2). On the same day of viral transduction being carried out, irradiated-MEF was seeded on 1% gelatin-coated six-well plates. Each tube of MEF (GlobalStem) consisted of 2 million cells whereby 2.5 x 10^5 of cells were plated in each well. MEF cells were incubated three days at 37°C, 5% CO_2. Transduced cells of H103 and H376 were passaged at 72hrs post-transduction onto the prepared MEF feeder plates. Each well was added approximately 1 x 10^2 transduced cells and cultured in OSCC growth medium. Day one upon transfer to MEF feeder layer, transduced cells were cultured with sequential transition of hESC medium and OSCC cell lines medium in ratios as shown in Table 3.8. Medium proportions and compositions are summarised in Tables 3.8 and 3.9 respectively. Subsequently from day 4 onwards, complete hESC medium was used to culture transduced/reprogrammed OSCC cell. The medium was changed daily over a period of 2 weeks till the appearance of colonies.

Table 3.8: Medium proportion

DAYS	HESCS MEDIUM (ML)	OSCC MEDIUM (ML)	RATIO
1	0.5	1.5	1:3
2	1	1	1:1
3	1.5	0.5	3:1
4	2	0	3:0

Table 3.9: Medium composition of hESC in 500ml

COMPOSITION	WORKING CONCENTRATION	TO PREPARE 500ML MEDIUM:
DMEM/F12	80%	389.865ml
Knock-Out Serum Replacment	20%	100ml
NEAA 100x	0.1mM	5ml
L-Glutamine 100x	4mM	5ml
B-Mercaptoethanol 14.3M	0.1mM	35µl
Human Fibroblast Growth Factor,50ug/ml	10ng/ml	100µl

3.8.2.1 Maintenance and Passaging of Reprogrammed OSCC Cell Lines

Colonies appeared at day 14-15 to an appropriate size for passaging. Colonies picked were based on the Embryonic Stem Cells (ESCs) like morphologies. Cells picked for the next passage were round in shape with large nucleus. Colonies also had sharp-edged with flat and scant cytoplasm. Picking was performed under a Eclipse TS100 inverted microscope (Nikon, Japan) in a pre-sterilised laminar hood. Newly derived ESCs-like cells were observed under the microscope and marked. About extra 2ml of hESCs medium was added into the wells with marked colonies. Colonies were then manually cut with 26G needle into grids. P200 pipette adjusted to 150µl -200µl was used pick up each grid which was transferred into another six-well plate layered by MEF feeder. Plates were incubated in 37°C, 5% CO_2. OSCC-IPCs colonies were continuously passaged above passage 5 and characterised for the pluripotency properties. Consequently, colonies were also isolated for cryopreservation from passage 5 and above at each passage number. Derived colonies were passaged every 4-5 days.

3.9 Characterization of OSCC-Induced Pluripotent Stem Cells (iPSCs)

3.9.1 Morphology Evaluation under Microscope Observation

The morphology evaluation was the primary screening for pluripotency properties prior to further in-depth characterisation. Stable reprogrammed colonies similar to ESC morphologies appeared and were grown in six-well plates coated with MEF feeder layers. The medium was changed every two days for formation of stable colonies. The morphologies of cells were observed under a Eclipse TS100 inverted microscope (Nikon, Japan) and all the images were duly recorded. Among the two OSCC cell lines reprogrammed, only H103 showed characteristic ESC-like morphologies upon passaging.

3.9.2 Gene Expression Assessment in OSCC- Induced Pluripotent Stem Cells (iPSCs)

3.9.2.1 Total Ribonucleic Acid (RNA) Extraction

The reprogrammed OSCC cells, approximately 5×10^6 - 1×10^7 number of cells, were isolated and lysed in 600ul of RLT buffer (Qiagen RNeasy® mini kit) (Qiagen, Germany). Cell pellets with RLT buffer were vortexed to mix well.

Lysed cells were then homogenized via Qiashredder by 2 minutes of centrifugation ($\geq$ 10000 rpm). One part of 70% ethanol (600 ul) was added to the lysate, mixed well by pipetting and then transferred into the Rneasy spin column. Spin column were centrifuged for 1 minute at $\geq$ 10000 rpm. Flow through was discarded after the centrifugation. Buffer RW1 (350ul) was added into the Rneasy column and again spinned for 1 minute at $\geq$ 10000 rpm. Flow through was discarded after the centrifugation. Genomic DNA elimination was performed. According to the manufacturer's protocol of the Genomic Elimination Kit (QIAGEN), 10 µl of Dnase 1stock mixed in 70µl of buffer RDD was added directly onto the Rneasy column membrane. The column was incubated for 15 minutes for complete genomic DNA removal. Again, 350ul buffer RW1 was applied to wash the column followed by 1 minute of centrifugation at $\geq$ 10000 rpm. Flow through was discarded after the centrifugation. A washing step performed by addition of 500µl buffer RPE to the column. The Rneasy column was then spinned for 1 minute of centrifugation at $\geq$ 10000 rpm and the flow through was discarded. This step was repeated by washing with 500ul buffer RPE but was centrifuged for 3 minutes to avoid ethanol carry over. The Rneasy column then transferred to a new collection tube provided by the Kit and was spinned at full speed for 1 minute to remove possible carry over. The column was transferred again to 1.5ml tube, also provided by the Kit. Approximately, 30µl of Rnase free water was added onto the membrane column which was centrifuged for 1.5 minutes at $\geq$ 10000 rpm as in the elution step. The elution was then repeated using the elute. Quality and quantity of

RNA extracted were assessed using the NanoPhotometer UV/Vis spectrophotometer. The RNA was then was run on pre-cast denaturing agarose gel. Buffer use consisted of 10x Mops (200ul) (Sigma-Aldrich), Formamide (1000 ul) (Merck Milipore, USA) and Formaldehyde (356 µl) (Merck Milipore, USA) Digested RNA was mixed with 1ul of 6x loading dye (Thermo Fisher Scientific, USA), loaded into the wells and then allowed to run on denaturing agarose gel for 45 minutes at 80V using 1kB RNA ladders (Amresco, USA) as markers. Post run, the agarose gel was stained in 3 x GelRed solutions (Biotium, USA) for 15 minutes and the visualized using molecular imager, BioSpectrum Imaging System under ultraviolet light (UVP LLC, USA). Intact total RNA was observed with clear 28s AND 18s bands with appropriate intensity of 28S:18S rRNA band of 2:1 ratio. The A260/280 value for pure RNA was accepted in the range of 1.9-2.0.

3.9.2.2 cDNA Conversion

Reverse transcription was performed to convert RNA extracted into cDNA prior to RQ-PCR experiments. Genomic elimination reaction was carried according to the manufacturer's protocol (QuantiTech Reverse Transcriptase Kit) (Qiagen, germany) before the reverse transcription steps. Extracted RNA templates, gDNA wipeout buffer, Quantiscript Reverse Transcriptase, Quantiscript RT buffer, RT primer mix and RNase-free water were all thawed on ice. Each tube was centrifuged briefly to collect the residual liquid from the sides of the tubes.

Genomic DNA elimination components were prepared as stated in Table 3.10. Then, mixtures were incubated for 2 minutes at 42°C and immediately placed on ice. Next, the reverse transcription master mixes were prepared accordingly as in Table 3.11. The reverse transcription master mix components were then mixed with 14µl of RNA template from the genomic elimination step. The reactions were incubated at 42^0C for 15 minutes at 95^0C for 3 minutes to inactivate the Quantiscript Reverse Transcriptase. All the cDNA were kept at 4^0C until RQ-PCR was set up and for long term storage they were placed at -80^0C.

Table 3.10: Genomic DNA elimination reaction components.

COMPONENTS	VOLUME/REACTION
gDNA Wipeout Buffer, 7x	2 µl
Template RNA (up to 1ug)	10 µl
Rnase-free water	2 µl
Total	**14 µl**

Table 3.11: Reverse-transcription reaction components.

COMPONENT	VOLUME/REACTION
Reverse-transcription master mix	1 µl
Quantiscript RT buffer 5x	4 µl
RT Primer mix	1 µl
Template RNA (from genomic elimination reaction – Table 3.9)	14 µl
Total	**20 µl**

3.9.2.3 Quantitative Real Time PCR (qPCR)

Both cell lines were characterized for mRNA expression to determine the endogenous reprogramming expression status and to ensure the susceptibility of reprogramming. Pluripotency of reprogrammed H103 and H376 cell lines were assessed via quantitative real time polymerase chain reaction (qPCR). Fluorescent reporter used includes double-stranded DNA (dsDNA)-binding dyes incorporated into the PCR product to quantify the mRNA targets during PCR cycle. The fluorescent signals from each sample were plotted against cycle numbers which represent the accumulation of product over the duration of the real-time PCR experiment. PCR amplification efficiency was determined based on all the primers optimised by using Embryonic Stem Cells which were commonly used as the gold standard for pluripotency genes expression. β-actin was used as a control gene in this experiment. Briefly, the experiment comprised initial denaturation at 95°C for 15 minutes, followed by 40 cycles of denaturation at 94°C for 30 seconds with annealing at 60°C for 30 seconds and extension at 72°C. Following PCR, fluorescent data collection was performed during extension. Real-time PCR was performed with iQ5 Bio-Rad qPCR machine (Bio-Rad, USA) using Quantitect Sybr Green PCR Master Mix (Qiagen, Germany). PCR reaction components prepared for one reaction (20ul/tube) were shown in Table 3.12. iQ5 Optical System Software, Version 2.0 was used for the analysis. List of primers used are shown in Appendix K.

Table 3.12: qPCR reaction components

COMPONENT	VOLUME/REACTION	FINAL CONCENTRATION
2x QuantiTect SYBR Green RT-PCR Master Mix	10 µl	1x
Primer 10 µM (Forward)	1 µl	0.5 µM
Primer 10 µM (Reverse)	1 µl	0.5 µM
Rnase Free Water	7 µl	-
Template RNA	1 µl	25ng
Total	**20 µl**	

3.9.2.4 Calculation and Analysis

Messenger RNA (mRNA) was assessed via Comparative C_T Method ($\Delta\Delta C_T$) normalised against Beta-Actin (ACTB) as endogenous control or house keeping gene. Experiments were carried out in triplicates to ensure accuracy and reproducibility of data obtained. The C_T mean value from each experiment was compared against parental and its reprogrammed counterpart and evaluated to determine the differential expression of gene of interest. Threshold cycles values (C_T) generated from qPCR were used in calculations to determine the fold changes of the samples.

Statistical data analysis was carried out with Paired t-Tests to compare the quantitative outcomes of parental, reprogrammed counterparts at passage 5 and

reprogrammed counterparts at passage 10 of H103 and H376 cell lines using SPSS Software version 22.0. All tests were conducted at the 95% confidence level. And data were presented as mean ± standard deviation (SD) or mean ± standard error of mean SEM. The differences were considered significant at $P<0.05$, $P<0.01$ and $P<0.001$ where apprpriate. Data are detailed in Appendix (L-M) and plotted into histograms in the Results section.

3.9.3   Immunofluorescence (IF) Staining

Immunofluorescence staining was performed on parental H103 and their counterparts to evaluate the pluripotency expression. This method is an immunochemical method that uses fluorescent dyes attached to antibodies whereby the antigens present in samples are determined when the sample is illuminated at a specific wavelength. Earlier, reprogrammed H103 showed similar morphologies and captured satisfactory signals from real-time pcr analysis compared to reprogrammed H376. Therefore, successfully induced pluripotent H103 cells were characterised further. Induced pluripotent cancer cells of H103 were seeded in a 12-well plate for immunofluorescence staining. Cells were fixed using 4% v/v paraformaldehyde (Sigma-Aldrich) for 30 minutes, washed three times with PBS containing 1% BSA and permeablised using Perm Buffer (BD Biosciences, USA) for 15 minutes at room temperature (Intracellular Markers). For the extracellular markers, immune-staining steps do not require

permeablisation and may proceed to blocking and incubation with PBS containing 1% BSA. After permeabilisation for intracellular staining, cells were blocked with PBS containing 1% BSA for 1 hour at room temperature. PBS containing 1% BSA was removed and washed three times with PBS. Cells were incubated with conjugated antibodies in PBS containing 1% BSA overnight at 4°C. Antibodies used in this study included Oct4-PE (BD Biosciences, USA), Sox2-PE (BD Biosciences, USA), Nanog-ALexa Fluor 488 (BD Biosciences, USA), Tra-1-60-PE (BD Biosciences, USA). After the overnight incubation, cells were washed three times with PBS and stained with Dapi Antifade Gold (Life Technologies, USA) for 10 minutes. Stained cells observed under Zeiss Imager A.1 Fluorescence Microscope (Carl Zeiss, Germany). Antibodies dilutions are summarised in Tables 3.13.

Table 3.13: Pluripotent specific antibodies dilution factors

ANTIBODIES	DILUTION FACTOR
OCT4-PE	1:50
SOX2-PE	1:50
NANOG-ALEXA FLUOR 488	1:50
TRA-1-60-PE	1:50

3.9.4 Embryoid Bodies (EBs)

Derived H103-IPCs were then manually cut (approximately 10 pieces per well) and transferred onto an ultra low attachment plate containing commercialised Embryoid Bodies medium (Milipore, USA). Transferred cells were grown in suspension for 8 days. The medium was consistently changed every 2–3 days up to 8 days without disrupting the EBs

3.9.4.1 Immunofluorescence Staining of Embryoid Bodies

Embryoid Bodies formed were carefully collected in 1.5ml tube for immunofluorescence staining to determine the presence of three germ layers. EBs were fixed with 4% paraformaldehyde, and washed three times to remove excessive fixing buffer by centrifugation. Cells were then blocked with PBS containing 1% BSA for 1 hour at room temperature and washed briefly by centrifugation. EBs were then incubated in fluorochrome-conjugated primary antibodies (Human Three Germ Layer 3-Color Immunostainining Kit) (R&D Systems, USA) for 2 hours at 4°C. EBs were stained for ectoderm differentiated cells with Northern Lights flourochromes repectively (NL) NL557-conjugated Otx2 (red), NL493-conjugated SOX1 (green), mesoderm differentiated cells NL557-conjugated Brachyury (red), and endoderm differentiated cells NL637-conjugated SOX17 (red), NL493-conjugated GATA-4 (green). After the

incubation, cells were washed three times with PBS and stained with Dapi Antifade Gold (Life Technologies, USA) for 10 minutes. Stained cells were observed under Zeiss Imager A.1 Fluorescence Microscope (Carl Zeiss, Germany). Antibodies dilutions are summarised in Table 3.14.

Table 3.14: Three germ layer specific antibodies dilution factors

ANTIBODIES	DILUTION FACTOR
Otx2 - NL557 (red)	1:10
Sox1- NL493 (green)	1:10
Brachyury - NL557	1:10
Sox17 - NL637 (red)	1:10
Gata4 - NL493 (green)	1:10

3.9.5 Directed Differentiation Assay

OSCC originates from endoderm and ectoderm lineages. Therefore, the trans-differentiation capability was assessed in successfully reprogrammed OSCC cell line. In this experiment, H103 was differentiated into adipocytes and osteocytes that are derived from mesoderm lineages.

3.9.5.1 Adipogenesis: Oil Red O Staining

Colonies were plated on gelatine coated six-well plates instead of MEF feeder layer and cultured with 3ml of adipogenic induction medium in each well. The medium was changed every 2-3 days. After 21 days of incubation at 37°C, in 5% CO_2, cells were stained in Oil Red O for visualisation of lipid droplets. 0.3% Oil Red O was prepared by dissolving 0.3g powder (Sigma-Aldrich, USA) in 100ml isopropanol (Merck Milipore, USA). Solution prepared was stored in the dark at room temperature. Adipogenic medium was removed from the culture and washed thoroughly with 1xPBS without any disruption to the monolayer cells. PBS aspirated out and the cells were fixed in 3ml of 10% formalin (Sigma-Aldrich, USA). Fixation was performed at room temperature for at least 30 minutes. During fixation, 3 parts of the Oil Red O stock solution was diluted with 2 parts distilled water and filtered with 0.45uM syringe filter. Fixation buffer was removed and cells were rinsed with distilled water. Next, 3ml of 60% isopropanol was added to the cells and incubated at room temperature for 5 min. Subsequently 60% isopropanol was aspirated out while Oil Red O staining solution was added enough to cover the cell monolayer. Staining was performed at room temperature for 15 min. Oil Red O staining solution was discarded and the cells were rinsed several times with double distilled water until the water became clear. Stained monolayer cells were carefully blotted on a paper towel to remove as much water as possible. Stained cells were then viewed under Eclipse TS100 inverted

microscope and images were captured for analysis. Mature adipocytes containing intracellular lipid vesicles showed bright red staining.

3.9.5.2 Osteogenesis: Alizarin Red Staining

Osteogenic induction medium was used to induce mineralisation indicating osteogenesis in reprogrammed OSCC cell line. IPCs clones were plated on gelatine coated six-well plates and cultured with 3ml of induction medium in each well. The medium was changed every 2-3 days. After 21 days of incubation at 37°C, in 5% CO_2, cells were stained in Alizarin Red for visualisation of calcium deposits. Approximately 2g of Alizarin Red S (Sigma-Aldrich, USA) was dissolved in 100 ml double distilled water. The solution was mixed and the pH was adjusted to 4.1 - 4.3 with 0.1% Ammonium Hydroxide (NH4OH) (Sigma-Aldrich, USA). The resultant dark brown solution was filtered and stored in the dark. The medium was discarded and cells were washed 1x PBS without any disruption to the monolayer cells. PBS was aspirated out and cells were fixed with 3ml of 10% formalin for 30 minutes. Fixed cells were carefully washed in double distilled water. Enough Alizarin Red S staining solution was added in to cover the cellular monolayer. Cells were stained in the dark for 45 minutes at room temperature. Alizarin Red S was removed and cells were washed three times with 1ml of doubledistilled water each time. Stained monolayer cells were then blotted on a paper towel to remove excess water. Stained cells were then evaluated under the

Eclipse TS100 inverted microscope and images were captured for analysis. Presence of mineralised osteoblasts was shown as bright orange-red precipitate.

3.10   Microsatellite Instability (MSI) Study via Polymerase Chain Reaction (PCR)

3.10.1 Deoxyribonucleic Acid (DNA) Extraction

The parental and reprogrammed H103 cells approximately 1×10^7 number of cells were isolated in 1x PBS and lysed with 20ul proteinase K to digest the protein and remove contamination prior to DNA extraction steps (Geneall Biotechnology, Korea). Samples (200ul) from early steps were then transferred into 1.5ml centrifuge tubes. A total of 200ul of lysis buffer (Buffer CL) were added in and vortexed to homogenise the lysed products. Mixtures were incubated in a water bath at 56°C for 30 minutes to further digest the cells. Upon incubation, 200ul of absolute ethanol was added into the sample tubes to precipitate the nucleic acids and mixtures were thoroughly mixed via vortexing. Samples were then transferred into elution column and centrifuged at 14000 rpm for 1 minute. Supernatants were discarded and columns were washed with buffer BW (600 ul) and centrifuged at 14000 rpm for 2 minutes. This step was repeated three times. The columns were again washed thoroughly (three times) with buffer TW (700 ul) and centrifuged at 14000 rpm for 2 minutes. Supernatants were discarded and the

columns were then transferred into new collection tubes. The columns in a new

collection tube were centrifuged at full speed to remove excess residual wash

buffer. Elution buffer (100 ul) was added into the column and incubated for 5

minutes before spinning at 14000 rpm for1 minute. The quality and quantity of

DNA extracted were assessed using the NanoPhotometer UV/Vis

spectrophotometer. DNA then was run on the agarose gel. Buffer used consisted of

1x TAE (Thermo Fisher Scientific, USA). Digested DNA was mixed with 1ul of

6x loading dye (Thermo Fisher Scientific, USA) and loaded into the wells then run

on the agarose gel for 45 minutes at 80V, using 1kB DNA ladders (Thermo Fisher

Scientific, USA) as markers. Post run, the agarose gel was stained in 3 x GelRed

solutions (Biotium, USA) for 15 minutes and visualised using the molecular

imager, BioSpectrum Imaging System under ultraviolet light (UVP LLC, USA).

The A260/280 value for extracted DNA was generally accepted in the range of

1.8-1.9. Extracted DNA was stored at -20°C if not used immediately.

3.10.2 Microsatellite Instability Analysis

MSI panels were screened by using conventional Polymerase Chain

Reaction (PCR) method through a series of informative microsatellite panel

markers and primers (Bioneer, Korea) as per stated in Table 3.15. This method

allows to distinguish the presence of MSI and LOH. PCR was performed with

Veriti Thermal Cycler (Life Technologies, USA) and the amplification condition

used in this experiment comprised initial denaturation at 94°C for 2 minutes, followed by 30 cycles of denaturation at 94°C for 30 seconds with annealing at (50-60°C) for 30 seconds, extension at 72°C for 60 seconds and final extension at 72°C for 5 minutes. PCR reaction components (Thermo Fisher Scientific, USA) were prepared for one reaction (20ul/tube) shown in Table 3.16. The PCR products were mixed with 6x loading dye (Thermo Fisher Scientific, USA) at 1:1 ratio were loaded into the wells then ran on 8% polyacrylamide gel (PAGE) for one hour and ten minutes at 120V, using 100bp DNA ladders (Thermo Fisher Scientific, USA) as markers. Post run, the polyacrylamide gel was stained in 3 x GelRed solutions (Biotium, USA) for 15 minutes and visualised using the molecular imager, BioSpectrum Imaging System under ultraviolet light (UVP LLC, USA).

3.15: MSI panel markers: Primers

MSI PANELS	PRIMERS
1. BAT 25	Forward: TCGCCTCCAAGAATGTAAGT
	Reverse: TCTGCATTTTAACTATGGCTC
2. BAT 26	Forward: TGACTACTTTTGACTTCAGCC
	Reverse: AACCATTCAACATTTTTAACCC
3. D2S123	Forward: AAACAGGATGCCTGCCTTA
	Reverse: GGACTTTCCACCTATGGGAC
4. D5S346	Forward: ACTCACTCTAGTGATAAATCGGG
	Reverse: AGCAGATAAGACAGTATTACTAGTT
5. D17S250	Forward: GGAAGAATCAAATAGACAAT
	Reverse: GCTGGCCATATATATATTTAAACC
6. D3S192	Forward: GAGCATAAAACTTGGGGATT
	Reverse: ATCTAGGTTAAACTGGGTGCTT
7. D3S966	Forward: AGGACCCAAACTAAGACAAGTA
	Reverse: CTGTGTCCTTCAAACAAAC
8. D3S647	Forward: TGGACACATACAGTTACACACA
	Reverse: GGGGTGTGAATTATATGAAGAG
9. D3S1228	Forward: TTAGTTCAGCTGTGGATGTAAC
	Reverse: ACTCCTGAGAATTGTAGGAAAG
10. D3S659	Forward: AACCTAAGTCTGTTTCAACCAC
	Reverse: AGTTTATCCTGCAAGGTCTGT

Table 3.16: PCR Reaction components

COMPONENTS	STOCK CONC.	WORKING CONC.	PER/TUBE (UL)
Taq Buffer	10x	1x	2
MgCl$_2$	25mM	4mM	3.2
Primer - Forward	10uM	0.5uM	1
Primer - Reverse	10uM	0.5uM	1
DNTPs	20mM	0.5mM	0.5
Taq Polymerase	5U/ul	0.05 U/ul	0.2
DNA	50ng/ul	50ng/ul	1
ddH20	-	-	11.1
Total			**20**

3.11   Global DNA Methylation Screening

The MethylFlash Methylated DNA Quantification Kit (Colorimetric) (Epigentek, USA) was used to quantify the global DNA methylation in parental H103 and the generated iPSCs. This assay was carried out according to the manufacturer's protocol whereby extracted genomic DNA was added onto the treated strip wells, followed by the addition of capture antibody reagents. Upon thorough washing steps, detection antibody reagents and enhancer solution were added in the later part. Final step involves addition of colour developing solution and reading the absorbance in a microplate spectrophotometer at 450 nm.

CHAPTER 4

RESULTS

4.1   Characteristics of Human Oral Squamous Cell Carcinoma

4.1.1   Microscopic Observation of OSCC Cell Lines

H103 cell line is a human oral squamous cell carcinoma line which was established from the tongue area of a 32-year old male patient with a tumour of < 20mm in size. This cell line was characterised as grade I cancer, a well - differentiated and node-negative tumour. The population of the cells was adherent to the tissue flasks and morphologically homogenous in culture with polygonal like appearance. H103 cells show proliferation and reached 70% - 80% confluency in two to three days of culture.

H3736 cell line is a human oral squamous cell carcinoma line, which was established from the floor of mouth (FOM) area of a 40-year old female patient with a tumour of 20-40mm in size. This cell line was characterised as grade III cancer, a well-differentiated and node-positive tumour and is more aggressive than H103. The population of the cells was adherent to the tissue flasks and

morphologically homogenous in culture similar to that of H103, with polygonal like appearance. H376 cells show proliferation and reached 80% - 90% confluency in two to three days of culture (Figure 4.1).
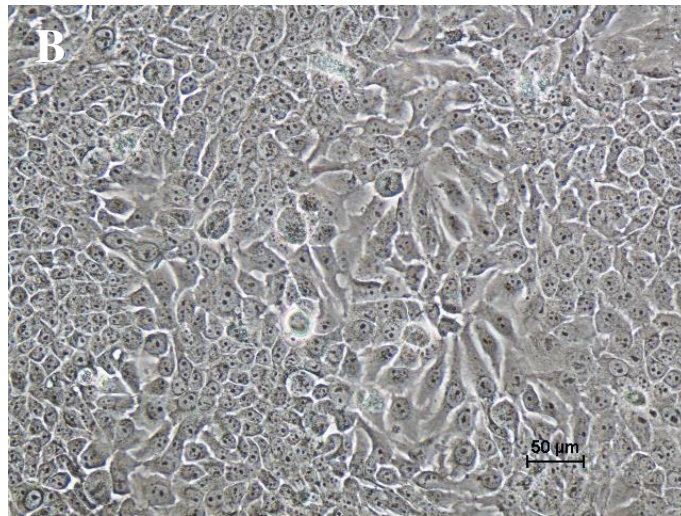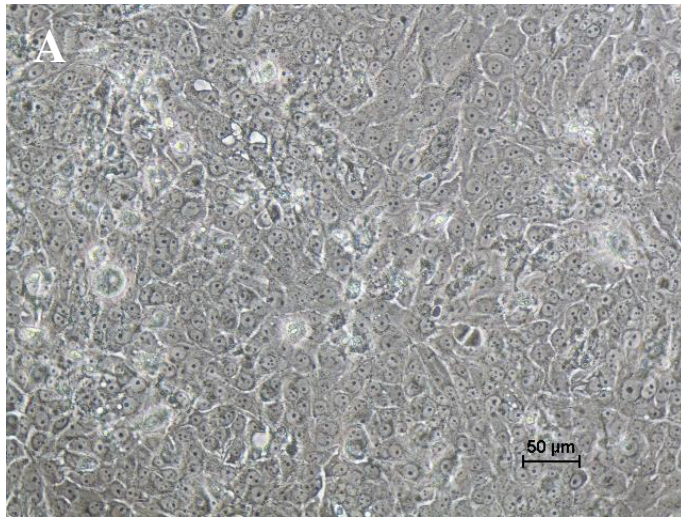
Figure 4.1 Adherent Oral Squamous Cell Carcinoma (OSCC) cells at 80% confluency. (A) Well-differentiated Grade I - H103 displayed polygonal morphology and originated from squamous cell carcinoma (SSC) of the tongue. (B) Well-differentiated Grade III – H376 displayed polygonal morphology and originated from the floor of the mouth. Nikon inverted microscope, magnification: 20x.

4.1.2 Microscopic Observation of Human Embryonal Kidney Cells (293FT)

293FT cells are ideal for generating high-titer viral stock for transfection, earlier isolated from human embryonal kidney cells transformed with SV40 large T antigen. This cell line yielded fast growing cells, which were adherent to the culture flasks but might detach easily if not healthy. Morphology of 293FT cells showed a mixture of endothelial, epithelial and fibroblast-like cells as the cell line was derived from the embryonic kidney. 293FT cells proliferated slowly upon thawing but tended to grow fast after two to three passages and reached 80% - 90% confluency in one to two days of culture (Figure 4.2).

4.1.3 Microscopic Observation of Mouse Embryonic Fibroblast Cells (MEF)

Mouse Embryonic Fibroblast cells are primary cells isolated from 12.5 to 13.5 postcoitum mouse embryos. The embryos are well dissociated and trypsinised into single suspension cells prior to storage in liquid nitrogen. MEF cells are crucial in ESCs culture as they prevent differentiation of ESCs. Yet, MEF cells are inactivated with Mytomycin-C or irradiated prior to use as feeder cells as to prevent the dilution of ESCs with dividing fibroblast cells. MEF proliferation reached 70% - 80% confluency in three to four days of culture (Figure 4.3).
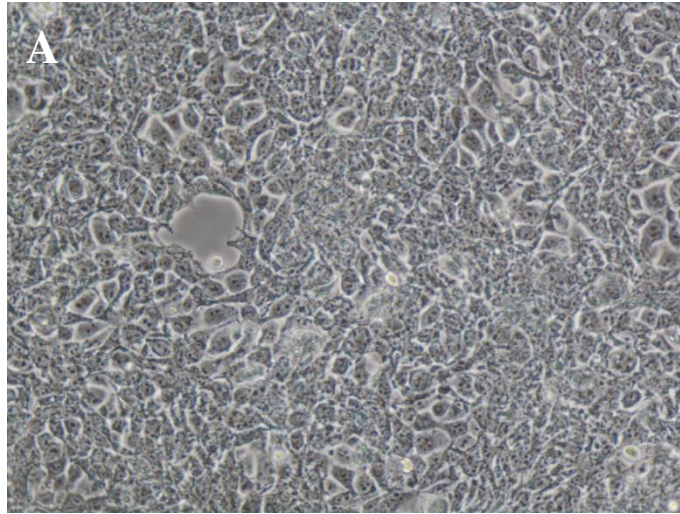
Figure 4.2 Adherent 293FT cell line at 60-70% confluency. (A) Displayed epithelial morphology and originated from tissues of embryonic kidney. Nikon inverted microscope, magnification: 20x.
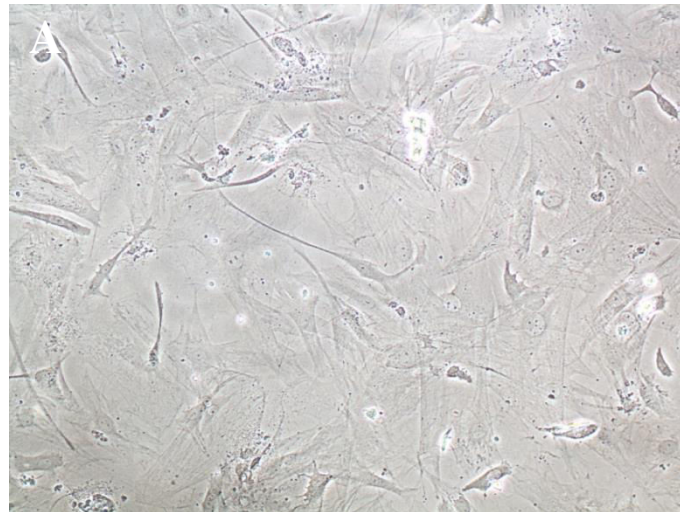
Figure 4.3 Adherent MEF cell line at 60-70% confluency. (A) Mouse Embryonic Fibroblast feeder cells for culturing pluripotent stem cells, mitotically arrested by irradiation and unable to proliferate. Nikon inverted microscope, magnification: 20x.

4.1.4   Microscopic Observation of Embryonic Stem Cells BG01 (ESCs)

ESCs derived from embryos at the blastocyst stage. Morphology of ESCs is characterised by the presences of clear borders from the MEF feeder layer, consisting of small rounded cells with spaces between cells and large nuclei with distinguished nucleoli. Passaging ESCs took five to seven day to form a colony (Figure 4.4).
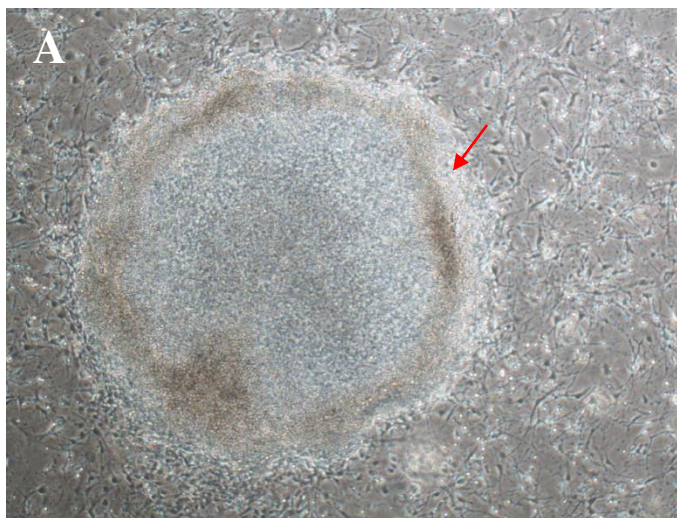
Figure 4.4 BG01 Embryonic Stem Cells attached to the MEF feeder layer. (A) ESC displayed a typical defined borders state (marked with *red arrow*) on feeders and contained small round cells with large nuclei and notable nucleoli. Nikon inverted microscope, magnification: 4x.

4.2 Transfection Efficiency via Green Fluorescent Protein (pMX-GFP)

4.2.1 Transfection Efficiency of 293FT Cell Line

GFP transfection serves as an internal control for transfection efficiency in target cells. Transfection was achieved in 293FT cell line by transfecting a positive control vector pMX-GF (3µg), that encodes the green fluoresecent protein signal into 4.5×10^6 293FT cell (70% – 80% confluency). Furthermore, negative control was performed to assess the potential influence of transfection on the viability of 293FT cells. GFP expression was successfully achieved at 48 hours and fluorescent signals were analyzed using Zeiss Imager A.1 Fluorescence Microscope (Figure 4.5).

4.2.2   Transduction of H103 and H376 Cell Lines with pMX-GFP

Transduction was achieved in both H103 and H376 cell lines with vector pMX-GF (3µg), that encodes the green fluoresecent protein signal into 7.0×10^5 cells (70% – 80% confluency) (Figure 4.6) (Figure 4.7). Transduction via GFP expressions was detected in H103 and H376 at 48 hours confirming the uptake of transgenes. Transduction efficiency of 75.50% ± 1.52 was achieved in H376 cell line compared to H103 which achieved a lower level of 38.20% ± 0.60 (Figure 4.8). Negative control was performed to assess the potential influence of

transfection on the viability of the cells. GFP expressions via fluorescent signals were analysed using Zeiss Imager A.1 Fluorescence Microscope.
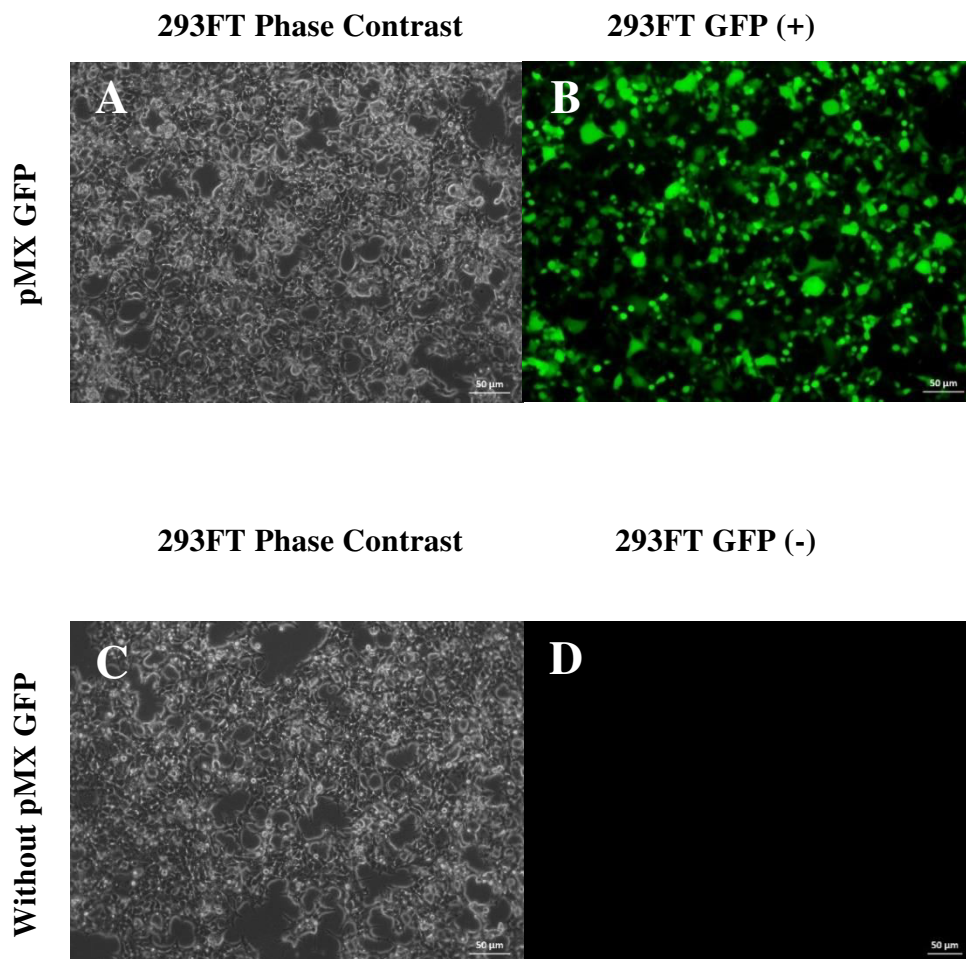
Figure 4.5 Post-transfection of 293FT at 48 hours. (A-B) 293FT cells transfected with retro - pMX GFP plasmid served as positive control. (C-D) Transfection of 293FT cells without retro-pMX GFP used as negative control. Zeiss Axiovert inverted microscope, magnification: 10x.

H103 Phase Contrast   **H103 GFP (+)**

H103 Phase Contrast   **H103 GFP (-)**
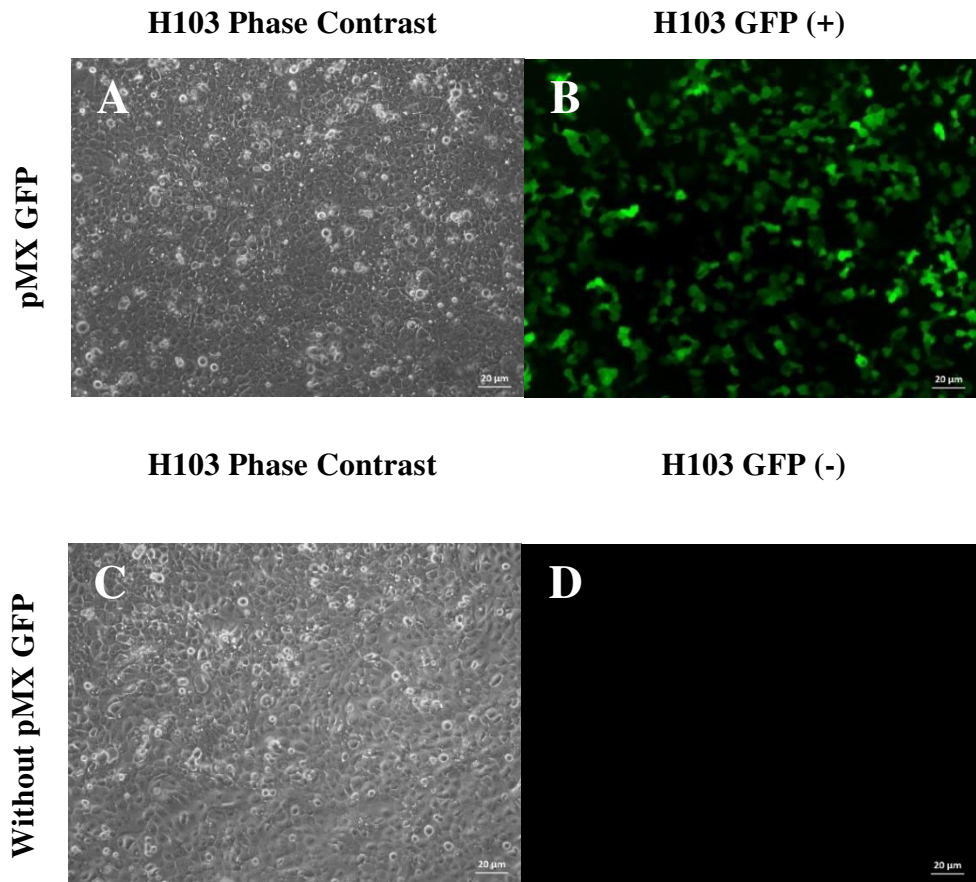
Figure 4.6 Post-transduction of H103 at 48 hours. (A-B) H103 cells transduced with retro - pMX GFP plasmid. GFP signals expressed at 48 hours. (C-D) Transfection of H103 without retro-pMX GFP used as negative control. Zeiss Axiovert inverted microscope, magnification: 20x.

H376 Phase Contrast   **H376 GFP (+)**

H376 Phase Contrast   **H376 GFP (-)**
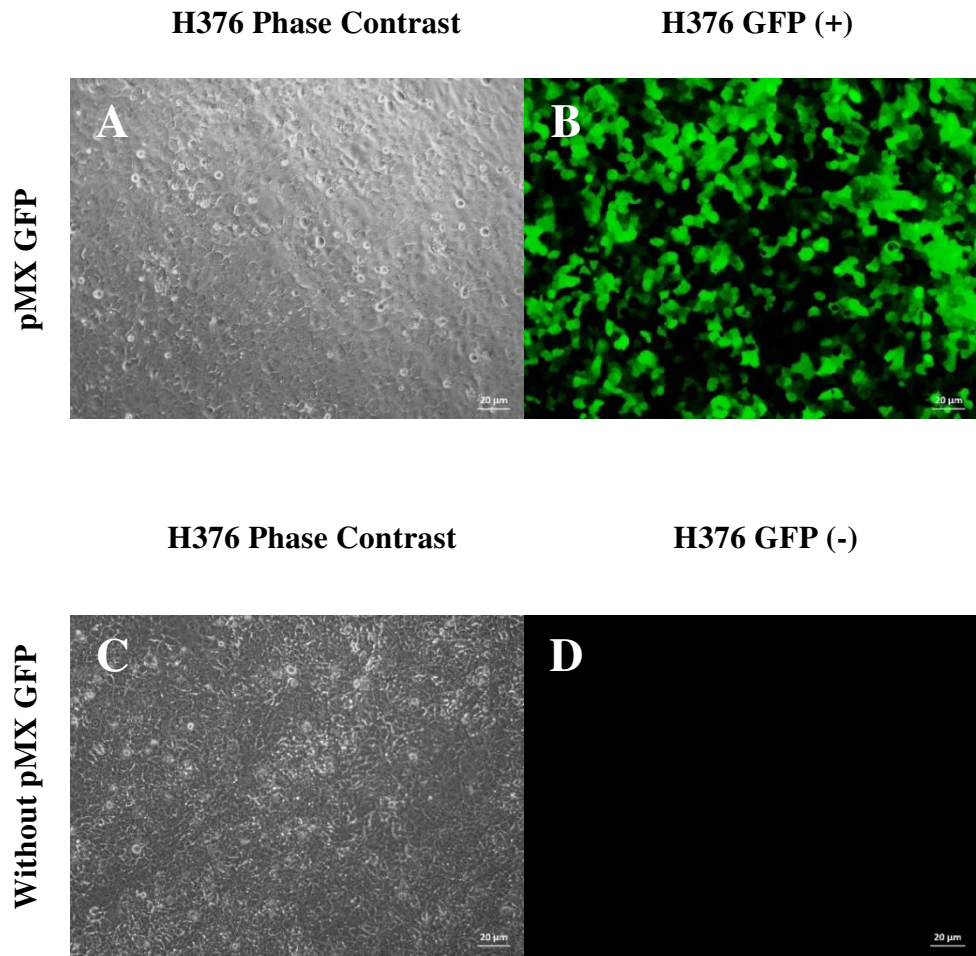
Figure 4.7 Post-transduction of H376 at 48 hours. (A-B) H376 cells transduced with retro - pMX GFP plasmid. GFP signals expressed at 48 hours. (C-D) Transfection of H103 cells without retro-pMX GFP used as negative control. Zeiss Axiovert inverted microscope, magnification: 20x.
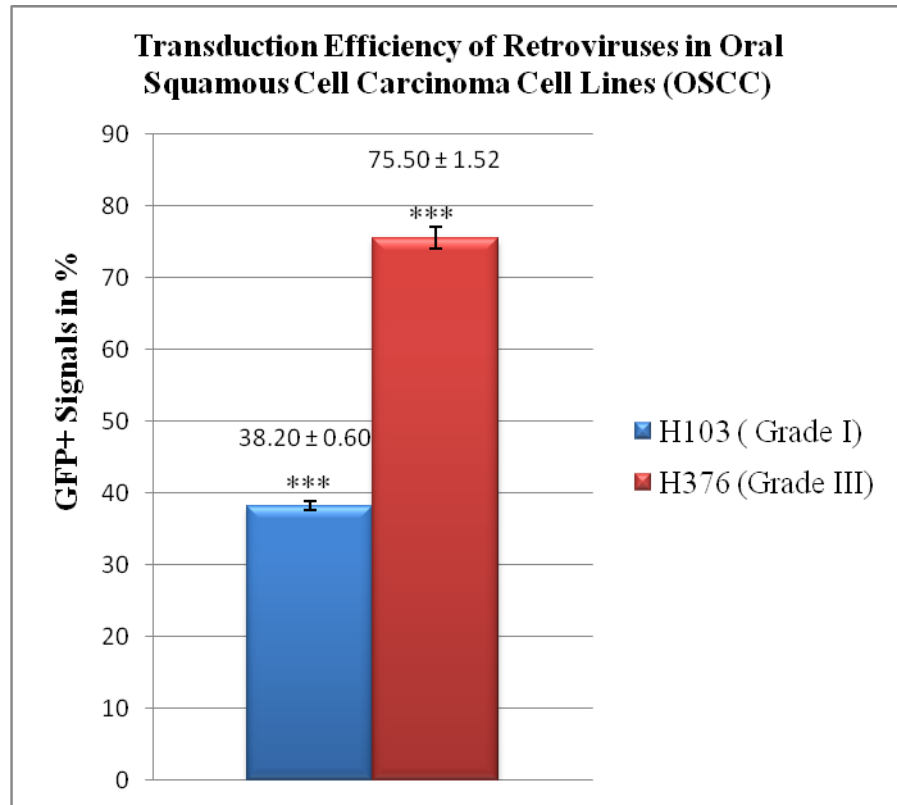
Figure 4.8 Transduction efficiency of OSKM in H103 and H376.
Data are expressed as mean ± standard deviation (SD). Statistical differences are indicated *** for P<0.001 using Student t-test.

4.3   Transduction with Plasmid OSKM

4.3.1   Transduction of H103 and H376 Cell Lines with Pasmid OSKM at 48 Hours Post-Transduction

Both H103 and H376 were transfected with plasmids encoding pluripotent genes (Oct4, Sox2, Klf4 and c-Myc). After Forty-eight hours post-transduction, distinct morphological changes were observed. Transduced cells showed higher number of cell death and were morphologically unhealthy. Positive control and negative control set of transduction were shown in Figure 4.9.

4.3.2   Transduction of H103 and H376 Cell Lines with Plasmid OSKM at Day 7 Post-Transduction

After 7 days of transduction, transduced H103 and H376 cell lines were grown on MEF feeder layer. Human Embryonic Stem Cells (hESCs) specific medium were changed every day and morphological changes were observed using an inverted microscope. Small colonies tended to form from small clumps with disorganized morphologies distinct from the control cells or non-transduced cells. (Figure 4.10).

4.3.3 Transduction Outcome in H103 and H376

First clone was successfully derived from both reprogrammed H103 and H376 cell lines. Only H103 clones were able to be passaged above passage 5 while clones derived from reprogrammed H376 did not survive and tended to differentiate at passage 2. Differentiated H376 cells showed disorganized morphology compared to reprogrammed H103 (Figure 4.11). Though, higher number of clones formed from transduced H376 (5.00 ± 1.73) than H103 (2.00 ± 1.00) (Figure 4.12) and higher GFP transfection capacity was achieved in H376, but stable clones were successfully generated only from H103 cell line as clones from this cell line was able to be passaged up to 20 weeks with ESCs like morphology (Figure 4.13).

H103 - Control

Non-transduced

H103 - Retro (OSKM)
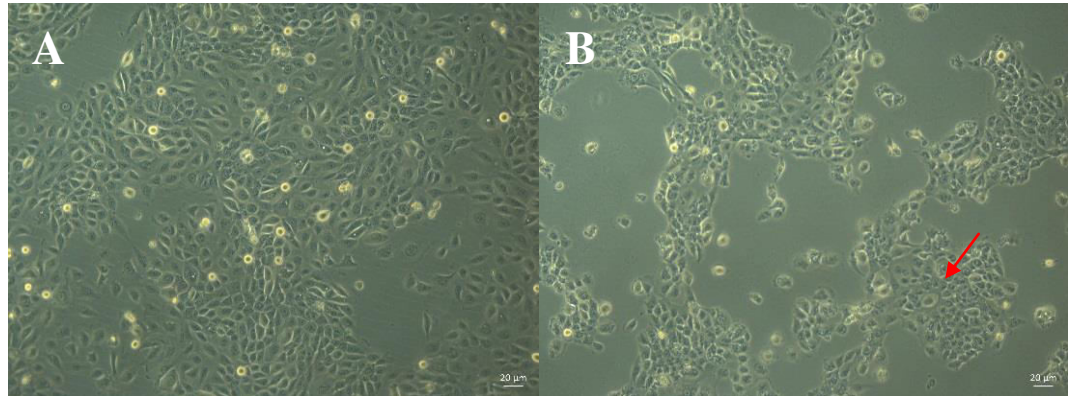
Transduced

H376 - Control

Non-transduced

H 376 - Retro (OSKM)
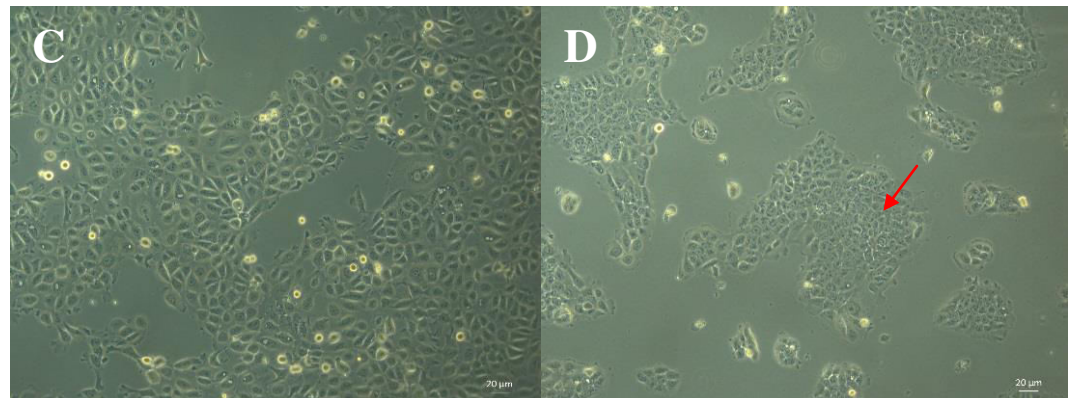
Transduced

Figure 4.9 Post-transduction at 48 hours. (A & C) Both H103 and H376 non-transduced cells showed normal healthy morphology while (B & D) cell death and unhealthy like cells with reduced number of cells observed (marked with *red arrow*) after Retro OSKM transduction. Nikon inverted microscope, magnification: 20x.

H103 - Control

Non-transduced

H103 - Retro (OSKM)

Transduced

H 376 - Control

Non-transduced

H 376 - Retro (OSKM)
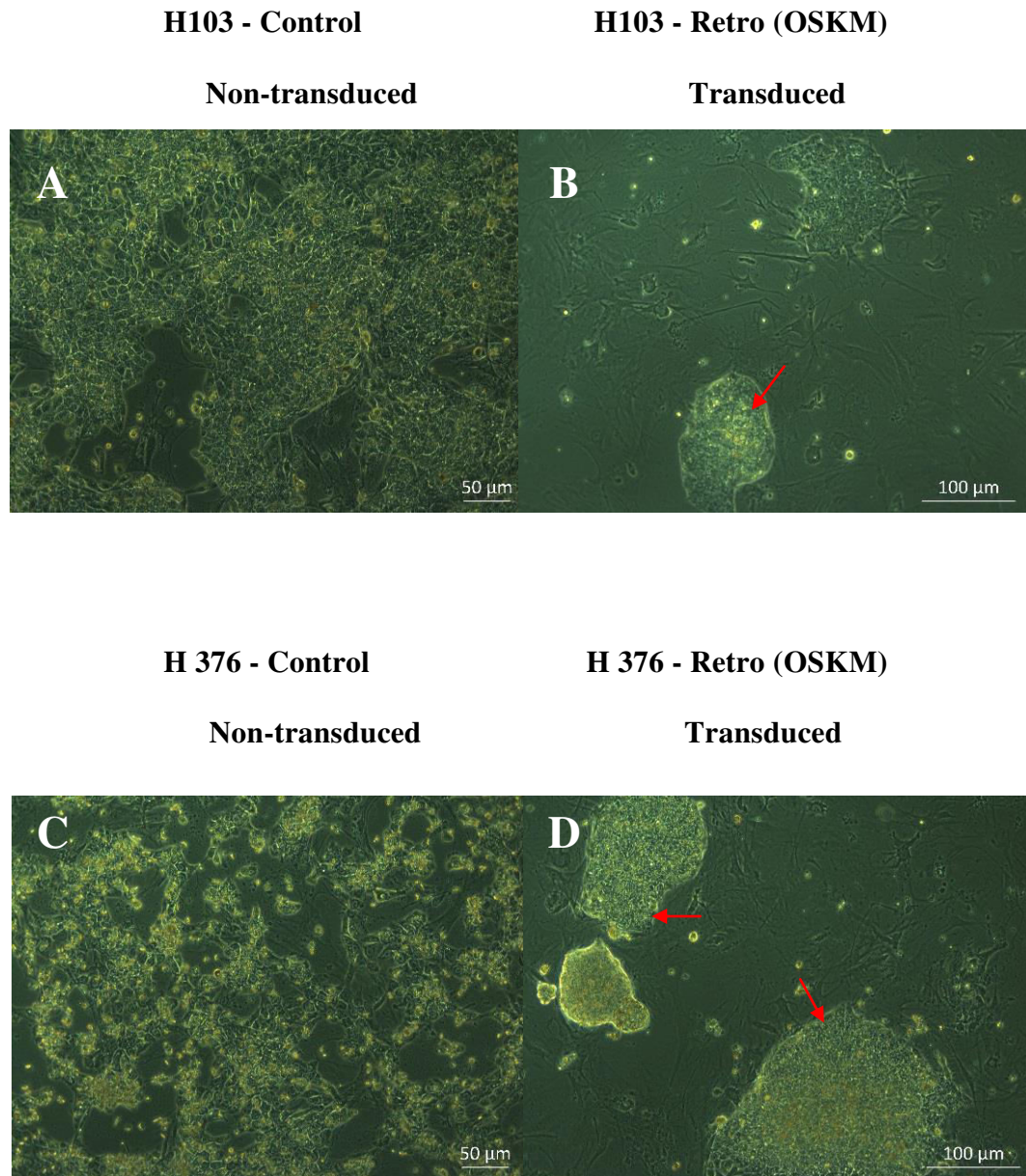
Transduced

Figure 4.10 Post-transduction at day - 7. (A& C) Both H103 and H376 non-transduced cells, continuously proliferate in hESC medium.(B & D) Small colonies resulting from small clumps with disorganized morphology (marked with *red arrow*) but distinct from the control cells. Nikon inverted microscope, magnification: 10x.
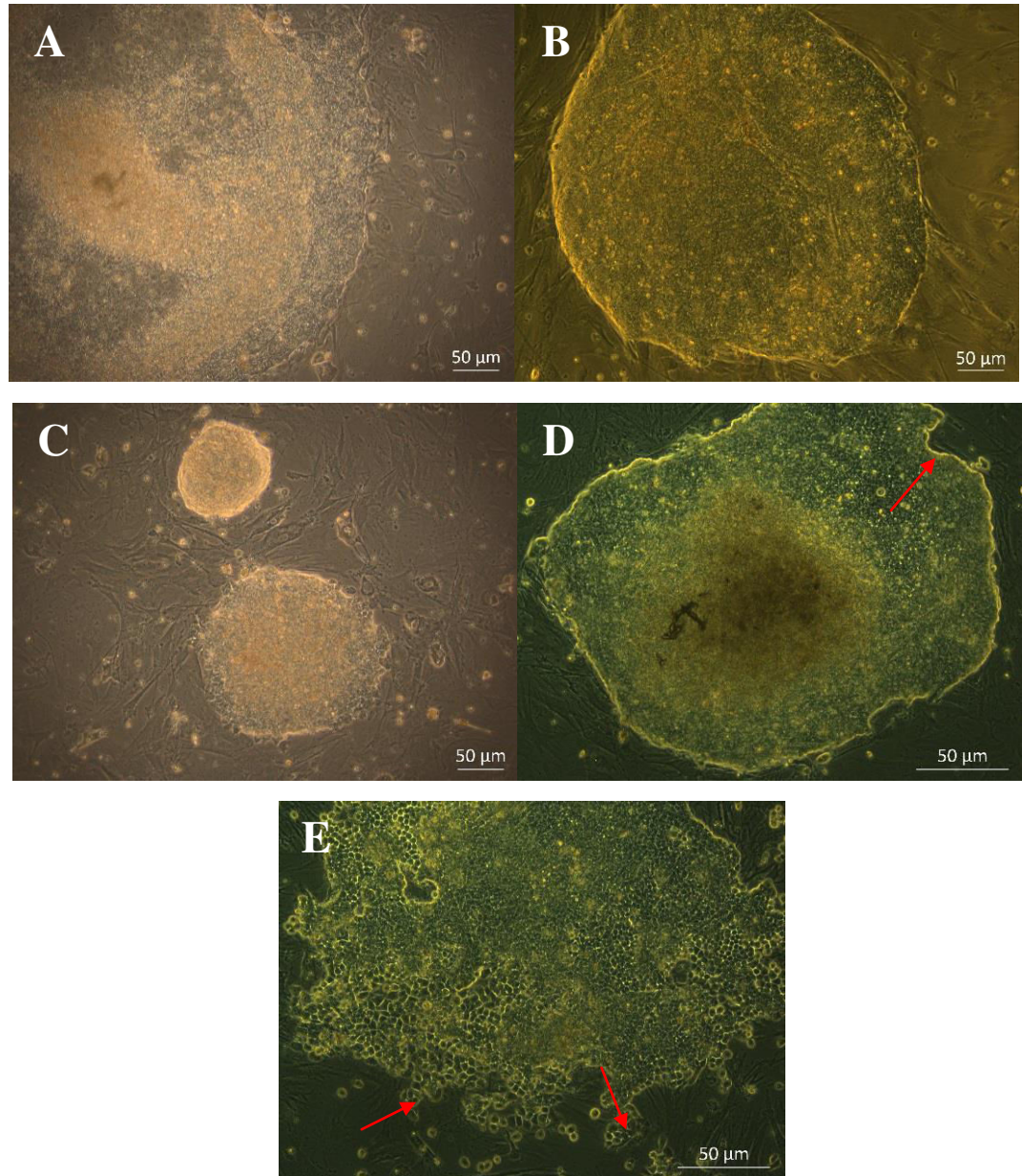
Figure 4.11 Emergence of clones at day 15. (A) First clone derived from reprogrammed H103. (B) Stable clone of reprogrammed H103 confirmed at passage 5. (C) First clone derived from reprogrammed H376, which did not survive the following passage. (D) Clone of reprogrammed H376 with disorganized morphology at passage 2 and its (E) differentiated state (marked with *red arrow*). Nikon inverted microscope, magnification: 10x.
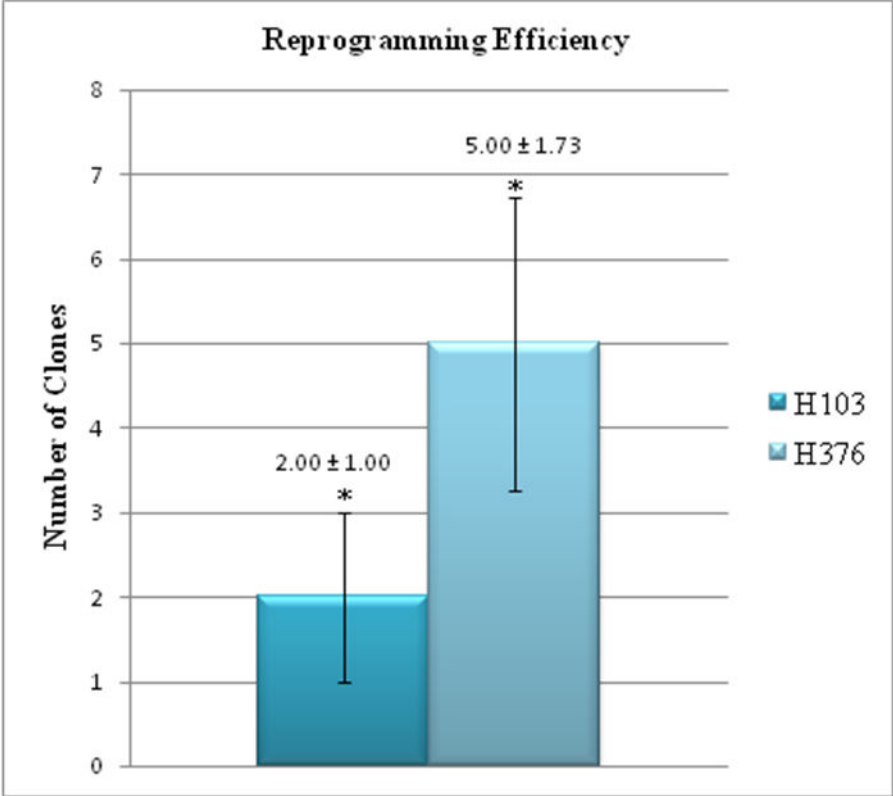
Figure 4.12 Reprogramming efficiency in H103 and H376. Data are expressed as mean ± standard deviation (SD). Statistical differences are indicated with * for P<0.05 using Student t-test.

4.4   Established Pluripotent Stem Cells from H103 Cell Line

4.4.1   H103 Derived Induced Pluripotent Stem Cells

Figure 4.13 showed representative images of reprogrammed cells at passage 10, passage 15 and passage 20. All derived clones resembled the morphology of ESCs with clear borders on mouse embryonic fibroblast feeder layer and consisted of high nucleus:cytoplasm ratio. The morphology of derived pluripotent stem cells is highly distinct from their parental cells and the clones had small cell size with spaces between them.
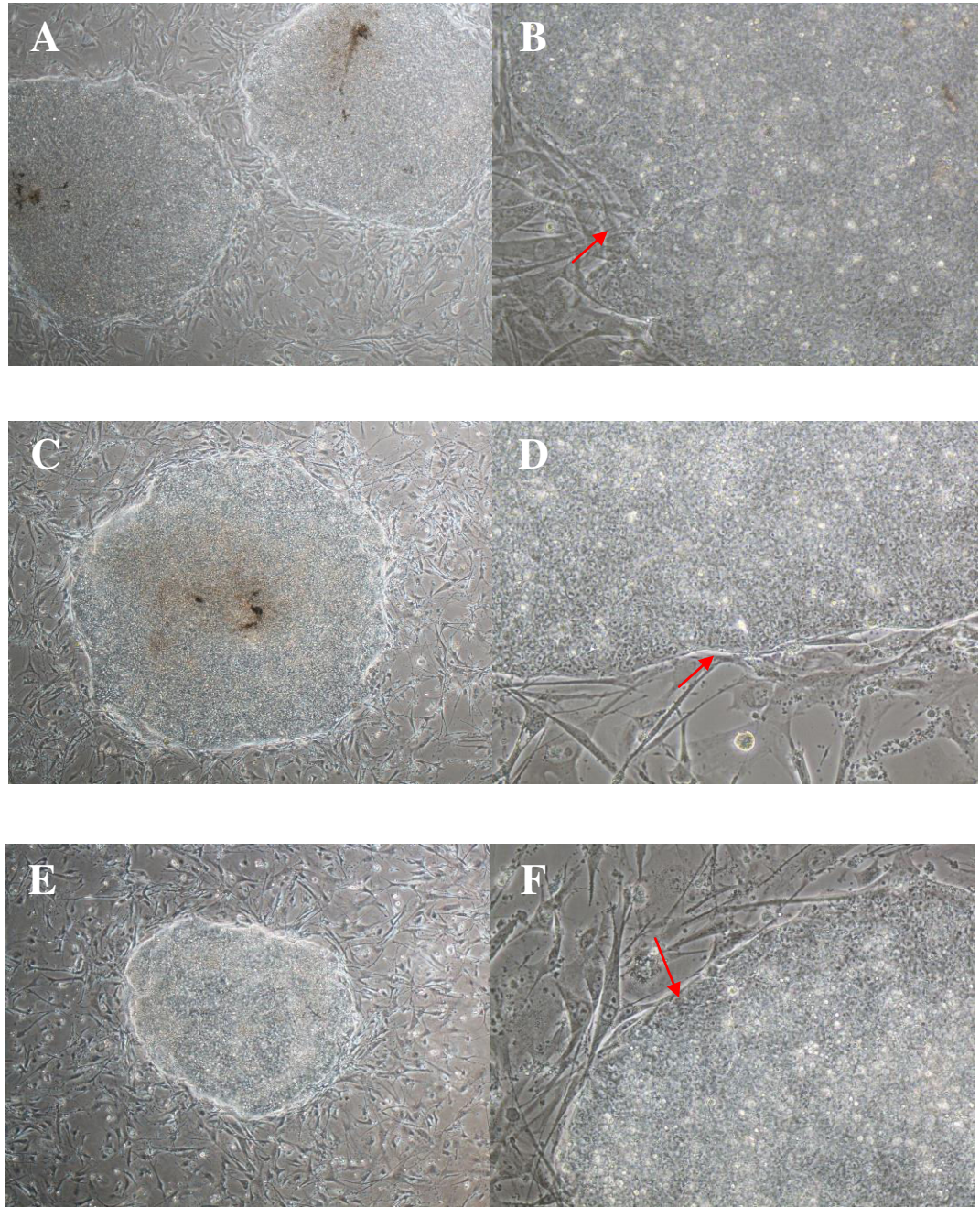
Figure 4.13 Established reprogrammed H103 cells from passage 10 (A-B), 15 (C-D) and 20 (E-F). A-F showed representative images of reprogrammed H103 cells exhibiting ESCs morphologies. (*Red arrows*) indicate the clear borders of reprogrammed colonies from H103. Nikon inverted microscope, magnification: 10x and 20x (B,D, F).

4.5   Differential mRNA Expression of Vector OSKM

4.5.1   mRNA Expression of Vector OSKM in Reprogrammed H103 and H376 Cell Lines

Expressions of mRNA were assessed in both reprogrammed H103 and H376 cells . Higher level of expressions of Oct4, Sox2 and Nanog were achieved in reprogrammed H103 cells compared to reprogrammed H376 cells. However, the suppression of Klf4 and c-Myc were shown in both reprogrammed cell lines.

In reprogrammed H103 cells of passage 5 and passage 10 against their parental counterparts, the fold changes were calculated by $\Delta\Delta\ C_T$ method between parental cells against two different passage of reprogrammed H103 were shown in details in Appendix L. Messenger RNA (mRNA) expressions of pluripotency genes were all relative to that of the parental. The real time PCR data in Figure 4.14 showed down-regulation of Oct4 expression at passage 5 but increased to 2.48 fold change at passage 10. While, Sox2 expression showed gradual up-regulation at passage 5 with 55.1 fold change and passage 10 with 77.11 fold change. Oncogenic Klf4 gene expression was down regulated upon reprogramming at passage 5 and passage 10 and similar patterns were observed in c-Myc gene expression. Nanog expression were up-regulated gradually at passage 5 with 2.84 fold change and passage 10 with 7.07 fold change. A decrease in fold

change was observed in Klf4 and c-Myc expressions against their parental counterparts indicates loss of oncogenic specific genes upon reprogramming.

The fold changes were also calculated by $\Delta\Delta\ C_T$ method between parental cells and two different passage of reprogrammed H376. The real time PCR data also showed down-regulation of Oct4 expression at passage 5 with 0.23 fold change and passage 10 with 1.07 fold change. Up-regulation of Sox 2 increased gradually from passage 5 to passage 10 but no change in oncogenic gene of c-Myc was observed. An increase in Klf4 expression was observed from 0.32 fold change at passage 5 to 0.53 at passage 10. Expression of c-Myc was almost not detected with 0.07 fold change at passage 5 and 0.01 at passage 10. As for Nanog expression, passage 5 showed very low expression that of H103, with 0.56 fold change relative to parental H376 but an increase of at 1.86 fold change was observed at passage 10.

On the whole, Nanog expression was known as the master pluripotent gene and appeared crucial to establish sustainable pluripotency in reprogrammed cells. Nanog expression was found progressively increased from passage 5 to passage 10 in reprogrammed H103, but for reprogrammed H376, Nanog expression was found reduced at passage 5 and showed little increase subsequently at passage 10. This pattern of Nanog expression may explain the failure to sustain pluripotency on passaging in H376 cells.

Parental H103 Against Reprogrammed Counterparts at P5 and P10
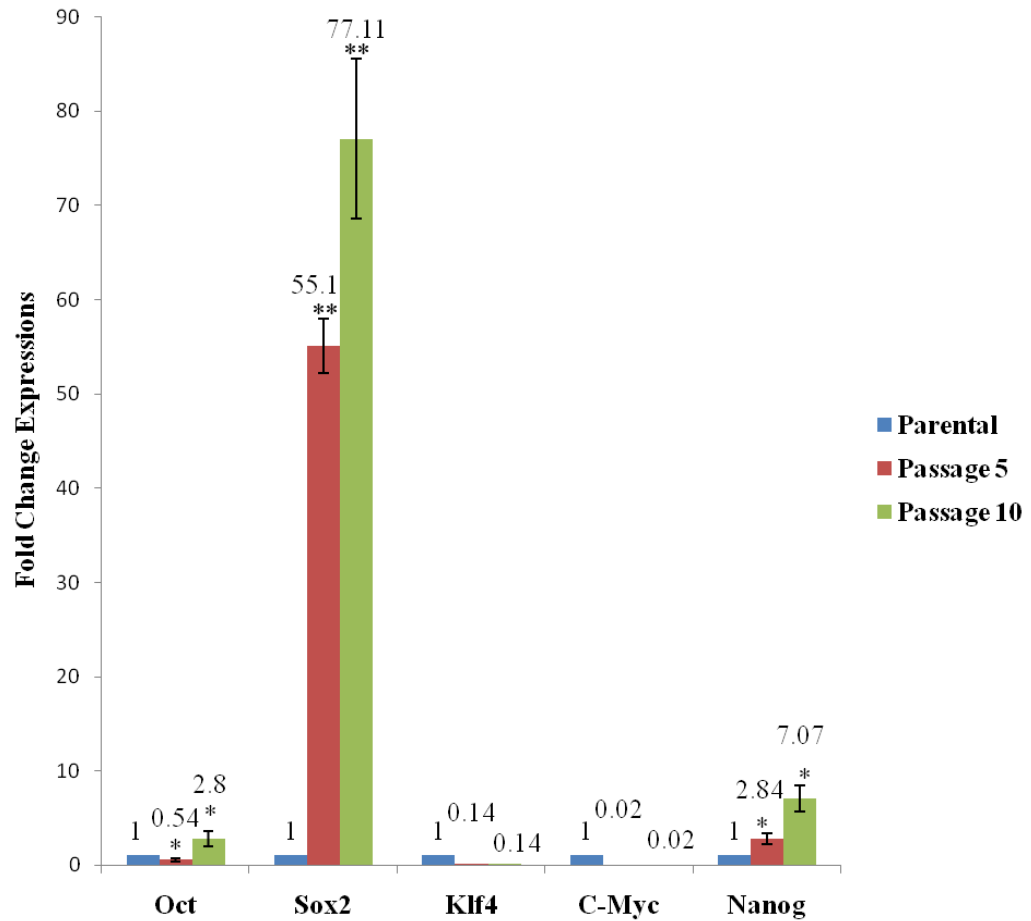
4.14 *In-Vitro* **mRNA expression of pluroipotent genes in reprogrammed H103 Relative to Parental (n=3).** Data presented as mean ± SEM. Statistical differences are indicated with * for $P<0.05$, ** for $P<0.01$ and *** for $P<0.001$ using paired t-test.

Parental H376 Against Reprogrammed Counterpart at P5 and P10
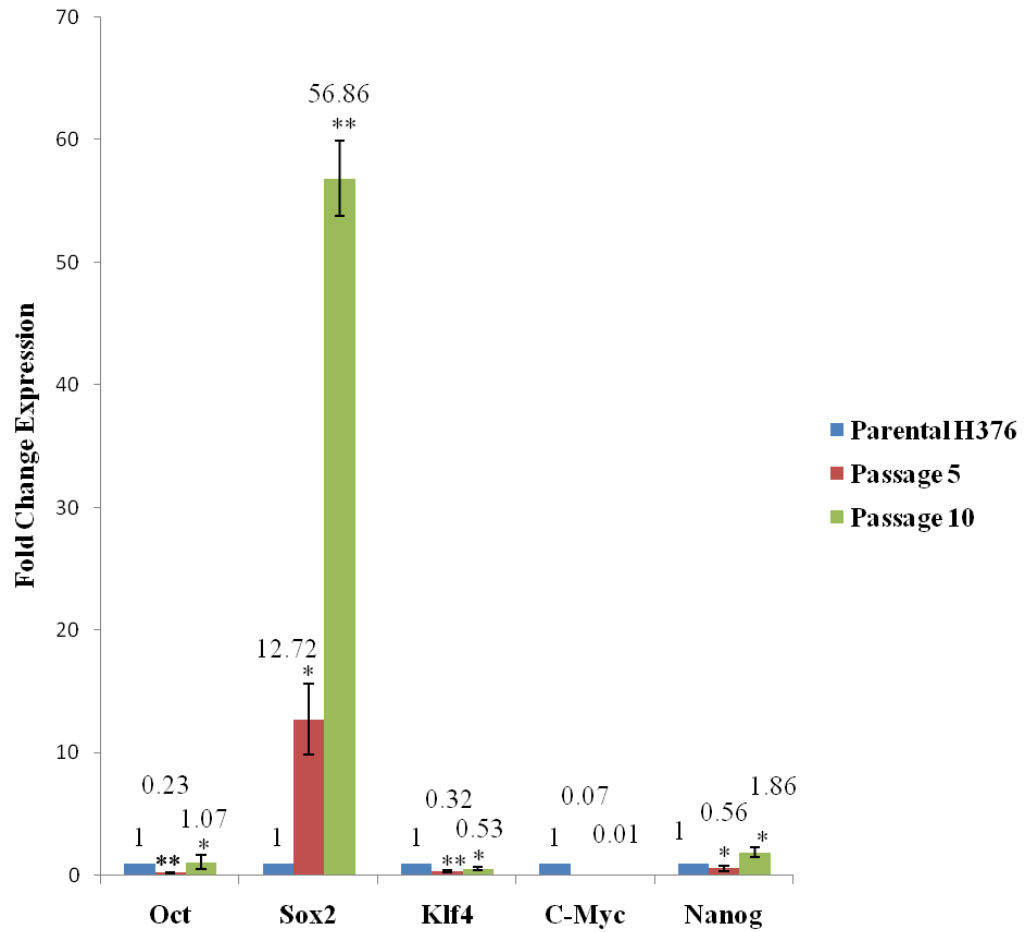
4.15 *In-Vitro* mRNA expression of pluripotent genes in reprogrammed H376 Relative to Parental (n=3). Data presented as mean ± SEM. Statistical differences are indicated with * for P<0.05, ** for P<0.01 and *** for P<0.001 using paired t-test.

4.6   Protein Expression of Pluripotency Markers

4.6.1 Protein Expression of Pluripotency Markers in Stable H103 Derived

   Pluripotent Stem Cells

Presence of distinct intracellular and extracellular pluripotency expressions (Oct4, Sox2, Nanog and Tra-1-60) were observed in stable reprogrammed H103 but none in parental H103. Distinct differences in protein expression observed between parental and its counterparts. Figure 4.16 and 4.17 shows the staining results of parental and the reprogrammed H103 cells.
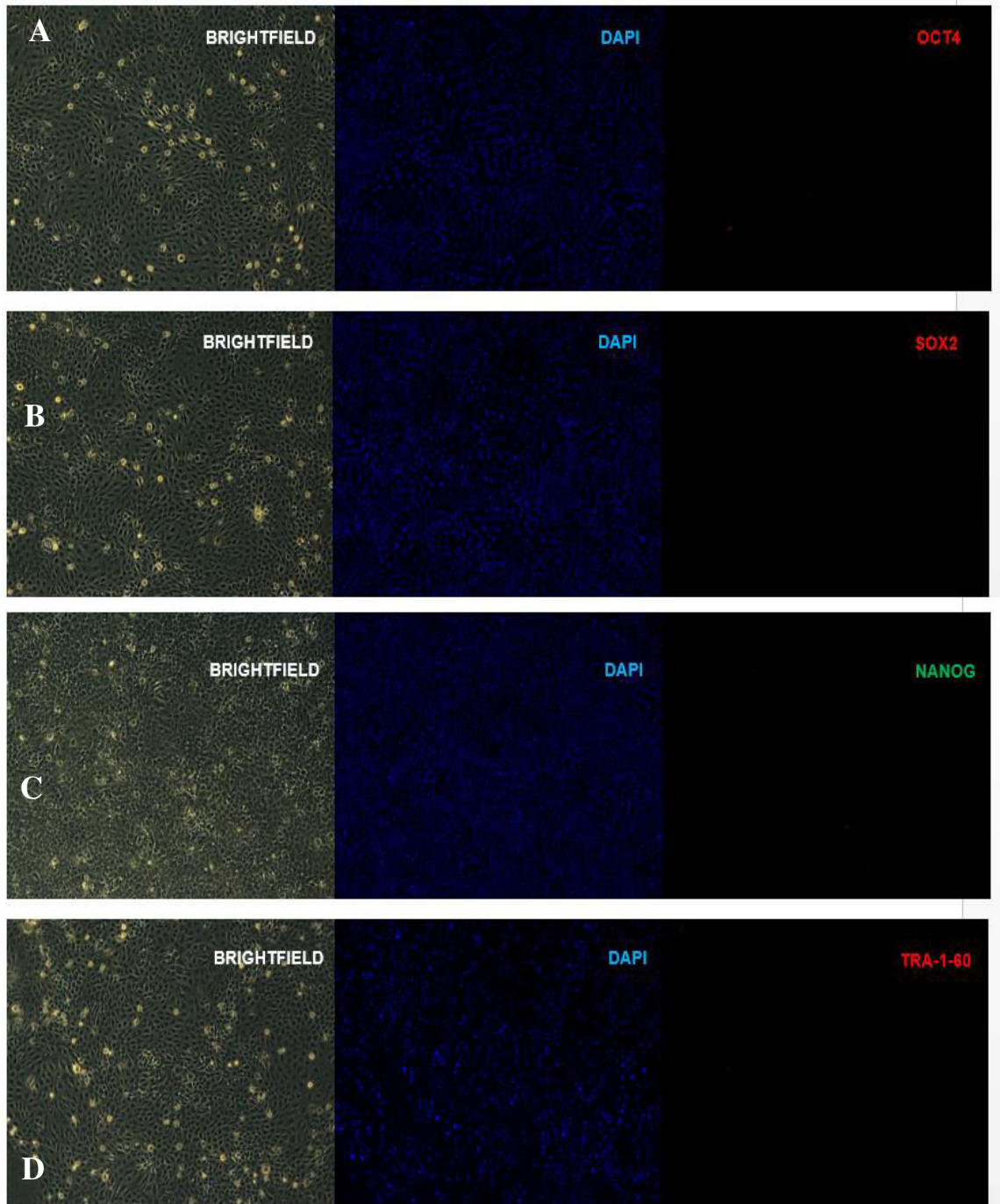
Figure 4.16 Immunofluorescence (IF) staining of parental H103 cells. (A-D) Representative images of parental H103 cells stained for pluripotency markers: Intercellular markers (Oct4, Sox2, Nanog) and Intracellular marker (Tra-1-60). Pluripotency expressions were not detected in parental H103. Nikon inverted microscope, magnification: 10x.
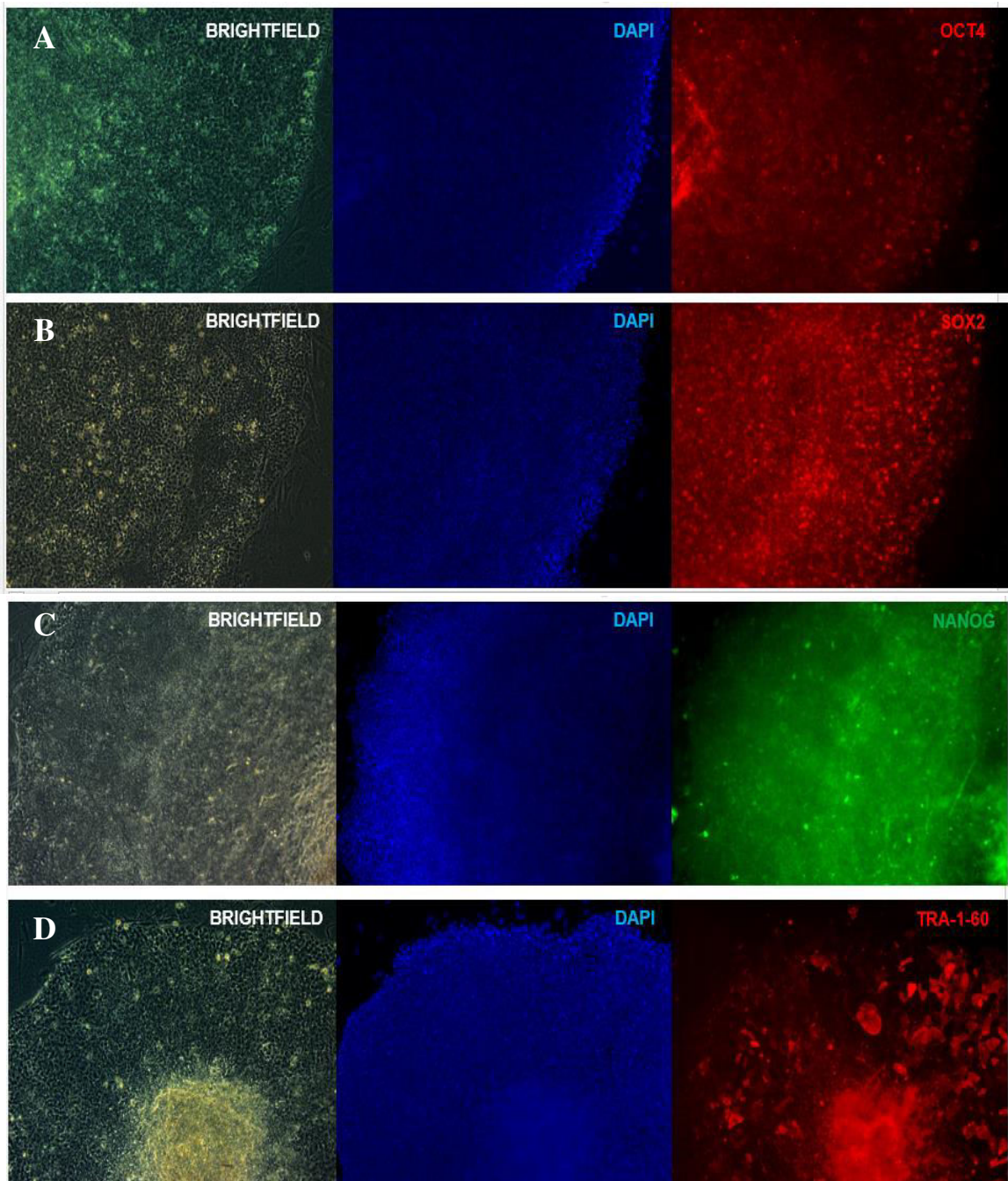
Figure 4.17 Immunofluorescence (IF) staining of reprogrammed H103 cells. (A-D) Representative images of parental H103 cells stained for pluripotency markers: Intercellular markers (Oct4, Sox2, Nanog) and Intracellular marker (Tra-1-60). Pluripotency expressions were detected in reprogrammed H103. Nikon inverted microscope, magnification: 10x.

4.7   Embryoid Bodies (EB) Formation

Derived pluripotent cells from H103 were able to form embryoid bodies after 8 days in EB specific medium. EB was induced from parental cell line of H103 to serve as control. Reprogrammed H103 showed morphologically compact EB with round border (Figure 4.18). Induced EB was characterised for the presence of three germ layers (endoderm, ectoderm and mesoderm) via immunofluorescence staining.

H103 cell line is derived from both ectodermal and endodermal lineage therefore ectoderm (Figure 19) and endoderm (Figure 20) expressions were detected in EB from parental and reprogrammed cells. However, mesoderm (Figure 21) expression was only detected in EB derived from reprogrammed H103 indicating presence of additional mesoderm lineage upon reprogramming into pluripotent stem cells.

4.8   Directed Differentiation Assay

In order to prove the differentiation potentiality of reprogrammed H103, reprogrammed cells were induced to differentiate into osteocytes and adipocytes. The differentiation potential was characterized for the presence of osteogenic and

adipogenic phenotypes and stained for lineage specific markers after 21 days of incubation.

4.8.1 Osteogenic Differentiation

Alizarin Red S is a standard staining method to identify matrix mineralization or calcium deposits during osteogenic differentiation from mesenchymal stem cells (Birmingham et al., 2012) and embryonic stem cells or pluripotent stem cells (Menendez et al., 2013). This staining detects calcium deposits, but presence of magnesium, manganese, barium, strontium, and iron may take up the staining as well. However, these elements (magnesium, manganese, barium, strontium, and iron) usually do not accumulate in great concentration in tissues to interfere with the staining (Lievremont et al., 1982). Therefore, mineralization during differentiation of reprogrammed H103 into osteocyte like cells is assessed via Alizarin Red S staining. Considering the fact that, endothelial cell death in human tumour results in calcium accumulation, parental H103 cell line (as control) was cultured in osteocytes induction medium. Alizarin red staining was detected in osteogenic induced differentiated reprogrammed H103 after 21 day of incubation but there were no Alizarin red-positive cells detected in the control cultures (Figure 4.22).

4.8.2   Adipogenic Differentiation

Presence of small cytoplasmic lipid droplets in induced adipocytes from pluripotent stem cells is commonly assessed using Oil Red O (Taura et al., 2009). Accumulation of lipids was often detected in diseased epithelial cells (Rizzo et al., 2008).   OSCC H103 cell line used in this study originated from oral epithelial keratinocytes.   Therefore, parental H103 cells (as control) were also cultured in adipocyte induction medium. Tiny vesicles containing lipid droplets were detected in adipocytes derived from reprogrammed H103 cells after 21 day of induction but not in the control cultures (Figure 4.22).
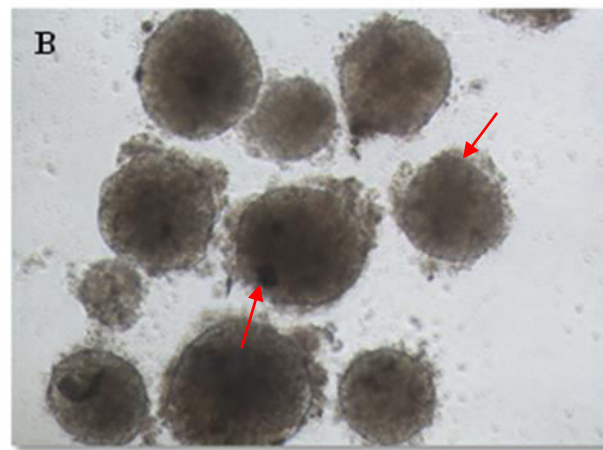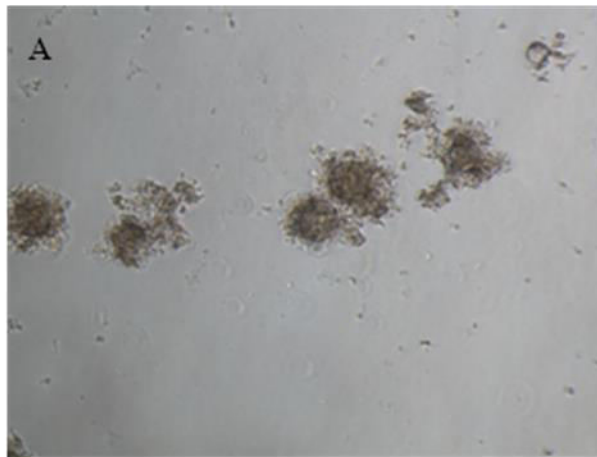
4.18 Embryoid bodies (EBs) formation. Representative images of (A) parental H103-EB and (B) reprogrammed H103-EB. The better organised compact structures with distinct round borders (marked with red arrow) were exhibited by reprogrammed H103-EB. These structures were less distinct in the parental H103-EB. Nikon inverted microscope, magnification:10x

ECTODERM

(A) PARENTAL   (B) H103-IPSCs
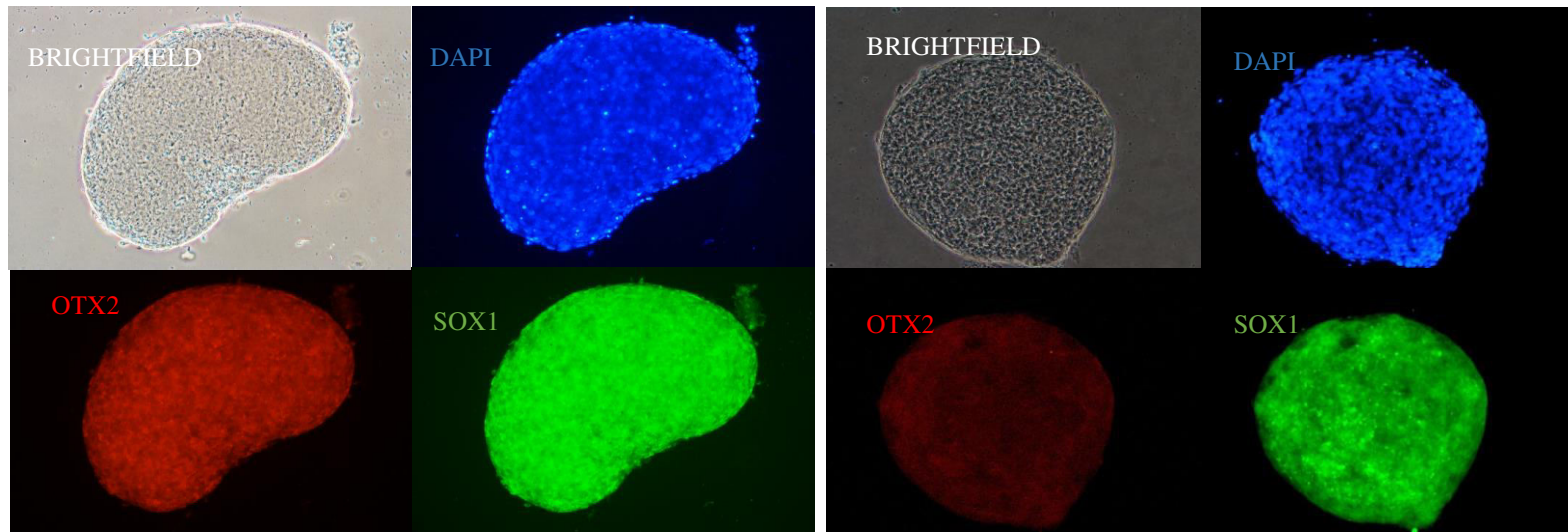
4.19 Immuno-fluorescence (IF) staining of parental H103-EB and reprogrammed H103-EB for ectoderm expression. (A&B) Representative images of parental H103-EB cells and reprogrammed H103-EB stained for ectoderm markers: (OTX2 and SOX1). Ectoderm markers were detected in both parental H103-EB and reprogrammed H103-EB. Nikon inverted microscope, magnification: 10x.

ENDODERM

(A) PARENTAL H103   (B) H103-IPSCs
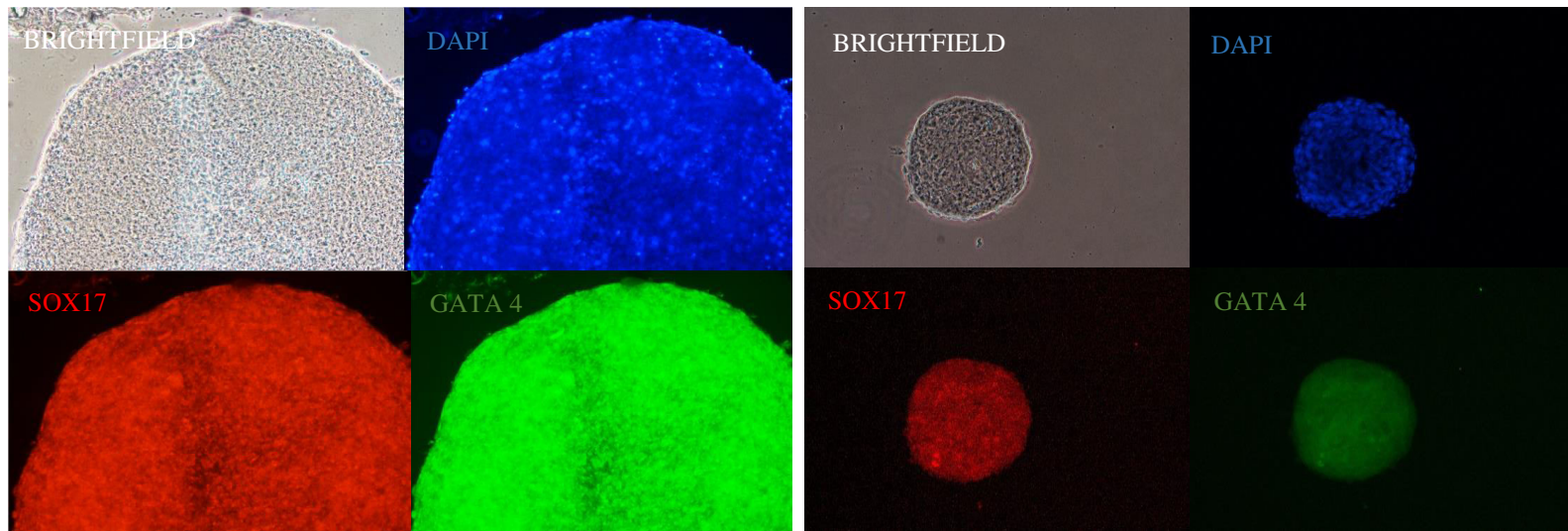
4.20 Immuno-fluorescent (IF) staining of parental H103-EB and reprogrammed H103-EB for endoderm expression. (A&B) Representative images of parental H103-EB and reprogrammed H103-EB stained for endoderm markers: (SOX17 and GATA4). Endoderm markers were detected in both parental H103-EB and reprogrammed H103-EB. Nikon inverted microscope, magnification: 10x.

MESODERM

(A) PARENTAL   (B) H103-IPSCs
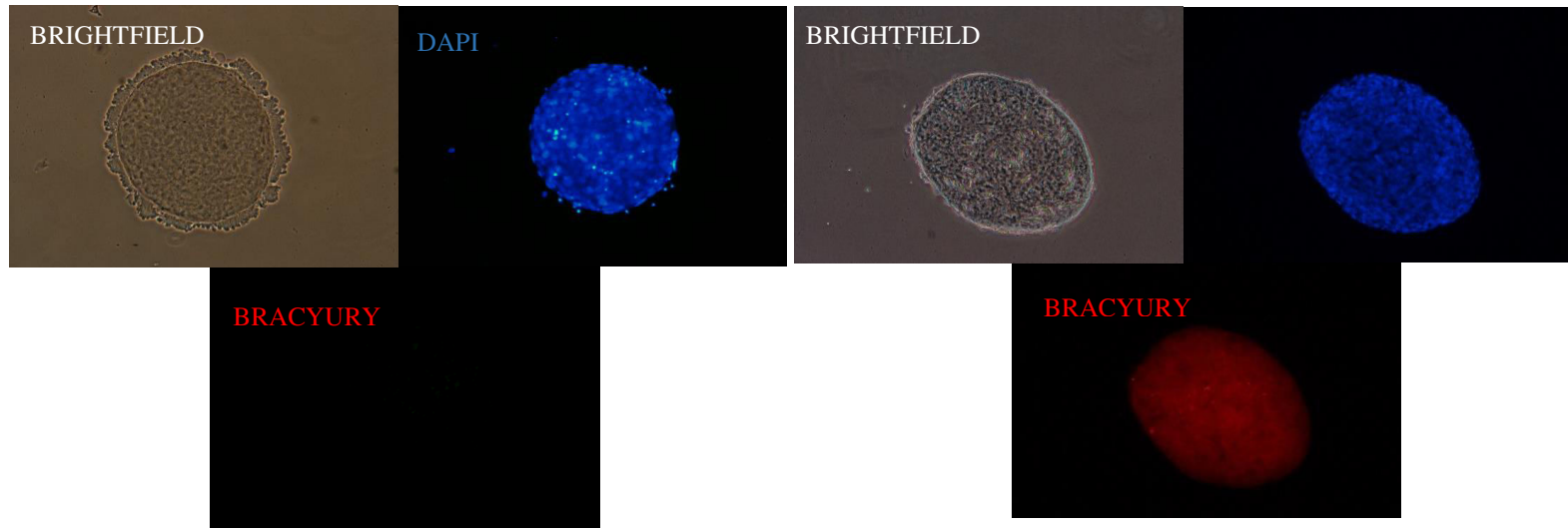
4.21 Immuno-fluorescent (IF) staining of parental H103-EB and reprogrammed H103-EB for mesoderm expression. (A&B) Representative images of parental H103-EB and reprogrammed H103-EB stained for mesoderm marker (BRACYURY). Mesoderm marker was not detected in parental H103-EB but expressed in reprogrammed H103-EB. Nikon inverted microscope, magnification: 10x.

Parental H103   **H103-IPSCS**

OSTEOCYTES

Parental H103   **H103-IPSCs**
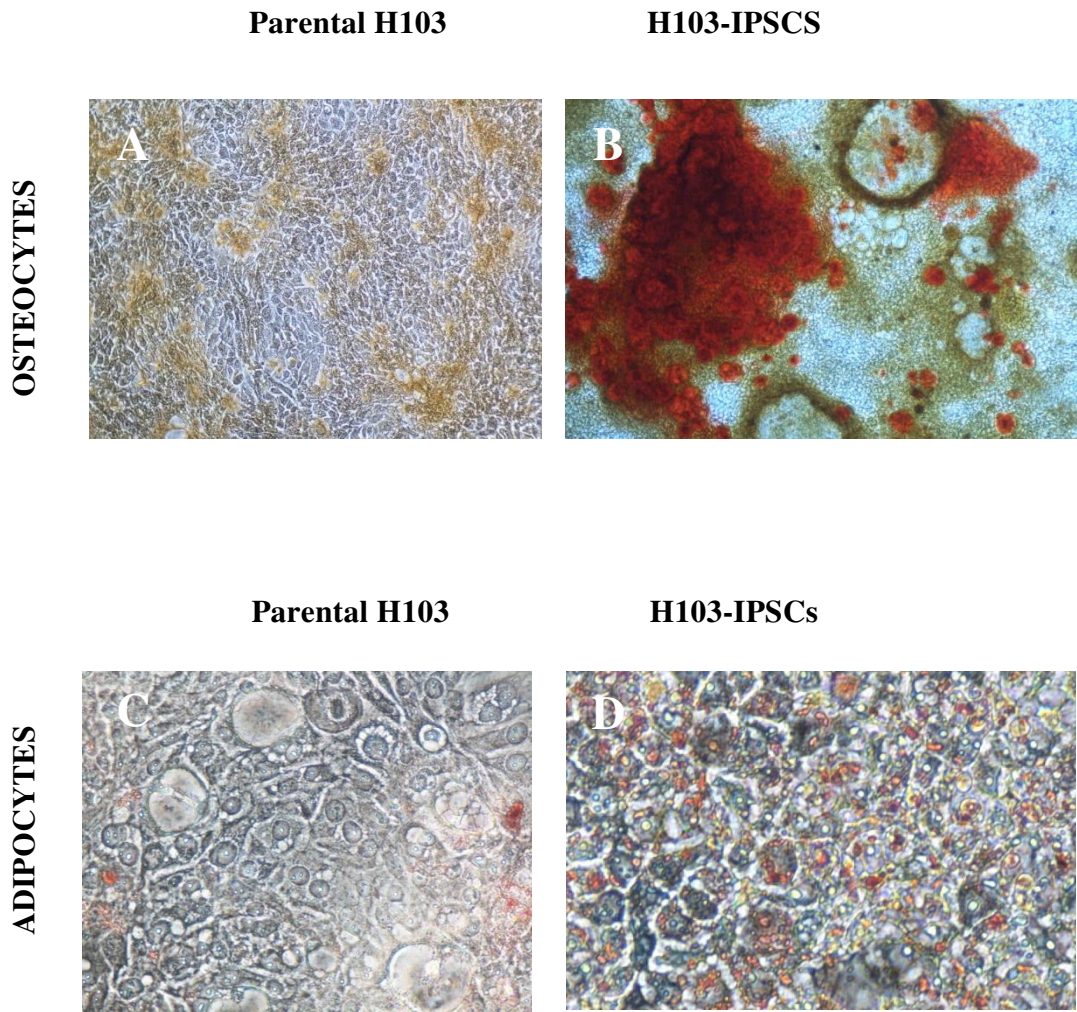
ADIPOCYTES

Figure 4.22 Directed differentiation into Osteocytes and Adipocytes. (A) Control parental H103 cells showing negative result for the Alizarin red staining (B) H103-IPScs cells showing positive result (red colour) for the Alizarin red staining indicating calcium deposits. (C) Negative staining for Oil-Red-O in control parental H103 cells. (D) Tiny lipid droplets observed in red colour after Oil-O-Red staining. Nikon inverted microscope, magnification: (A & B) 10x, (C & D) 40x.

4.9 Microsatellite Instability (MSI)

Ten microsatellite panel markers were selected to screen parental H103 cells and their reprogrammed counterparts. One selected marker D3S1228 showed the presence of loss of heterozygosity (LOH).

MSI PANEL	LOH
1. BAT 25	-
2. BAT 26	-
3. D2S123	-
4. D5S346	-
5. D17S250	-
6. D3S192	-
7. D3S966	-
8. D3S647	-
9. D3S1228	+
10. D3S659	-

Table 4.1: Microsatellite panel markers . LOH was observed in D3S1228. Representative gel image of D3S1228 was shown in Appendix N.

4.10   Global Methylation in Reprogrammed H103 Cells

Higher numbers of genes were methylated in reprogrammed H103 cells as shown in Figure 4.24, compared to the parental cells indicating many genes were switched off upon reprogramming.
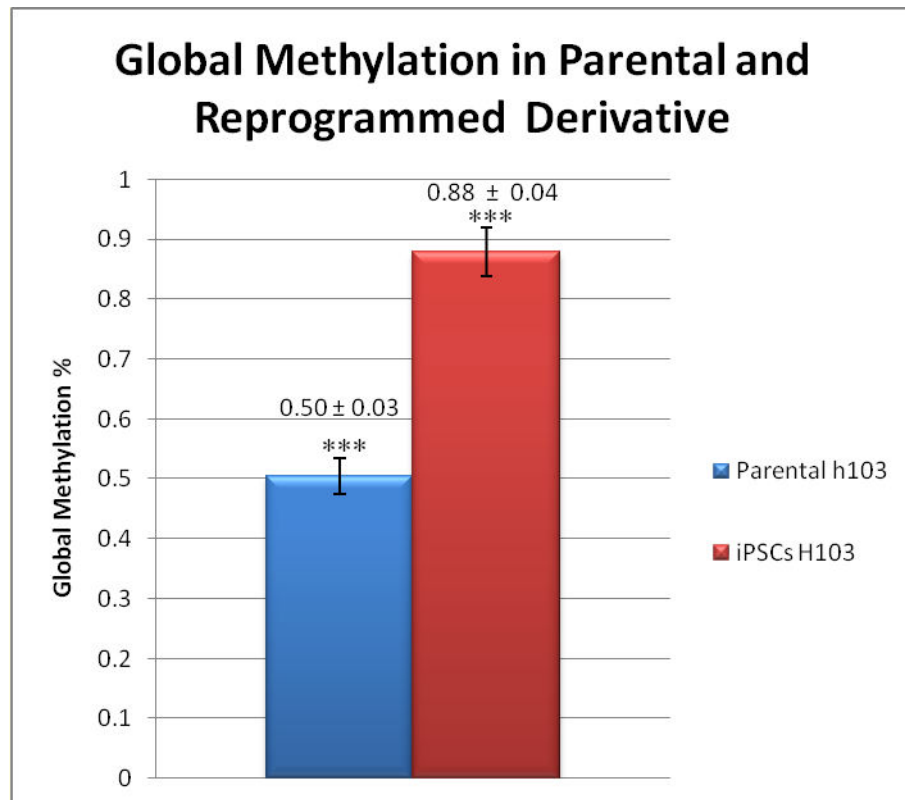
Figure 4.23 Global Methylation Status in parental H103 cells and reprogrammed (iPSCs) H103 cells. The average number of high (>0.6) methylated CpG sites: iPSCs had more methylated sites than the parental cells. Data presented as mean ± SD. Statistical differences are indicated with *** for P<0.001 using Student t-test.

CHAPTER 5

DISCUSSION

5.1   The Outcome of Reprogramming H103 and H376

The aims of this study are to reprogramme two Human Oral Squamous Cell Carcinoma cell lines into iPSCs like cells and to characterize their pluripotency signatures. Previous study had reported that iPSCs from somatic cells generated were used in regenerative medicine due to their self-renewal properties and ability to differentiate to targeted cell types (Fernandez et al., 2013). Recently, iPSCs from cancer cells have become a new area of interest and they are being explored for cancer disease modelling *in-vitro,* personalised drug testing models and cancer immunotherapy (Knorr and Kaufman, 2010). IPSCs from cancer cells provide   an opportunity to study human cancer states by understanding cancer pathogenesis and progression (Sharkis et al., 2012).

When two human Oral Squamous Cell Carcinoma cell lines (H103 and H376) were reprogrammed in this study, iPSCs were successfully derived from H103. The reprogrammed H103 cells morphologically exhibit Embryonic Stem Cells (ESCs) like characteristics based on cell morphology and are distinguishable from that of the parental cell line. The reprogrammed

H103 cells could undergo prolonged culture *in-vitro* up to 20 passages and above without any change of stem cell-like properties indicating their self-renewal capacity (Figure 4.13). On the other hand, reprogramming H376 cells had not been successful as ESCs –like morphology was not sustainable from passage two onwards. These reprogrammed cells appeared to spontaneously differentiate into the original H376 phenotype (Figure 4.11). This differentiated phenotype indicates partial loss of transgenes and a probable incomplete reprogramming of H376, using the Retroviral-OSKM mediated system.

Human iPSCs shared similar properties with ESCs as in colony morphology, gene expressions, epigenetic signatures, and self-renewal capacities (Takahashi et al., 2007). Derived IPSCs could be identified as flat cell colonies *in-vitro* with defined borders, tightly packed cells, high cell density, high N/C ratio, and small cell size (Shohei Wakao, 2012, Ono et.al, 2012, Ooi and Lieu, 2012). These features were observed in reprogrammed H103. In previous reports, iPSCs derived from human melanoma cells and chronic myeloid leukaemia cells (KBM7 cells) were morphologically distinct from that of the parental cancer cells and resembled that of ESCs morphologies (Lin et al., 2008, Carette et al., 2010). Subsequently, more cancer cell lines were reprogrammed using different methods and consistent ESCs morphology were also observed (Kim and Zaret, 2015).

Green fluorescence protein (GFP) reporter gene is commonly used as the control in transduction. Transduction efficiency in infected cells is determined via GFP signals confirming the uptake of transgenes (Hasegawa et al., 2010). As such, the transduction efficiency in both H103 and H376 was assessed via green fluorescence protein (GFP) expressions at 48 hours post-transduction. H376 showed higher GFP transgene uptake of 75.50% ± 1.52 compared to H103 showing an uptake of 38.20% ± 0.60 (Figure 4.8). In fact, H376 also exhibited higher tendency to form clones at day 15 upon reprogramming with Retrovirus-OSKM. It had been theorised that cells with higher transduction efficiency possess higher chance of being reprogrammed into iPSCs (Liao et al., 2008). However, in this study H376 exhibited high transduction efficiency but failed to sustain the stem cell-like features under long term *in-vitro* culture. Choong et al. recently demonstrated reprogramming of four osteosarcoma cell lines (U-2 OS, MG-63, Saos-2, G-292) via Retroviral-OSKM mediated system. The authors had highlighted the correlation between the transduction efficiencies and the success towards reprogramming. Two cell lines, U-2 OS and MG-63 with higher transduction efficiencies could not be maintained on long-term ESCs culture (< 30 passages) (Choong et al., 2014). Similar reprogramming pattern was identified in the reprogrammed H376 cell and therefore, depending on the cell types,

uptake of GFP transgene may not necessarily be correlated with transduction efficiency.

Reprogramming resistance was observed in H376 cell line compared to H103. Numerous reprogramming roadblocks involving genetic, epigenetic and signalling pathways were previously reported in pluripotent reprogramming (Ebrahimi, 2015). Reprogramming roadblocks contributed by diverse molecular properties and biophysical nature of the cell type, could result in inefficient reprogramming (Vierbuchen and Wernig, 2012). It has been shown that activation of p53 tumour suppressor gene activity is a reprogramming barrier. Additionally, p53 also safeguards the cellular genome integrity and this function was previously confirmed in ESCs (Spike and Wahl, 2011b, Olivier et al., 2010). Recent studies have also reported the effect of p53, which interrupted reprogramming efficiency and kinetics by removing DNA damaged cells at the early steps of the reprogramming stepwise process via apoptosis. Although both H103 and H376 harbour the mutant p53 gene, H376 carries a p53 gene which has a nonsense mutation and expresses the truncated form of the protein which basically do not show any detectable mutant p53 expression (Yeudall et al., 1995). Despite the fact that the mutated form of p53 gene may provide a more favourable condition for reprogramming cancer cells, the presence, rather than the absence of the mutant p53 expression has been reported to enhance reprogramming efficiency (Sarig et al., 2010, Tapia and Schöler, 2010) as in

the case of H103 which was able to maintain its pluripotent features under prolonged passage.

Transforming growth factor beta-I (TGF-β), a tumour suppressor gene identified in normal oral epithelial lineage, transformed into oncogenic activator which activates EMT most likely due to pathological stress (Krisanaprakornkit and Iamaroon, 2012). EMT initiates metastasis and invasion which indicates poor prognostic and high risk of survival rate in OSCC patients (da Silva et al., 2015). It has been shown that TGF- β triggers EMT (Ebrahimi, 2015). Presence of TGF- β signalling transduction was previously reported to be among the root cause of roadblocks in reprogramming (Li et al., 2010a). On the other hand, successful reprogramming towards pluripotency is shown to be facilitated by mesenchymal-to-epithelial transition (MET) followed by suppression of epithelial-to mesenchymal transition (EMT) regulation (Chen et al). Paterson et al. determined the effect of TGF-β in OSCC H-series cell lines in which H376 cell line was shown to be highly responsive to TGF- β than H103 (Paterson et al., 1995). Hence, H376 cell line may potentially harbours higher EMT activity that makes it more resistance towards reprogramming.

Despite repeated reprogramming attempts on H376 and H103, reprogramming was only successful for H103. This may be due to the differences in the inherent genetic make-ups between H103 and H376 cell lines which determined their capacity to be reprogrammed into iPSCs (Donate

and Blasco, 2011, Bojovic and Crowe, 2013). Since, reprogramming with OSKM factors gradually induces pluripotency transition through sequential gene expression states, intrusion by any of these biological barriers would impede reprogramming efficiencies (Hochedlinger and Plath, 2009).

The fundamental pluripotency regulators (Oct4, Sox2 and Nanog) in reprogrammed H103 were expressed at higher levels than that of H376 at both passage 5 and passage 10. Distinct Nanog differential expression was observed in stable reprogrammed H103 with significant increase in expression from parental to passage 5 and passage 10 (Figure 4.14) while partially reprogrammed H376 encountered significant down-regulation of Nanog from parental to passage 5 and gaining back the expression at passage 10 to a level similar to that of the parental (Figure 4.15), indicating its resistance towards reprogramming.

Expressions of Oct4 and Sox2 genes are important to regulate pluripotency and stemness (Rizzino, 2013) in undifferentiated ESCs. In addition, both Oct4 and Sox2 associated pluripotency and stemness are governed by a network of genes focused on Nanog (Palla et al., 2015). The interactions between Oct4, Sox2 and Nanog had been demonstrated via mutagenesis *in-vitro* assay and *in-vivo* functional study described previously in which suppression of Oct4 and Sox2 expression respectively decreases the promoter activity of Nanog (Rodda et al., 2005). Deficiency in Nanog expression results in partially reprogrammed cells which were unable to shift

into pluripotency state due to impaired regulation of pluripotency network (Festuccia et al., 2013). Importance of Nanog expression and its role in pluripotency was expounded in reprogramming of gastrointestinal cell lines by Myoshi and group previously (Miyoshia et al., 2009). Gastrointestinal cell lines selected for reprogramming expressed low level of Nanog mRNA, however these cell lines acquired significant up-regulation of Nanog expression upon reprogramming with four pluripotent transcription factors though Nanog was not induced exogenously.

Oct4 was proposed as an important regulator of proliferation and stemness in Embryonic Stem Cells (ESCs) (Heng *et al.*, 2010). Up-regulation of Oct4 expression in pluripotent stem cells facilitates reprogramming. Radzisheuskaya et al. had previously demonstrated the biological role of Oct4 in pluripotency acquisition, self-renewal, as well as *in vitro* and *in vivo* cell differentiation (Radzisheuskaya et al., 2013). Another study by Sajini, A.A et al. showed that embryoid bodies from murine embryonic stem cells progressively lost their Oct4 expression upon differentiation suggesting differentiated pluripotent stem cells are not able to sustain Oct4 expression (Hermitte and Chazaud, 2014). On the other hand, iPS cells derived from liver cancer cells exhibited low methylation of Oct4 indicating up-regulation of the gene (Zhang et al., 2014). Studies in tumour, however, reported high level of Oct4 expression in recurrent and metastatic OSCC specimens. Targeting Oct4 in OSCC was thus hypothesised to provide potential therapeutic approach in the future (Tsai et al., 2014). In this study, Oct4 was found to be expressed in

parental cancer cells of H103 and H376. Repression of Oct4 expression was observed at passage 5 after reprogramming in both H103 and H376 cell lines but this gene expression increased at passage 10 to a similar level like the parental counterpart for reprogrammed H376 and was highly increased in reprogrammed H103.

Klf4 is known to act either as a tumour suppressor gene or an oncogene depending on the need of the tumour cells and the types of cancer (Evans and Liu, 2008) and c-Myc is a crucial oncogene that confers immortality in cancer cells via a shift from senescence state to oncogenic progression (Erenpreisa and Cragg, 2013). These transcription factors have been highly implicated in influencing cancer progression (Erenpreisa and Cragg, 2013). The down-regulation pattern of oncogenic gene expression, namely c-Myc and Klf4 in both H103 and H376 were also absent in reprogrammed human osteosarcoma cells (Zhang et al., 2013). When, *in-vivo* tumorigenecity properties were assessed in human osteosarcoma cells with regards to down regulation of Klf4 and c-Myc, the parental cancer cells were shown to form tumour at a faster rate than that of the reprogrammed counterpart (Zhang et al., 2013). Furthermore, down regulation of c-Myc was previously highly associated with epigenetic remodelling due to hypermethylation of H3K4 gene (Koga et al., 2014). This oncogene was found to be responsible in determining the fate of oncogenes and tumour suppressor genes in targeted cells after cellular reprogramming (Mahalingam et al., 2012). Down-regulation of both c-Myc and Klf4 in OSCC suggests reprogramming

may initiate an epigenetic reversal process on the oncogenic gene networks in cancer cells and this phenomenon could be utilize as a therapeutic strategy for treatment of OSCC.

5.2 Pluripotency Expression and Differentiation Capacity in H103 iPSCs

The evidence for pluripotency was further explored on successfully reprogrammed H103 via the immunofluorescence staining for common intracellular (Oct4, Sox2, Nanog) and extracellular (Tra-1-60) pluripotent markers which were used in pluripotent stem cells characterization. All intracellular and extracellular pluripotent markers were detected on reprogrammed H103 (Figure 4.17) indicating H103 expresses important pluripotency expressions at the protein levels.

Subsequently, H103 iPSCs were subjected to *in-vitro* differentiation assay by embryoid bodies (EB) formation and induced differentiation into adipocytes and osteocytes. EB formed vary in size and presence of three germ layers in EB was assessed by immuno-fluorescence staining. Three germ layers specific markers (Ectoderm: OTX2, Sox1; Endoderm: Sox17, Gata4; Mesoderm: Bracyury) were all detected in EB derived from H103 iPSC. H103 cell lines originated from the endoderm and ectoderm lineages (Jones and Klein, 2013) . Hence, presence of positive signals for ectoderm and endoderm is not indicative of the pluripotency properties. However, positive signal of

mesoderm markers (Figure 4.21) do suggest that reprogrammed H103 acquired pluripotency because "EB" from parental H103 did not show mesoderm positive signal. Our observation is consistent with other studies, in which differentiation into three germ layer were achieved upon reprogramming (Carette et al., 2010).

Oil-Red O and Alizarin red staining respectively confirmed lineage-specific differentiation of reprogrammed H103, into adipocytes and osteocytes. These methods were used as standard protocols to assess differentiation capacity of adult stem cells such as mesenchymal stem cells. These methods have been extended on iPSCs though these methods do have certain limitations. Alizarin red S is not specific for calcium deposits as this staining may also take up by magnesium, manganese, barium, strontium, and iron. Tumours are also known to show calcium deposits as tumour tissues are abnormal tissue where dystrophic calcium deposits can occur. However, as per mentioned in Chapter 4, these elements usually do not accumulate in such great concentration in tissues compared to the amount of calcium deposit in bone formation. (Lievremont et al., 1982). Formation of lipid droplets occurs during adipogenic differentiation of in H103 iPSCs though these changes also developed in a diseased tissue as a degeneration process. The provision of controls and the short duration of the experiments argue against the observed phenomena being due to changes associated with degeneration. In addition, other assays have been used in osteoblast detection which include identification of osteocalcin, alkaline phosphatase and type I collagen via

immunohistochemistry and reverse transcription polymerase chain reaction (RT-PCR) (Arpornmaeklong et al., 2009). While, evaluation of adipocytes-specific fatty acid binding protein could be detected via gene expression and protein expression of Adipoq, Pparγ, fatty acid binding protein 4 (FABP4) (Cuaranta-Monroy et al., 2014). Differentiation of reprogrammed osteosarcoma cells into embryoid bodies and directed differentiation into adipocytes and osteocytes were demonstrated in previous studies using similar approaches (Choong et al., 2014). Myoshi et al. 2009 previously demonstrated adipogenesis on their iPSCs and detected FABP4 expression via immunohistochemistry (Myoshi et al., 2009). In our study, H103 exhibited capacity to differentiate into mesodermal lineage though H103 cells originate from both ectoderm and endoderm lineage indicating their potential to acquire cross lineage differentiation capacity into mesoderm lineage cells of adipocytes and osteocytes. In contrast, parental OSCC setup as controls, were not able to demonstrate such differentiation capacity.

Carette et al. observed their iPSCs cell derived from leukemia cells lost their oncogenic properties of the BCR-ABL fusion gene. Yet, the BCR-ABL properties were restored upon differentiation of the iPSCs towards haematopoietic lineage. Their findings indicate reprogramming facilitates the elimination of the oncogene properties (but not the mutation), which later could be reinstated via differentiation (Carette et al., 2010). Moderating oncogene properties such as reprogramming indeed may serve as a new approach in cancer therapy (Yap and Workman, 2012).

5.3   Microsatellite Analysis in H103 iPSCs

DNA repair is crucial to maintain the genomic integrity in each and every cell type and presence of genomic instability indicates reduced ability in DNA repair mechanism involving the Mismatch Repair (MMR) genes (Yu et al., 2006). Perturbation of MMR genes may lead to cancer. Microsatellite instability (MSI) is a molecular attribute that can be used to study DNA repair mechanism and frequently used in cancer research to screen for perturbation of MMR genes. Microsatellite sequences are short base pairs, up to six base pairs in a sequence that are repeated along DNA sequence at gene promoters, exons, and introns (Campregher et al., 2010). Microsatellite sequence is similar in each and every cell in an individual body but it differs between a cancer cell and a normal cell and that is why MSI markers were often screened between normal tissues and tumours (Horvat and Stabuc, 2011). DNA repair mechanism was investigated previously comparing human iPSCs derived from human foreskin fibroblast and human lung fibroblast and their non-pluripotent parental counterparts. Greater repair ability and response towards apotosis was shown in iPSCs derivatives (Luo et al., 2012).

Upon review of literature, there was little information on MSI between generated iPSCs from cancer cells and their parental counterparts. In our study, allelic imbalance in one of Microsatellite marker (D3S1228) was detected in H103 iPSCs at 112-120bp. LOH was shown previously by researchers, in oral tumour tissues against normal tissues and this finding was

correlated to the mapping of the FHIT gene, a tumour suppressor gene, which was often found activated in the OSCC (Ashazila et al., 2011). Therefore, it remains to be determined whether FHIT gene is affected in reprogramming of the OSCC which is beyond the scope of the present study.

5.4   Global Methylation Status in H103 iPSCs

Global methylation status from both parental and reprogrammed H103 revealed higher number of methylated genes acquired upon reprogramming with 88% of methylations detected. Similar studies were carried on pluripotent stem cell derivatives and it was reported that higher reprogramming efficiency correlates with the hypermethylation. Hypermethylation in differential methylated regions (DMRs) was associated with suppression of gene expression and apparently, 80% of DMRs were captured as hypermethylated in human skin fibroblast iPSCs against their parental cells (Nishino et al., 2011). Recent studies showed that genes which were usually up-regulated in lung cancer were suppressed or hypermethylated upon reprogramming in reprogrammed lung cancer cells. These findings indicated that reprogramming may induce reversion of abnormal gene expression to normal expression via epigenetic remodelling (Mahalingam et al., 2012, Barrero et al., 2012).

## 5.5	Practical Implications

Our findings indicated that the critical roles of Oct4, Sox2 and Nanog, towards successful reprogramming. Down-regulation of oncogenes c-Myc and Klf4 was observed in derived iPSCs from H103 cells, a potential clue to therapeutic intervention. The reprogrammed cells shall be subjected to further analysis to explore their potential as a model to study multiple stages of oncogenesis in OSCC, thus enabling access to cancer biological properties from the initial tumour initiation to the later malignant/metastatic states. In addition, reprogramming creates an opportunity to derive an *in-vitro* model of carcinogenesis for OSCC and differentiated neoplastic progenitors of multiple stages from iPSCs for discovery of novel anti-cancer drugs.

CHAPTER 6

CONCLUSION AND FUTURE RECOMMENDATIONS

6.1   Conclusion

Traditional approaches using primary cancer cells to study tumour properties have their limitations. Cells isolated from tumours possess limited lifespan and technical constraints under prolonged tissue culture *in-vitro.* Tumour tissues are often not easily obtained from patients and primary cell lines could often not be established successfully (Shirako et al., 2015). Reprogramming OSCC cells provides an alternative method for studying tumour properties as iPSCs are sustainable under prolonged *in-vitro* cell culture condition with self-renewable characteristics (Curry et al., 2015, Grskovic et al., 2011). iPSCs are species-specific and individual-specific. iPSCs derived from OSCC carry OSCC specific mutations after reprogramming and these can be accessed via genomic and proteomic based assays to reveal the content of genetic and epigenetic variability of the disease in patients (Kim and Zaret, 2015). iPSCs derived from OSCC (iPSCs-OSCC) in our study exhibit pluripotency and differentiation capacity. These cells maybe differentiated towards OSCC specific lineages to determine the oncogenic mutations at specific tumour developmental states. Furthermore, cellular based assays can be designed for drug discovery, toxicological studies

and high-throughput drug screening by utilizing differentiated iPSCs-OSCC that recapitulate specific tumour formation *in-vitro* (Ebert et al., 2012).

6.2   Future Recommendations

Viral delivery system increases the risk of tumourigenesis by gene modification during reprogramming (Okita and Yamanaka, 2011b). Though viral delivery system provides higher transduction efficiencies, non-viral delivery system could be an alternative in reprogramming OSCC cells in the future to facilitate translational studies for clinical application (Park et al., 2012).

Available genetic engineering technologies could be employed to resolve tumourigenic properties via H103 iPSCs, which would be an advantage to study the aberrations in tumour suppressor genes and oncogenes expressions in malignant states and correlate the aberrations with the clinical aggressiveness of OSCC. Assays used in screening genetic constituents and functions of iPSCs-OSCC, including knockdown with RNA interference , differential expression analysis via microarray platform, and next gene sequencing (Santostefano et al., 2015, Zhang et al., 2013, Mahalingam et al., 2012), may be employed to establish gene expressions and epigenetic profiles between metastatic and reprogrammed cells. This could help to explain various genes that are differentially expressed in association with the metastatic potential cancer cells.

127

Oncogenic model could be developed to elucidate the existence of Cancer Stem cell (CSC) (Abhold et al.) (Trosko, 2014). The CSC subpopulation in OSCC was identified to contribute in cancer recurrence and chemotherapeutics resistance due to apoptotic evasion and aggressive proliferation in nature (Patel et al., 2014). iPSCs-OSCC model could serves as an alternative model to discover the biological characteristics, functional relevance of CSC and the underlying mechanisms that regulate tumour development and metastasis.

REFERENCES

Aasen, T., et al., 2008. Efficient and rapid generation of induced pluripotent stem cells from human keratinocytes. *Nature Biotechnology,* 26**,** pp.1276-84.

Abhold, E. L., et al., 2012. EGFR kinase promotes acquisition of stem cell-like properties: a potential therapeutic target in head and neck squamous cell carcinoma stem cells. *PLoS One,* 7**,** pp. e32459.

Adams,. et al., 2013. Functional Vascular Endothelium Derived from Human Induced Pluripotent Stem Cells. *Stem Cell Reports,* 1**,** pp.105-113.

Alizadeh, R., Mehrabi, S. and Hadjighassem, M., 2014. Cell Therapy in Parkinson's Disease. *Archieves of Neuroscience,* 1**,** pp.43-50.

Ardeshiry lajimi., et al., 2013. Feasibility of Cell Therapy in Multiple Sclerosis: A Systematic Review of 83 Studies. *International Journal of Hematology-Oncology and Stem Cell Research*, 7**,** pp.15-33.

Arpornmaeklong, P., Brown, S. E., Wang, Z and Krebsbach, P.H. 2009. Phenotypic characterization, osteoblastic differentiation, and bone regeneration capacity of human embryonic stem cell-derived mesenchymal stem cells. *Stem Cell and Development*, 18**,** pp.955-968.

Arzenani, M. K., et al., 2011. Genomic DNA hypwemethylation by Histone Deacetylase inhibition implicates DNMT1 nuclear dynamics. *Molecular and Cellular Biology*, 31, pp. 4119-4128.

Ashazila, M. J., et al., 2011. Microsatellite instability and loss of heterozygosity in oral squamous cell carcinoma in Malaysian population. *Oral oncology,* 47**,** pp.358-364.

Barrero, M. J., et al., 2012. DNA hypermethylation in somatic cells correlates with higher reprogramming efficiency, *Stem Cells,* 30**,** pp.1696-702.

Begley, C. G. and Ellis, L. M., 2012. Drug development: Raise standards for preclinical cancer research. *Nature,* 483**,** pp.531-533.

Birnmingham, E., et al., 2012. Osteogenic differentiation of mesenchymal stem cells is regulated by osteocyte and osteoblast cells in a simplified bone niche. *European Cells and Materials*, 23, pp.13-27.

Bojovic, B. and Crove, D.L., 2013. Dysfunctional telomeres promote genomic instability and metastasis in the absence of telomerase activity in oncogene induced mammary cancer. *Molecular Carcinogenesis,* 52**,** pp:103-17.

Boulting, G.L., et al., 2011. A functionally characterized test set of human induced pluripotent stem cells. *Nature Biotechnology,* 29**,** pp.279-286.

Brave, A.,Liungberg,K., Wahren, B. and Liu, M. A., 2007. Vaccine delivery methods using viral vectors. *Molecular Pharmacology,* 4**,** pp.18-32.

Buganim, Y., Faddah, D. A. & Jaenisch, R,. 2013. Mechanisms and models of somatic cell reprogramming. *Nature reviews. Genetics,* 14**,** pp.427-439.

Campregher, C., et al., 2010. The nucleotide composition of microsatellites impacts both replication fidelity and mismatch repair in human colorectal cells. *Human Molecular Genetic,* 19**,** pp.2648 - 2657.

Carette, J. E., et al., 2010. Generation of iPSCs from cultured human malignant cells. *Blood,* pp. 4039-4042.

Cekanova, M. and Rathore, K., 2014. Animal models and therapeutic molecular targets of cancer: utility and limitations. *Drug Design Development and Therapy,* 8**,** pp.1911-21.

Chan, R. J. and Yoder, M. C., 2013. JMML patient-derived iPSCs induce new hypotheses. *Blood,* 121**,** pp. 4815-4817.

Chandra, A., Sebastian, B. and Agnihotri, A., 2013. Oral squamous cell carcinoma pathogenesis and role of p53 protein. *University Research Journal of Dentistry,* 3**,** pp.128-130.

Chen, L. and Daley, G. Q., 2008. Molecular basis of pluripotency. *Human Molecular Genetics,* 17**,** pp. R23-R27.

Chen, L. W., et al., 2011. Potential application of induced pluripotent stem cells in cell replacement therapy for Parkinson's disease. *CNS Neurological Disorders-Drug Targets,* 10**,** pp.449-458.

Choong, P. F., et al., 2014. Heterogeneity of osteosarcoma cell lines led to variable responses in reprogramming. *International Journal of Medical Science,* 11**,** pp.1154-60.

Colley, H. E., et al., 2011. Development of tissue-engineered models of oral dysplasia and early invasive oral squamous cell carcinoma. *British Journal of Cancer,* 105**,** pp.1582-1592.

Correia, A. S., Anisimov, S. V., Li, J. Y. and Brundin, P., 2005. Stem cell-based therapy for Parkinson's disease. *Annals of Medicines,* 37**,** pp.487-498.

Chen, J., Han. Q., 2011a. EMT and MET as paradigms for cell fate switching. *Journal of Molecular Cell Biology*, *4*(2), pp.66-69.

Cuaranta-Monroy, I., et al., 2014., Highly efficient differentiation of embryonic into adipocytes by ascorbic acid. *Stem Cell Research*, 13, pp.88-97.

Curry, E. L., Moad. M., Robson, C. N and Heer, R., 2015. Using induced pluripotent stem cells as a tool for modelling carcinogenesis. *World Journal of Stem Cells*, 7, pp. 461-9.

Da Silva, S. D., et al., 2015. Epithelial-mesenchymal transition (EMT) markers have prognostic impact in multiple primary oral squamous cell carcinoma. *Clinical and Experimental Metastasis*,3291), pp.55-63.

De Camargo Cancela, M., et al., 2010. Oral cavity cancer in developed and in developing countries: Population-based incidence. *Head & Neck,* 32**,** pp.357-367.

Deng, X. Y., et al., 2015. . Non-Viral Methods For Generating Integration-Free, Induced Pluripotent Stem Cells. *Current Stem Cell Research & Therapy,* 10**,** pp.153-158.

Deshmukh, R. S., Kovacs. K. A. and Dinnyes. A., 2012. Drug Discovery Models and Toxicity Testing Using Embryonic and Induced Pluripotent Stem-Cell-Derived Cardiac and Neuronal Cells. *Stem Cells International,* 2012**.**

Dewi, D., et al., 2012. Reprogramming of gastrointestinal cancer cells. *Cancer Science*, 103, pp.393-399.

Donate, L. E. and Blasco, M. A., 2011. Telomeres in cancer and ageing. *Philosophical Transaction of the Royal Society B: Biological Sciences*, 366, pp.76-84.

Doshi Neena, P., Shah Siddharth, A., Patel Keyuri, B. and Jhabuawala Munira, F., 2011. Histological grading of oral cancer: a comparison of different systems and their relation to lymph node metastasis. *National Journal of Community Medicine,* 2**,** pp.136-142.

Ebert, A. D., Liang, P. and Wu, J. C., 2012. Induced pluripotent stem cells as a disease modeling and drug screening platform. *Journal of Cardiovascular Pharmacology*, 60, pp.408-416.

Ebrahimi, B. 2015 Reprogramming barriers and enhancers: strategies to enhance the efficiency and kinetics of induced pluripotency. *Cell Regeneration*, 4, pp. 1-12.

Elston, R. and Inman, G, J., 2012. Crosstalk between p53 and TGF-signalling. *Journal of Signal Transduction*, 2012, pp.294-297.

Ebert, A. D., et al., 2009. Induced pluripotent stem cells from a spinal muscular atrophy patient. *Nature,* 457**,** pp277-280.

El-Aneed, A., 2004. An overview of current delivery systems in cancer gene therapy. *J Control Release,* pp.94**,** 1-14.

Erenpreisa, J. and Cragg, M. S., 2013. Three steps to the immortality of cancer cells: senescence, polyploidy and self-renewal. *Cancer Cell Int,* 13**,** pp.92.

Evans, P. M. and Liu, C., 2008. Roles of Krupel-like factor 4 in normal homeostasis, cancer and stem cells. *Acta Biochim Biophys Sin (Shanghai), 40(7),* pp.554-564.

Eve, D. J., et al., 2008. Stem Cell Research and Health Education. *American journal of health education / American Alliance for Health, Physical Education, Recreation, and Dance,* 39**,** pp.167-179.

Fernandez, T.D.S., de Souza Fernandez, C. and Mencalha, A.L., 2013. Human induced pluripotent stem cells from basic research to potential clinical applications in cancer. *BioMed research international*, *2013*.

Farini, D., et al., 2005. Growth factors sustain primordial germ cell survival, proliferation and entering into meiosis in the absence of somatic cells. *Dev Biol,* 285**,** pp. 49-56.

Feller, L., et al., 2013. Alcohol and oral squamous cell carcinoma. *Journal of the South African Dental Association,* 68**,** pp.176-180.

Festuccia, N., Osorno, R.., Wilson, V. and Chambers, I., 2013. The role of pluripotency gene regulatory network components in mediating transitions between pluripotent cell states. *Current Opinion in Genetics & Development,* 23**,** pp.504-511.

Focosi, D., et al., 2014. Induced pluripotent stem cells in hematology: current and future applications. *Blood Cancer Journal,* 4**,** pp.e211.

Gandre-Babbe, S., et al., 2013. Patient-derived induced pluripotent stem cells recapitulate hematopoietic abnormalities of juvenile myelomonocytic leukemia. *Blood*, 121(24), pp.4925-4929.

Ganguly, J. A. and Parihar, S. P., 2009. Human papillomavirus E6 and E7 oncoproteins as risk factors for tumorigenesis. *J Biosci,* 34**,** 113-123.

Gardlik, R., et al., 2005. Vectors and delivery systems in gene therapy. *Medical Science Monitor,* 11**,** pp. RA110-RA121.

Gasche, J. A. and Goel, A., 2012. Epigenetic mechanisms in oral carcinogenesis. *Future Oncolology, 8*(11), pp.1407–1425.

Gasche, J. A., Hoffman, J., Boland, C. R. and Goel, A., 2011. Interleukin-6 promotes tumorigenesis by altering DNA methylation in oral cancer cells. *International Journal of Cancer,* 129**,** pp.1053-1063.

Glauche, I., Herberg, M. and Roeder, I., 2010. Nanog variability and pluripotency regulation of embryonic stem cells--insights from a mathematical model analysis. *PLoS One,* 5**,** pp.e11238.

Gonzalez, F., Boue, S. and Belmonte, J. C. I., 2011. Methods for making induced pluripotent stem cells: reprogramming à la carte. *Nature Reviews Genetics,* 12**,** pp.231-242.

Grskovic, M., Javaherian, A., Strulovici, B. and Daley, G.Q., 2011. Induced pluripotent stem cells—opportunities for disease modelling and drug discovery. *Nature reviews Drug discovery*, 10(12), pp.915-929.

Guzzo, R. M., et al., 2013. Efficient differentiation of human iPSC-derived mesenchymal stem cells to chondroprogenitor cells. *Journal of Cellular Biochemistry,* 114**,** pp.480-490.

Han, J. W. and Yoon, Y. S., 2011. Induced Pluripotent Stem Cells: Emerging Techniques for Nuclear Reprogramming. *Antioxidants & Redox Signaling,* 15**,** pp.1799-1820.

Han, W., Zhao, Y. and Fu, X., 2010. Induced Pluripotent Stem Cells: The Dragon Awakens. Journal of *BioScience,* 60**,** pp.278-285.

Hanahan, D. and Weinberg, R. A., 2011. Hallmarks of Cancer: The Next Generation. *Cell,* 144**,** pp.646-674.

Handy, D.E., Castro, R. and Loscalzo, J., 2011. Epigenetic modifications basic mechanisms and role in cardiovascular disease. *Circulation*, 123(19), pp.2145-2156.

Hao, J., et al., 2009. Human parthenogenetic embryonic stem cells: one potential resource for cell therapy. *Sci China C Life Sci, 52*(7), pp.599-602.

Hasegawa, K., et al., 2010. Comparison of reprogramming efficiency between transduction of reprogramming factors, cell–cell fusion, and cytoplast fusion. *Stem Cells*, 28(8), pp.1338-1348.

Hayashi, R.., et al., 2012. Generation of corneal epithelial cells from induced pluripotent stem cells derived from human dermal fibroblast and corneal limbal epithelium. *PLoS One,* 7**,** pp.e45435.

Heng, J.C.D., et al., 2010. The nuclear receptor Nr5a2 can replace Oct4 in the reprogramming of murine somatic cells to pluripotent cells. *Cell stem cell*, 6(2), pp.167-174.

Hermitte, S. and Chazaud, C., 2014. Primitive endoderm differentiation: from specification to epithelium formation. *Philosophical Transactions of the Royal Society of London B: Biological Sciences*, 369(1657), pp.20130537.

Hochedlinger, K. and Plath, K., 2009. Epigenetic reprogramming and induced pluripotency. *Development*, 136(4), pp.509-523.

Horvat, M. and Stabuc, B., 2011. . Microsatellite instability in colorectal cancer. *Radiology and Oncology,* 45**,** pp.75-81.

Hu, K. and Slukvin, I., 2013. Generation of transgene-free iPSC lines from human normal and neoplastic blood cells using episomal vectors. *Pluripotent Stem Cells: Methods and Protocols*, pp.163-176.

Huang, L., Wu, R.L. and Xu, A.M., 2015. Epithelial-mesenchymal transition in gastric cancer. *American Journal of Translational Research*, 7(11), p.2141.

Hug, K., 2005. Sources of human embryos for stem cell research: ethical problems and their possible solutions. *Medicina (Kaunas),* 41**,** pp.1002-1010.

Hughes, I. A., 2004. A perspective on stem cells by a clinician. *European Journal of Endocrinology,* 151 Suppl 3**,** pp.U3-U5.

Hyun, I., 2010. The bioethics of stem cell research and therapy. *The Journal of Clinical Investigation,* 120**,** pp.71-75.

Jessri, M., Dalley, A. J. and farah, C. S., 2015. hMSH6: a potential diagnostic marker for oral carcinoma in situ. *Journal of Clinical Pathology,* 68**,** pp.86-90.

Ithesh, P. V., et al., 2013. The epigenetic landscape of oral squamous cell carcinoma. *British Journal of Cancer,* 108**,** pp. 86-90.

Jithesh, P.V., et al., 2013. The epigenetic landscape of oral squamous cell carcinoma. *British journal of cancer*, 108(2), pp.370-379.

Johansson, H. and Simonsson, S., 2010. Core transcription factors, Oct4, Sox2 and Nanog, individually form complexes with nucleophosmin (Npm1) to control embryonic stem (ES) cell fate determination. *Aging (Albany NY)*,2(11), pp.815-822.

Jones, K. B. and Klein, O. D., 2013. Oral epithelial stem cells in tissue maintenance and disease: the first steps in a long journey. *International Journal of Oral Sciences,* 5**,** pp.121-129.

Kalladka, D. and Muir, K. W., 2014. Brain repair: cell therapy in stroke. *Stem Cells and Cloning : Advances and Applications,* 7**,** pp.31-44.

Kamat, N., et al., 2012. High incidence of microsatellite instability and loss of heterozygosity in three loci in breast cancer patients receiving chemotherapy: a prospective study. *BMC Cancer,* 12**,** pp.1.

Kandi, S., et al., 2014. Alcoholism and Its Role in the Development of Oxidative Stress and DNA Damage: An Insight. *American Journal of Medical Sciences and Medicine,* 2**,** pp.64-66.

Kasamatsu, A., et al., 2011. Loss of heterozygosity in oral cancer. *Oral Science International,* 8**,** pp.37-43.

Kelesidis, T., et al., 2011. Human Papillomavirus (HPV) Detection Using In Situ Hybridization in Histologic Samples: Correlations With Cytologic Changes and Polymerase Chain Reaction HPV Detection. *American Journal of Clinical Pathology,* 136**,** pp.119-127.

Kim, J., et al., 2013. An iPSC Line from Human Pancreatic Ductal Adenocarcinoma Undergoes Early to Invasive Stages of Pancreatic Cancer Progression. *Cell Reports,* 3**,** pp.2088-2099.

Kim, J. and Zaret, K. S., 2015. Reprogramming of human cancer cells to pluripotency for models of cancer progression. *The EMBO Journal,* 34**,** pp.739-747.

Knorr, D.A. and Kaufman, D.S., 2010. Pluripotent stem cell-derived natural killer cells for cancer therapy. *Translational Research*, *156*(3), pp.147-154.

Ko, H. C. and Gelb, B.D., 2014. Concise Review: Drug Discovery in the Age of the Induced Pluripotent Stem Cell. *Stem Cells Translational Medicine,* 3**,** pp.500-509.

Koga, C., et al., 2014. Reprogramming using microRNA-302 improves drug sensitivity in hepatocellular carcinoma cells. *The annals of surgical Ocology, 21*(4), pp.591-600.

Kotini, A.G., et al., 2015. Functional analysis of a chromosomal deletion associated with myelodysplastic syndromes using isogenic human induced pluripotent stem cells. *Nature biotechnology*, *33*(6), pp.646-655.

Krisnaprokornkit, S. and Iamaroon, A., 2012. Epithelial-Mesenchymal Transition in Oral Squamous Cell Carcinoma. *ISRN Oncology,* 2012.

Kulis, M. and Esteller, M., 2010. DNA methylation and cancer. *Advances in Genetics,* 70**,** pp.27-56.

Landry, D.W. and Zucker, H.A., 2004. Embryonic death and the creation of human embryonic stem cells. *The Journal of clinical investigation*, 114(9), pp.1184-1186.

Lang, J. Y., Shi, Y. and Chin, Y.E. 2013. Reprogramming cancer cells: back to the future. *Oncogene, 32*(18), pp.2247-2248.

Lee, D. F., et al., 2015. Modeling Familial Cancer with Induced Pluripotent Stem Cells. *Cell,* 161**,** pp.240-254.

Lei, T., et al., 2007. Xeno-free derivation and culture of human embryonic stem cells: current status, problems and challenges. *Cell Res,* 17**,** pp.682-688.

Lerou, P. H. and Daley, G. Q., 2005. Therapeutic potential of embryonic stem cells. *Blood Reviews,* 19**,** pp.321-331.

Li, H.Y., et al., 2011. Reprogramming induced pluripotent stem cells in the absence of c-Myc for differentiation into hepatocyte-like cells. *Biomaterials*, 32(26), pp.5994-6005.

Li, J., Song, W., Pan, G. Zhou, J., 2014. Advances in understanding the cell types and approaches used for generating induced pluripotent stem cells. *Journal of Hematology and Oncology,* 7**,** pp.50.

Li, L., Cole, J. and Margolin, D. A. 2013. Cancer Stem Cell and Stromal Microenvironment. *The Ochsner Journal,* 13**,** pp.109-118.

Li, R., Liang, et al., 2010. A mesenchymal-to-epithelial transition initiates and is required for the nuclear reprogramming of mouse fibroblasts.*Cell stem cell*, 7(1), pp.51-63.

Li, Y., et al., 2011. c-Met signaling induces a reprogramming network and supports the glioblastoma stem-like phenotype. *Proceedings of the National Academy of Sciences*, 108(24), pp.9951-9956.

Liao, J., et al., 2008. Enhanced efficiency of generating induced pluripotent stem (iPS) cells from human somatic cells by a combination of six transcription factors. *Cell research*, 18(5), p.600.

Lievremont, M., Potus, J. and Guillou, B., 1982. Use of alizarin red S for histochemical staining of Ca2+ in the mouse; some parameters of the chemical reaction in vitro. *Cells Tissues Organs*, 114(3), pp.268-280.

Lin, G., et al., 2007. A highly homozygous and parthenogenetic human embryonic stem cell line derived from a one-pronuclear oocyte following in vitro fertilization procedure. *Cell Research,* 17**,** pp.999-1007.

Lin, S. and Talbot, P., 2011. Methods for culturing mouse and human embryonic stem cells. *Methods in Molecular Biology,* 690**,** pp.31-56.

Lin, S. L., et al., 2008. Mir-302 reprograms human skin cancer cells into a pluripotent ES-cell-like state. *RNA,* 14**,** 2115-2124.

Lo, B. and Parham, L., 2009. Ethical Issues in Stem Cell Research. *Endocrine Reviews,* 30**,** pp.204-213.

Lu, X. and Zhao, T., 2013. Clinical Therapy Using iPSCs: Hopes and Challenges. *Genomics, Proteomics & Bioinformatics,* 11**,** pp.294-298.

Luo, L. Z.,et al., 2012. DNA repair in human pluripotent stem cells is distinct from that in non-pluripotent human cells. *PLoS One,* 7**,** pp.e30541.

Mahalingam, D., et al., 2012. Reversal of aberrant cancer methylome and transcriptome upon direct reprogramming of lung cancer cells. *Sci Rep,* 2.

Mai, Q., et al., 2007. Derivation of human embryonic stem cell lines from parthenogenetic blastocysts. *Cell Research,* 17**,** 1008-19.

Majchrzak, E., et al., 2014. Oral cavity and oropharyngeal squamous cell carcinoma in young adults: a review of the literature. *Radiology and Oncology,* 48**,** pp.1-10.

Marian, A. J., 2011. Modeling Human Disease Phenotype in Model Organisms: "It's Only a Model!". *Circulation Research,* 109**,** pp.356-359.

Markopoulos, A. K., 2012. Current Aspects on Oral Squamous Cell Carcinoma. *The Open Dentistry Journal,* 6**,** pp.126-130.

Mascolo, M., et al., 2012. Epigenetic Disregulation in Oral Cancer. *International Journal of Molecular Sciences,* 13**,** pp.2331-2353.

Mason, J. B. and Choi, S. W., 2005. Effects of alcohol on folate metabolism: implications for carcinogenesis. *Alcohol,* 35**,** pp.235-41.

Maccall, M. D., Toso, C., Baetge, E. E. and Shapiro, A. M., 2010. Are stem cells a cure for diabetes? *Clinical Science,* 118**,** pp.87-97.

Mcdowell, J. D., 2006. An overview of epidemiology and common risk factors for oral squamous cell carcinoma. *Otolaryngologic Clinics of North America,* 39**,** pp.277-294

Medvedev, S. P., Shevchenko, A. I. and Zakian, S. M., 2010a. Induced Pluripotent Stem Cells: Problems and Advantages when Applying them in Regenerative Medicine. *Acta Naturae,* 2**,** pp.18-28.

Medvedev, S.P., Shevchenko, A.I. and Zakian, S.M., 2010. Molecular basis of mammalian embryonic stem cell pluripotency and self-renewal. *Acta Naturae,* 2(3 (6)).

Menendez, L., et al., 2013. Directed differentiation of human pluripotent cells to neural crest stem cells. *Nature protocols*, 8(1), pp.203-212.

Messadi, D. V., Wilder-Smith, P. and Wolinsky, L., 2009. Improving Oral Cancer Survival: The Role of Dental Providers. *Journal of the California Dental Association,* 37**,** pp.789-798.

Miller, J. D. and Schlaeger, T.M., 2011. Generation of induced pluripotent stem cell lines from human fibroblasts via retroviral gene transfer. *Methods of Molecular Biology,* 767**,** pp.55-65.

Miyoshia, N., et al., 2009. Defined factors induce reprogramming of gastrointestinal cancer cells. *PNAS,* 107**,** pp.40-45.

Nelson, T. J., 2010. Induced pluripotent stem cells: advances to applications. *Stem Cells and Cloning : Advances and Applications,* 3**,** pp.29-37.

Nishino, K., et al., 2011. DNA Methylation Dynamics in Human Induced Pluripotent Stem Cells over Time. *PLoS Genetics,* 7**,** e1002085.

Noguchi, K., et al., 2015. Susceptibility of pancreatic cancer stem cells to reprogramming. *Cancer science*, *106*(9), pp.1182-1187.

O'Doherty, R., Greiser, U. and Wang, W., 2013. Nonviral Methods for Inducing Pluripotency to Cells. *BioMed Research International,* 2013.

O' Neil, A. C. and Ricardo, S. D., 2013. Human Kidney Cell Reprogramming: Applications for Disease Modeling and Personalized Medicine. *Journal of the American Society of Nephrology,* 24**,** pp.1347-1356.

OH, S. I., et al., 2012., Technological Progress in Generation of Induced Pluripotent Stem Cells for Clinical Applications. *The Scientific World Journal***,** 417809.

Okita, K. and Yamanaka, S., 2011. Induced pluripotent stem cells: opportunities and challenges. *Philos Trans R Soc Lond B Biol Sci,* 366**,** pp.2198-2207.

Olivier, M., Hollstein, M. and Hainaut, P., 2010. TP53 mutations in human cancers: origins, consequences, and clinical use. *Cold Spring Harbor perspectives in biology*, *2*(1), pp.a001008.

Omar, E. A., 2013. The Outline of Prognosis and New Advances in Diagnosis of Oral Squamous Cell Carcinoma (OSCC): Review of the Literature. *Journal of Oral Oncology***,** 13.

Onder, T. T. and Daley, G. Q., 2011. microRNAs become macro players in somatic cell reprogramming. *Genome Medicine,* 3**,** pp.40.

Ono, M., et al., 2012. Generation of induced pluripotent stem cells from human nasal epithelial cells using a Sendai virus vector. *PLoS One,* 7(8), pp.e4285.

Ooi, J. and Liu, P., 2012. Pluripotency and its layers of complexity. *Cell Regen (Lond),* 1**,** pp.1.

Palla, A. R., et al., 2015. The pluripotency factor NANOG promotes the formation of squamous cell carcinomas. *Science Report,* 5.

Park, H.Y., et al., 2012. Efficient generation of virus-free iPS cells using liposomal magnetofection. *PLoS One*, 7(9), pp.e45812.

Patel AP., et al., 2014. Single-cell RNA-seq highlights intratumoral heterogeneity in primary glioblastoma. Science 344: 1396–1401

Paterson, I.C., Patel, V., Sandy, J.R., Prime, S.S. and Yeudall, W.A., 1995. Effects of transforming growth factor beta-1 on growth-regulatory genes in tumour-derived human oral keratinocytes. *British journal of cancer*, *72*(4), pp.922.

Pawitan, J. A., 2012. Prospect of Induced Pluripotent Stem Cell Genetic Repair to Cure Genetic Diseases. *Stem Cells International,* 2012:498197.

Pennarossa, G., et al., 2011. Parthenogenesis in mammals: pros and cons in pluripotent cell derivation. *Central European Journal of Biology,* 6**,** pp.770-775.

Pires, F. R.,et al., 2013. Oral squamous cell carcinoma: clinicopathological features from 346 cases from a single oral pathology service during an 8-year period. *Journal of Applied Oral Sciences,* 21**,** pp.460-7.

Pouton, C. W. and Haynes, J. M., 2007. Embryonic stem cells as a source of models for drug discovery. *Nature Reviews Drug Discovery,* 6**,** pp.605-616.

Prime, S.S., et al., 1994. Epidermal growth factor and transforming growth factor alpha characteristics of human oral carcinoma cell lines. *British journal of cancer*, 69(1), p.8.

Prime, S. S., et al., 1990. The behaviour of human oral squamous cell carcinoma in cell culture. *Journal of Pathology, 160(3),* pp. 259-269.

Radzisheuskaya, et al., 2013. A defined Oct4 level governs cell state transitions of pluripotency entry and differentiation into all embryonic lineages. *Nature cell biology*, 15(6), pp.579-590.

Ram, H., et al., 2011. Oral Cancer: Risk Factors and Molecular Pathogenesis. *Journal of Maxillofacial & Oral Surgery,* 10**,**pp. 132-137.

Ramos-Mejia, V., Fraga, M. F. and Menendez, P., 2012. "iPSCs from cancer cells: challenges and opportunities". *Trends in Molecular Medicines. ,* 18(5)**,** pp.245-247.

Rao, M. S. and Malik, N., 2012. Assessing iPSC Reprogramming Methods for Their Suitability in Translational Medicine. *Journal of cellular biochemistry,* 113**,** pp.3061-3068.

Rizzino, A., 2013. The Sox2-Oct4 Connection: Critical players in a much larger interdependent network integrated at multiple levels. *Stem cells (Dayton, Ohio),* 31**,** pp.1033-1039.

Rizzo, W.B., et al., 2008. Abnormal fatty alcohol metabolism in cultured keratinocytes from patients with Sjögren-Larsson syndrome. *Journal of lipid research*, 49(2), pp.410-419.

Rodda, D. J., et al., 2005. Transcriptional Regulation of Nanog by OCT4 and SOX2. *Journal of Biological Chemistry,* 280**,** pp.24731-24737.

Roshandel, G., Boreiri, M., Sadjadi, A. and Malekzadeh, R., 2014. A Diversity of Cancer Incidence and Mortality in West Asian Populations. *Annals of Global Health,* 80**,** pp.346-357.

Santostefano, K.E., et al., 2015. A practical guide to induced pluripotent stem cell research using patient samples. *Laboratory Investigation*, 95(1), pp.4-13.

Sarig, R., et al., 2010. Mutant p53 facilitates somatic cell reprogramming and augments the malignant potential of reprogrammed cells. *The Journal of experimental medicine*, 207(10), pp.2127-2140.

Schwartz, P.H., Brick, D.J., Nethercott, H.E. and Stover, A.E., 2011. Traditional human embryonic stem cell culture. *Human Pluripotent Stem Cells: Methods and Protocols*, pp.107-123.

Scully, C., Bagan, J.V., Hopper, C. and Epstein, J.B., 2008. Oral cancer: current and future diagnostic techniques. *Am J Dent*, 21(4), pp.199-209.

Semi, K., Matsuda, Y., Ohnishi, K. and Yamada, Y., 2013. Cellular reprogramming and cancer development. *International Journal of Cancer*,*132*(6), pp.1240-1248.

Shao, L. and Wu, W.S., 2010. Gene-delivery systems for iPS cell generation. *Expert opinion on biological therapy*, 10(2), pp.231-242.

Sharkis, S.J., Jones, R.J., Civin, C. and Jang, Y.Y., 2012. Pluripotent stem cell–based cancer therapy: Promise and challenges. *Science translational medicine*, *4*(127), pp.127ps9-127ps9.

Shetty, S. and Gokul, S., 2012. Keratinization and its disorders. *Oman Med J*, *27*(5), pp.348-357.

Shilpa, V. and Lakshmi, K., 2014. Molecular Mechanisms of Mismatch Repair Genes in Cancer–A Brief Review. *Journal of Proteomics and Genomics*, *1*(1), p.1.

Shin, D., Vigneswaran, N., Gillenwater, A. and Richards-Kortum, R., 2010. Advances in fluorescence imaging techniques to detect oral cancer and its precursors. *Future Oncology*, *6*(7), pp.1143-1154.

Shirako, Y., et al., 2015. Heterogeneous tumor stromal microenvironments of oral squamous cell carcinoma cells in tongue and nodal metastatic lesions in a xenograft mouse model. *Journal of Oral Pathology & Medicine*, 44(9), pp.656-668.

Singh, T. and Schenberg, M., 2013. Delayed diagnosis of oral squamous cell carcinoma following dental treatment. *Annals of the Royal College of Surgeons of England*, 95(5), p.369.

Singh, V.K., Kalsan, M., Kumar, N., Saini, A. and Chandra, R., 2015. Induced pluripotent stem cells: applications in regenerative medicine, disease modeling, and drug discovery. *Frontiers in cell and developmental biology*, *3*.

Sinnecker, D., et al., 2012. Induced pluripotent stem cells in cardiovascular research. In *Reviews of Physiology, Biochemistry and Pharmacology, 163*, pp.1-26.

Solter, D., 2006. From teratocarcinomas to embryonic stem cells and beyond: a history of embryonic stem cell research. *Nature Reviews Genetics*, *7*(4), pp.319-327.

Soto-Gutierrez, A., Tafaleng, E., Kelly, V., Roy-Chowdhury, J. and Fox, I.J., 2011. Modeling and therapy of human liver diseases using induced pluripotent stem cells: How far have we come?. *Hepatology*, 53(2), pp.708-711.

Spike, B.T. and Wahl, G.M., 2011. P53, stem cells, and reprogramming tumor suppression beyond guarding the genome. *Genes & cancer*, *2*(4), pp.404-419.

Strauer, B.E. and Kornowski, R., 2003. Stem cell therapy in perspective. *Circulation*, 107(7), pp.929-934.

Stricker, S.H., et al., 2013. Widespread resetting of DNA methylation in glioblastoma-initiating cells suppresses malignant cellular behavior in a lineage-dependent manner. *Genes & development*, 27(6), pp.654-669.

Stadtfeld, M. and Hochedlinger, K., 2010. Induced pluripotency: history, mechanisms, and applications. *Genes & Development, 24*, pp.2239-2263.

Strauer, B. E. and Kornowski, R., 2003. Stem Cell Therapy in Perspective. *Circulation,* 107**,** pp.929-934.

Sugii, S., et al., 2010. Human and mouse adipose-derived cells support feeder-independent induction of pluripotent stem cells. *Proceedings of the National Academy of Sciences of the United States of America,* 107**,** pp.3558-3563.

Supic, G., et al., 2011. Interaction between the MTHFR C677T polymorphism and alcohol--impact on oral cancer risk and multiple DNA methylation of tumor-related genes. *Journal of Dental Research,* 90**,** pp.65-70.

Takahashi, K., et al., 2007. Induction of pluripotent stem cells from adult human fibroblasts by defined factors, *Cell***,** pp.861-872.

Takahashi, K. and Yamanaka, S., 2006. Induction of pluripotent stem cells from mouse embryonic and adult fibroblast cultures by defined factors, *cell*,126(4), pp.663-676.

Tapia, N. and Schöler, H.R., 2010. p53 connects tumorigenesis and reprogramming to pluripotency, *The Journal of experimental medicine*, 207(10), pp.2045-2048.

Tat, P.A., Sumer, H., Pralog, D. and Verma, P. j., 2011. . The efficiency of cell fusion-based reprogramming is affected by the somatic cell type and the in vitro age of somatic cells, *Cell Reprogram,* 13**,** pp.331-344.

Taura, D., et al., 2009. Adipogenic differentiation of human induced pluripotent stem cells: comparison with that of human embryonic stem cells. *FEBS letters*, *583*(6), pp.1029-1033.

Tchieu, J., et al., 2010. Female human iPS cells retain an inactive X-chromosome. *Cell stem cell,* 7**,** pp.329-342.

Termine, N., et al., 2008. HPV in oral squamous cell carcinoma vs head and neck squamous cell carcinoma biopsies: a meta-analysis (1988–2007). *Annals of Oncology,* 19**,** pp.1681-1690.

Tewarie, R.S.N., Hurtado, A., Bartels, R.H., Grotenhuis, A. and Oudega, M., 2009. Stem cell–based therapies for spinal cord injury. *The journal of spinal cord medicine*, *32*(2), p.105.

Tolar, J., et al., 2011a. Hematopoietic differentiation of induced pluripotent stem cells from patients with mucopolysaccharidosis type I (Hurler syndrome). *Blood,* 117,pp**.** 839-847.

Tolar, J., et al., 2011b. Induced Pluripotent Stem Cells from Individuals with Recessive Dystrophic Epidermolysis Bullosa. *Journal of Investigative Dermatology,* 131**,** pp.848-856.

Torre, L. A., et al., 2015. Global cancer statistics, 2012. *Journal of Clinical Cancer Research,* 65(2), pp.87-108.

Trosko, J.E., 2014. Induction of iPS cells and of cancer stem cells: the stem cell or reprogramming hypothesis of cancer?. *The Anatomical Record,297*(1), pp.161-173.

Tsai, L.L., et al., 2014. Oct4 mediates tumor initiating properties in oral squamous cell carcinomas through the regulation of epithelial-mesenchymal transition. *PloS one*, *9*(1), p.e87207.

Unternaehrer, J. J. and Daley, G. Q., 2011. Induced pluripotent stem cells for modelling human diseases. *Philosophical Transactions of the Royal Society B: Biological Sciences,* 366**,** pp. 2274-2285.

Vaish, M. and Mittal, B., 2002. DNA mismatch repair, microsatellite instability and cancer. *Indian Journal of Experimental Biology,* 40**,** pp.989 - 994.

Vierbuchen, T. and Wernig, M., 2012. Molecular roadblocks for cellular reprogramming. *Molecular cell*, 47(6), pp.827-838.

Wan, W., et al., 2015. Applications of Induced Pluripotent Stem Cells in Studying the Neurodegenerative Diseases. *Stem Cells International*. pp.11.

Warnakulasuriya, S., 2009. Global epidemiology of oral and oropharyngeal cancer. *Oral Oncology,* 45**,** (4-5), pp.309-316.

Watt, F. M. and Driskell, R. R., 2010. The therapeutic potential of stem cells. *Philosophical Transactions of the Royal Society B: Biological Sciences,* 365**,** pp.155-163.

Weber, S. M., et al., 2011. Tobacco-specific carcinogen nitrosamine 4-(methylnitrosamino)-1-(3-pyridyl)-1-butanone induces AKT activation in head and neck epithelia. *International journal of oncology,* 39**,** pp.1193-1198.

Wert, G. D. and Mummery, C., 2003. Human embryonic stem cells: research, ethics and policy. *Human Reproduction,* 18**,** pp.672-682.

Wijeyekoon, R. and Barker, R. A., 2009. Cell replacement therapy for Parkinson's disease. *Biochimica et Biophysica Acta (BBA) - Molecular Basis of Disease,* 1792**,** pp.688-702.

Wilding, J.L. and Bodmer, W.F., 2014. Cancer cell lines for drug discovery and development. *Cancer research*, *74*(9), pp.2377-2384.

Winning, T.A. and Townsend, G.C., 2000. Oral mucosal embryology and histology. *Clinics in dermatology*, *18*(5), pp.499-511.

Wong, G.R., et al., 2014. Seropositivity of HPV 16 E6 and E7 and the risk of oral cancer. *Oral Diseases,* 20**,** pp.762-767.

Yamamoto, N., et al., 2015. Molecular biological change in oral cancer, summary of our researches. *Japanese Dental Science Review,* 51**,** pp.25-33.

Yap, T.A. and Workman, P., 2012. Exploiting the cancer genome: strategies for the discovery and clinical development of targeted molecular therapeutics. *Annual review of pharmacology and toxicology*, *52*, pp.549-573.

Yeudall, W.A., Paterson, I.C., Patel, V. and Prime, S.S., 1995. Presence of human papillomavirus sequences in tumour-derived human oral keratinocytes expressing mutant p53. *European Journal of Cancer Part B: Oral Oncology*, *31*(2), pp.136-143.

Yu, J., et al., 2006. DNA repair pathway profiling and microsatellite instability in colorectal cancer. *Journal Clinical Cancer Research,* 12**,** pp.5104 - 5111.

Yu, J., Vodyanik, M.A., Smuga-Otto, K., Antosiewicz-Bourget, J., Frane, J.L., Tian, S., Nie, J., Jonsdottir, G.A., Ruotti, V., Stewart, R. and Slukvin, I.I., 2007. Induced pluripotent stem cell lines derived from human somatic cells. *Science*, *318*(5858), pp.1917-1920.

Zhang, D.M., Li, J.J., Yan, P. and Hu, J.T., 2014. Establishment and identification of induced pluripotent stem cells in liver cancer patients. *Asian Pacific journal of tropical medicine*, *7*(4), pp.253-256.

Zhang, X., et al., 2013. Terminal differentiation and loss of tumorigenicity of human cancers via pluripotency-based reprogramming. *Oncogene,* 32**,** pp.2249-60.

Zhou, Y. Y. and Zeng, F. 2013. Integration-free Methods for Generating Induced Pluripotent Stem Cells. *Genomics, Proteomics & Bioinformatics,* 11**,** pp.284-287.

Zwaka, T. P and Thomson, j. A., 2005. A germ cell origin of embryonic stem cells? *Development,* 132**,** pp.227-233.

APPENDICES

Appendix A

Full Sequence Map for pMXs-hOCT3/4
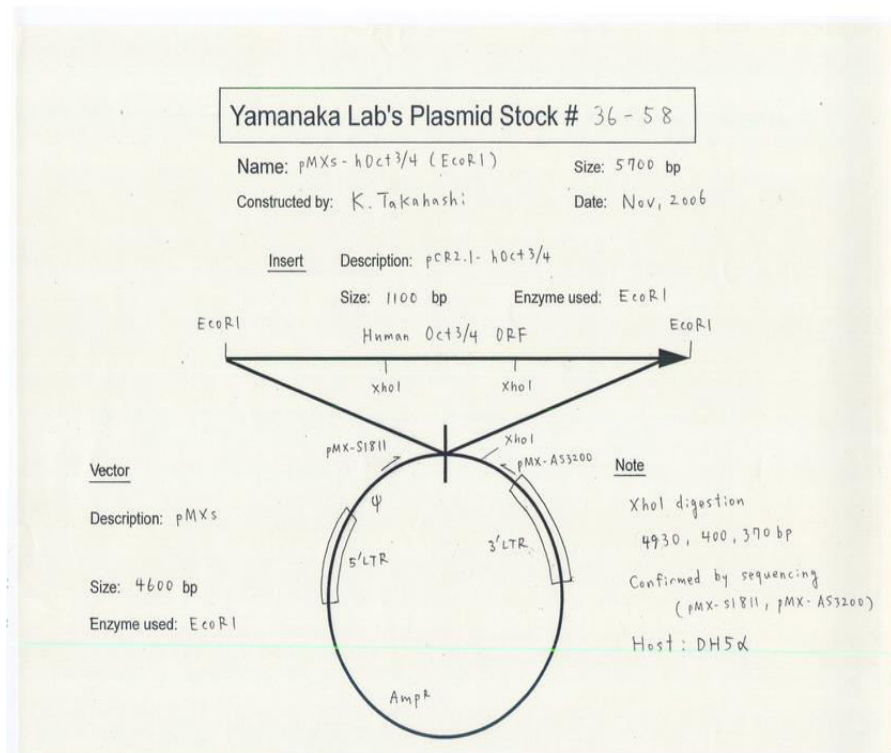
Appendix B

Full Sequence Map for pMXs-hSOX2
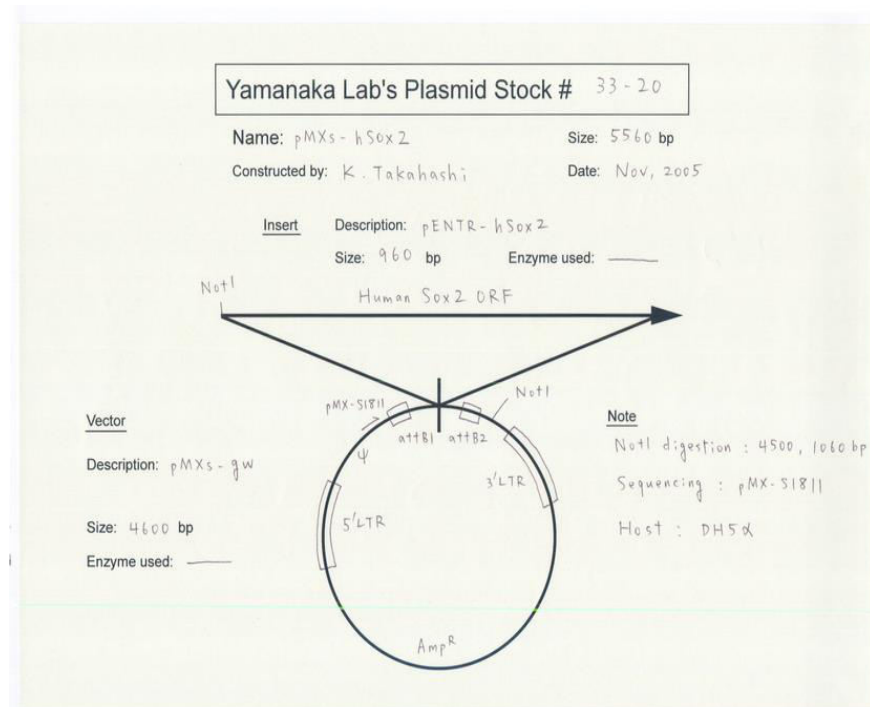
Appendix C

Full Sequence Map for pMXs-hKLF4
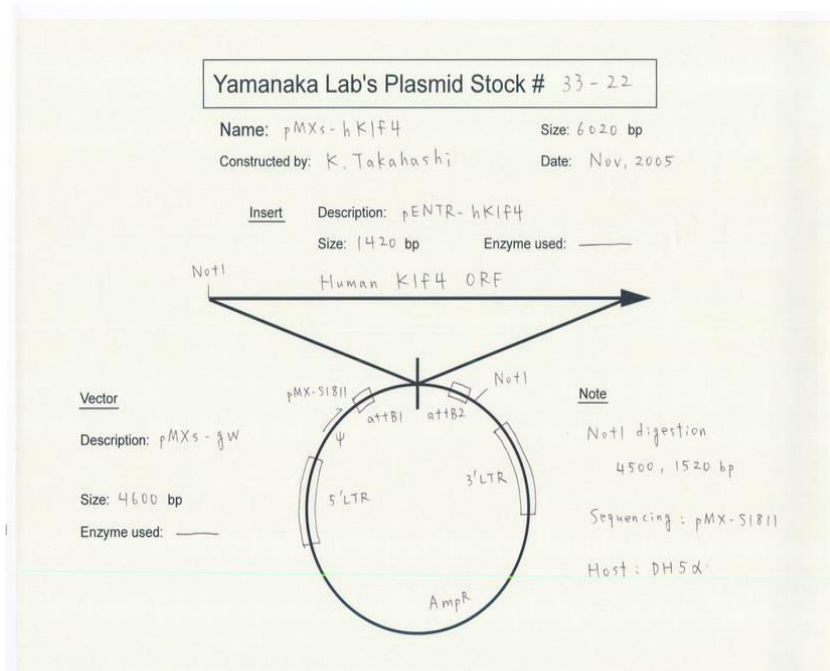
Appendix D

Full Sequence Map for pMXs-hc-MYC
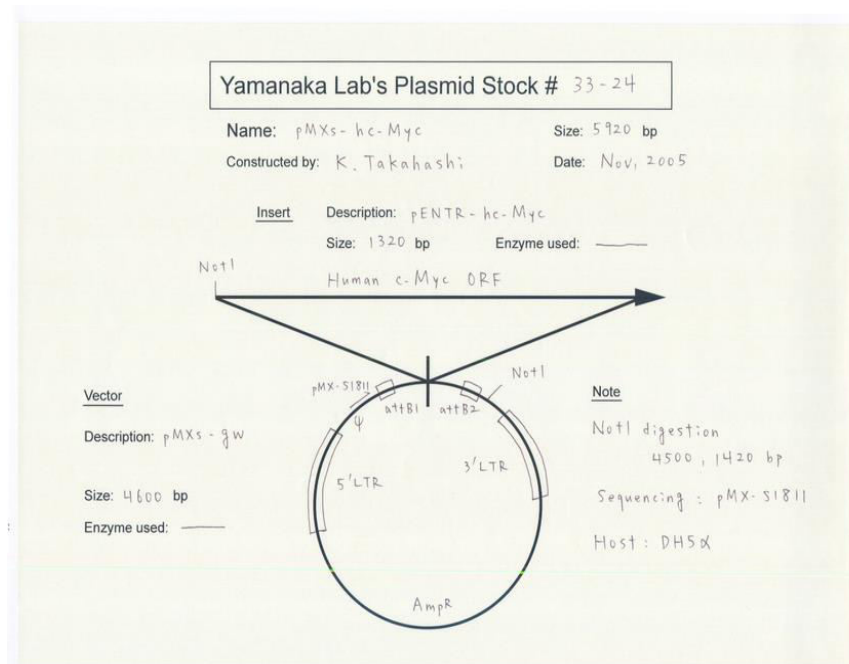
Appendix E

Full Sequence Map for Packaging Plasmid Gag-Pol
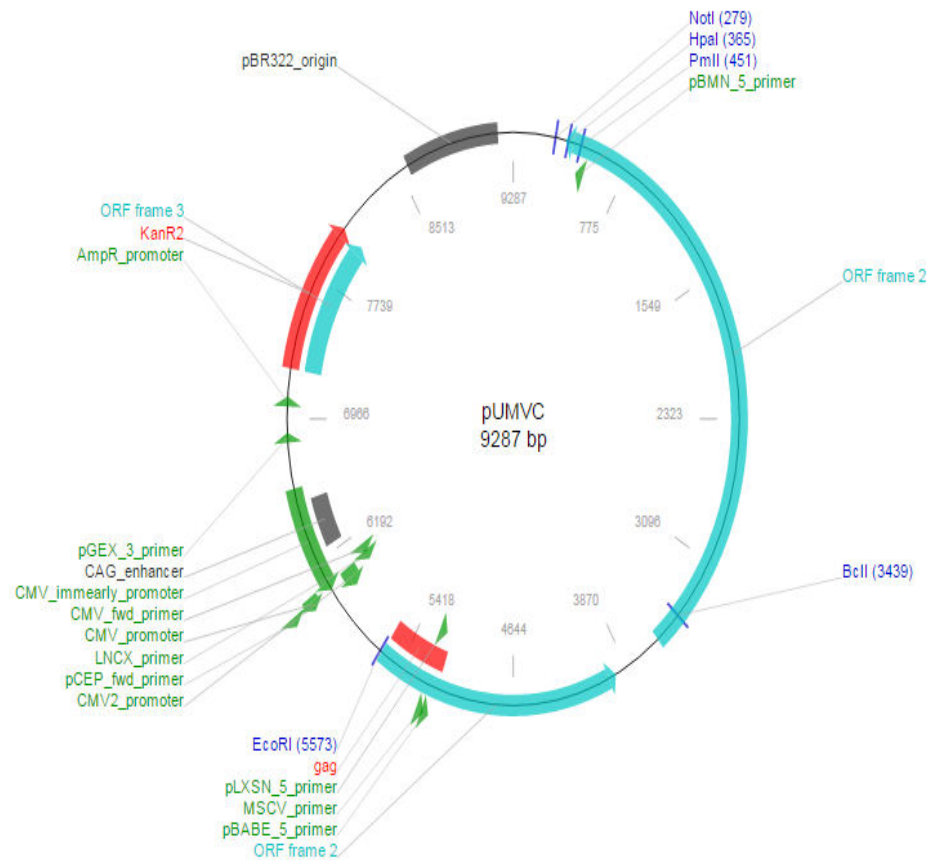
Full Sequence Map for Packaging Plasmid VSV-G
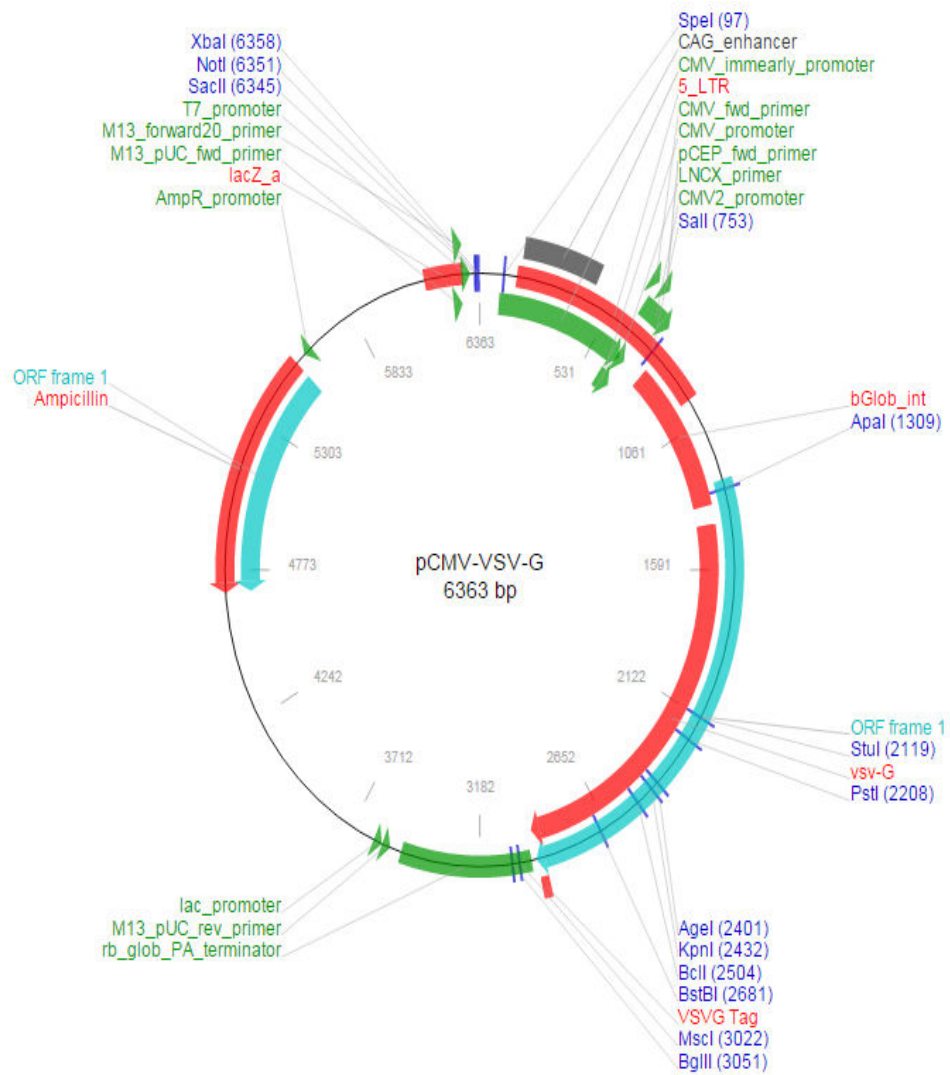
Appendix G

Full Sequence Map for pMX-GFP
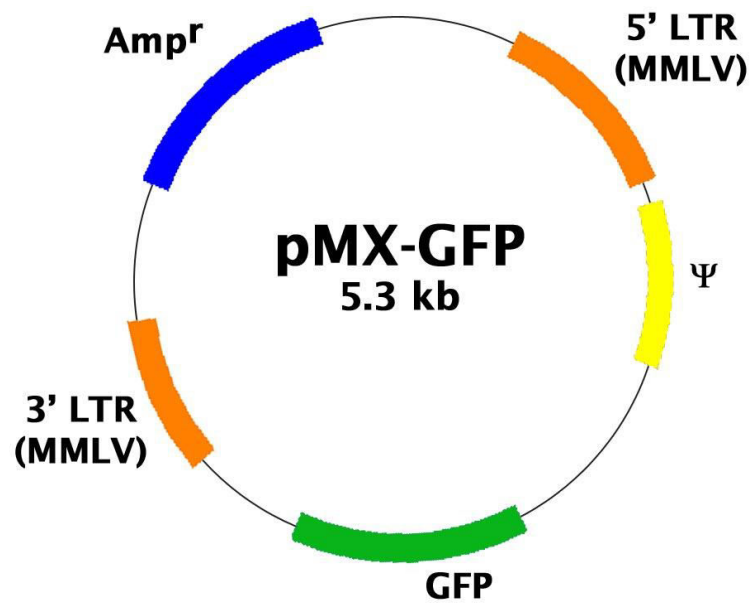
Appendix H

Plasmid Concentration and purity

PLASMID	CONC (NG/UL)	A260/280	A260/230
GFP	755.8	1.804	2.160
GAG-POL	596.5	1.955	3.161
VSV-G	674	1.891	2.779
PMX-OCT4	3166	1.867	2.348
PMX-SOX2	3196	1.872	2.338
PMX-KLF4	3295	1.860	2.275
PMX-CMYC	3823	1.837	2.242

Appendix I

Types of Restriction Enzymes and Plasmid DNA (OSKM) Sizes

PLASMID	SIZE (BP)
PMX-OCT4	4600,bp, 1100bp (ECOR1)
PMX-SOX2	4500bp, 1060bp (NOT1)
PMX-KLF4	4500bp, 1520bp (NOT1)
PMX-CMYC	4500bp, 1420bp (NOT1)

Appendix J

Plasmid DNA and Restriction Enzme Digestion of Plasmid

154
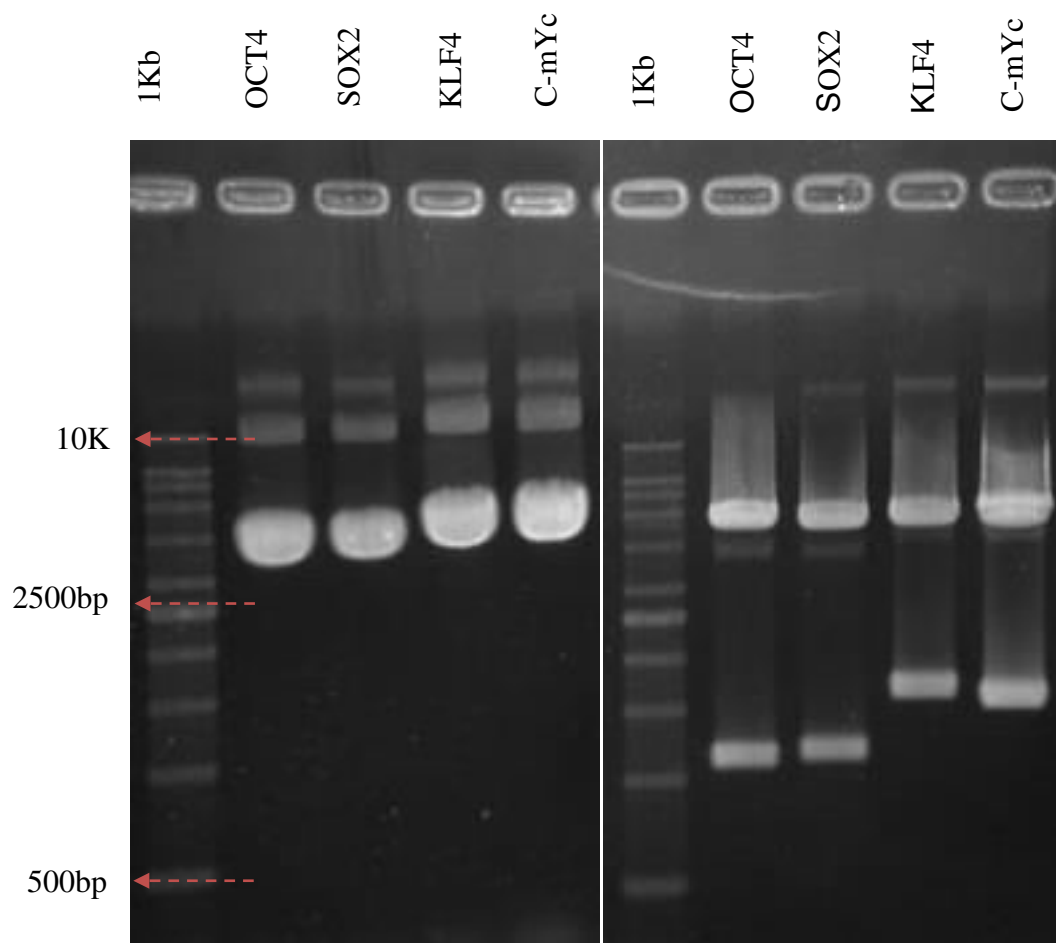
Appendix K

List of Primers

NO	PRIMER NAME	PRIMER SEQUENCE (5' => 3')
1	pMXs-AS3200 TG(R-OSK)	TTATCGTCGACCACTGTGCTGCTG
2	pMXs-L3205 TG(R-M)	CCCTTTTTCTGGAGACTAAATAAA
3	OCT4 TG (F)	CCC CAG GGC CCC ATT TTG GTA CC
4	SOX2 TG (F)	GGC ACC CCT GGC ATG GCT CTT GGC TC
5	KLF4 TG/ENDO (F)	ACG ATC GTG GCC CCG GAA AAG GAC C
6	C-MYC TG (F)	CAA CAA CCG AAA ATG CAC CAG CCC CAG
7	OCT4 ENDO (F)	GAC AGG GGG AGG GGA GGA GCT AGG
8	OCT4 ENDO (R)	CTT CCC TCC AAC CAG TTG CCC CAA AC
9	SOX2ENDO (F)	GGG AAA TGG GAG GGG TGC AAA AGA GG
10	SOX2 ENDO (R)	TTG CGT GAG TGT GGA TGG GAT TGG TG
11	KLF4 ENDO (R)	TGA TTG TAG TGC TTT CTG GCT GGG CTC C
12	C-MYC ENDO (F)	GCG TCC TGG GAA GGG AGA TCC GGA GC
13	C-MYC ENDO (R)	TTG AGG GGC ATC GTC GCG GGA GGC TG
14	NANOG ENDO (F)	TTT GGA AGC TGC TGG GGA AG
15	NANOG ENDO (R)	GAT GGG AGG AGG GGA GAG GA

REPLICATE 1

Fold Change of Pluripotent Genes Expression in Reprogrammed H103 Relative to Parental by ΔΔCT Method

	GENE	AVERAGE C_T (TARGET GENE)	AVERAGE C_T T (ACTB)	ΔC_T = TARGET GENE - ACTB	$\Delta\Delta C_T = \Delta C_T$ TARGET GENE - ΔCT CONTROL	$2^{-\Delta\Delta C_T}$
Parental H103	Oct4	34.08 ± 0.68	18.95 ± 0.44	15.13 ± 0.81	0 ± 0.81	1
	Sox2	33.93 ± 1.50	18.95 ± 0.44	14.98 ± 0.44	0 ± 0.44	1
	Klf4	27.83 ± 0.85	18.95 ± 0.44	8.88 ± 0.96	0 ± 0.96	1
	C-Myc	24.99 ± 0.84	18.95 ± 0.44	6.04 ± 0.95	0 ± 0.95	1
	Nanog	36.69 ± 0.21	18.95 ± 0.44	17.74 ± 0.49	0 ± 0.49	1
IPSC H103 (P5)	Oct4	34.50 ± 0.65	18.54 ± 0.56	15.96 ± 0.86	0.83 ± 0.86	0.81
	Sox2	27.63 ± 0.68	18.54 ± 0.56	9.09 ± 0.88	-5.89 ± 0.88	59.30
	Klf4	30.92 ± 0.43	18.54 ± 0.56	12.38 ± 0.86	3.50 ± 0.86	0.09
	C-Myc	32.07 ± 0.43	18.54 ± 0.56	13.53 ± 0.86	7.49 ± 0.86	0.01
	Nanog	34.74 ± 0.47	18.54 ± 0.56	16.20 ± 0.73	-1.54 ± 0.73	2.91
IPSC H103 (P10)	Oct4	32.75 ± 0.35	18.89 ± 0.29	13.86 ± 0.45	-1.27 ± 0.45	2.41
	Sox2	27.40 ± 1.52	18.89 ± 0.29	8.51 ± 1.55	-6.47 ± 1.55	88.65
	Klf4	30.80 ± 0.44	18.89 ± 0.29	11.91 ± 0.53	3.03 ± 0.53	0.12
	C-Myc	31.25 ± 0.50	18.89 ± 0.29	12.36 ± 0.58	6.32 ± 0.58	0.01
	Nanog	33.76 ± 1.83	18.89 ± 0.29	14.87 ± 1.85	-2.87 ± 1.85	7.31

Fold Change of Pluripotent Genes Expression in Reprogrammed H103 Relative to Parental by ΔΔCT Method

	GENE	AVERAGE C_T (TARGET GENE)	AVERAGE C_T T (ACTB)	ΔC_T = TARGET GENE - ACTB	$\Delta\Delta C_T = \Delta C_T$ TARGET GENE - ΔCT CONTROL	$2^{-\Delta\Delta CT}$
Parental H103	Oct4	33.53 ± 2.05	18.50 ± 0.79	15.03 ± 2.20	0 ± 2.20	1
	Sox2	33.50 ± 1.12	18.50 ± 0.79	15.00 ± 1.37	0 ± 1.37	1
	Klf4	27.87 ± 0.20	18.50 ± 0.79	9.37 ± 0.81	0 ± 0.81	1
	C-Myc	25.13 ± 0.84	18.50 ± 0.79	6.63 ± 1.15	0 ± 1.15	1
	Nanog	36.20 ± 0.29	18.50 ± 0.79	17.70 ± 0.84	0 ± 0.84	1
IPSC H103 (P5)	Oct4	34.94 ± 1.64	18.79 ± 0.77	16.15 ± 1.81	1.12 ± 1.81	0.46
	Sox2	27.97 ± 0.41	18.79 ± 0.77	9.18 ± 0.87	-5.82 ± 0.87	56.49
	Klf4	30.58 ± 2.12	18.79 ± 0.77	9.80 ± 2.25	2.42 ± 2.25	0.19
	C-Myc	31.79 ± 0.25	18.79 ± 0.77	11.79 ± 0.81	5.16 ± 0.81	0.03
	Nanog	34.57 ± 1.22	18.79 ± 0.77	15.78 ± 1.44	-1.92 ± 1.44	3.78
IPSC H103 (P10)	Oct4	31.99 ± 1.50	17.69 ± 0.19	14.30 ± 1.51	-0.73 ± 1.51	1.66
	Sox2	26.77 ± 0.82	17.69 ± 0.19	9.08 ± 0.84	-5.92 ± 0.84	60.55
	Klf4	30.74 ± 0.66	17.69 ± 0.19	13.05 ± 0.69	3.68 ± 0.69	0.08
	C-Myc	31.09 ± 0.50	17.69 ± 0.19	13.40 ± 0.53	6.77 ± 0.53	0.01
	Nanog	32.16 ± 1.17	17.69 ± 0.19	14.47 ± 1.19	-3.23 ± 1.19	9.38

REPLICATE 3

Fold Change of Pluripotent Genes Expression in Reprogrammed H103 Relative to Parental by $\Delta\Delta$CT Method

	GENE	AVERAGE C_T (TARGET GENE)	AVERAGE C_T T (ACTB)	ΔC_T = TARGET GENE - ACTB	$\Delta\Delta C_T = \Delta C_T$ TARGET GENE - ΔCT CONTROL	$2^{-\Delta\Delta CT}$
Parental H103	Oct4	33.19 ± 1.84	18.98 ± 0.65	14.21 ± 1.95	0 ± 1.95	1
	Sox2	33.03 ± 1.15	18.98 ± 0.65	14.05 ± 1.32	0 ± 1.32	1
	Klf4	27.97 ± 1.40	18.98 ± 0.65	8.99 ± 1.54	0 ± 1.54	1
	C-Myc	24.77 ± 0.19	18.98 ± 0.65	5.79 ± 0.68	0 ± 0.68	1
	Nanog	35.99 ± 1.23	18.98 ± 0.65	17.01 ± 1.40	0 ± 1.40	1
IPSC H103 (P5)	Oct4	34.59 ± 0.35	18.89 ± 0.19	15.70 ± 0.40	1.49 ± 0.40	0.36
	Sox2	27.31 ± 0.36	18.89 ± 0.19	8.42 ± 0.41	-5.63 ± 0.41	49.52
	Klf4	30.73 ± 1.10	18.89 ± 0.19	11.84 ± 1.12	2.85 ± 1.12	0.14
	C-Myc	31.61 ± 0.40	18.89 ± 0.19	12.72 ± 0.44	6.93 ± 0.44	0.01
	Nanog	35.02 ± 0.37	18.89 ± 0.19	16.13 ± 0.42	-0.88 ± 0.42	1.84
IPSC H103 (P10)	Oct4	31.95 ± 0.32	19.85 ± 0.25	12.1 ± 0.41	-2.11 ± 0.41	4.32
	Sox2	27.54 ± 1.40	19.85 ± 0.25	7.69 ± 1.42	-6.36 ± 1.42	82.14
	Klf4	31.07 ± 1.39	19.85 ± 0.25	11.22 ± 1.41	2.23 ± 1.41	0.21
	C-Myc	30.27 ± 0.78	19.85 ± 0.25	10.42 ± 0.82	4.63 ± 0.82	0.04
	Nanog	34.68 ± 0.59	19.85 ± 0.25	14.83 ± 0.64	-2.18 ± 0.64	4.53

In Vitro mRNA Expression of Pluroipotent Genes in Reprogrammed H103 Relative to parental (n-3)

Sample	Gene	Fold Changes				
		Replicate 1	Replicate 2	Replicate 3	Mean	SEM
Parental H103	Oct4	1	1	1	1	0
	Sox2	1	1	1	1	0
	Klf4	1	1	1	1	0
	C-Myc	1	1	1	1	0
	Nanog	1	1	1	1	0
IPSC H103 (P5)	Oct4	0.81	0.46	0.36	0.54	0.14
	Sox2	59.30	56.49	49.52	55.10	2.91
	Klf4	0.09	0.19	0.14	0.14	0.03
	C-Myc	0.01	0.03	0.01	0.02	0.01
	Nanog	2.91	3.78	1.84	2.84	0.56
IPSC H103 (P10)	Oct4	2.41	1.66	4.32	2.80	0.79
	Sox2	88.65	60.55	82.14	77.11	8.49
	Klf4	0.12	0.08	0.21	0.14	0.04
	C-Myc	0.01	0.01	0.04	0.02	0.01
	Nanog	7.31	9.38	4.53	7.07	1.41

PAIRED t-TEST (H103-Oct4)

Paired Samples Statistics

		Mean	N	Std. Deviation	Std. Error Mean
Pair 1	Parental	1.0000	3	.00000	.00000
	iPSC5	.5433	3	.23629	.13642
Pair 2	Parental	1.0000	3	.00000	.00000
	iPSC10	2.7967	3	1.37151	.79184
Pair 3	iPSC5	.5433	3	.23629	.13642
	iPSC10	2.7967	3	1.37151	.79184

Paired Samples Correlations

		N	Correlation	Sig.
Pair 1	Parental & iPSC5	3	.	.
Pair 2	Parental & iPSC10	3	.	.
Pair 3	iPSC5 & iPSC10	3	-.444	.707

Paired Samples Test

		Paired Differences							
					95% Confidence Interval of the Difference				
		Mean	Std. Deviation	Std. Error Mean	Lower	Upper	t	df	Sig. (2-tailed)
Pair 1	Parental - iPSC5	.45667	.23629	.13642	-.13031	1.04365	3.347	2	.079
Pair 2	Parental - iPSC10	-1.79667	1.37151	.79184	-5.20368	1.61035	-2.269	2	.151
Pair 3	iPSC5 - iPSC10	-2.25333	1.49149	.86111	-5.95839	1.45173	-2.617	2	.120

PAIRED t-TEST ((H103-Sox2)

Paired Samples Statistics

		Mean	N	Std. Deviation	Std. Error Mean
Pair 1	Parental	1.0000	3	.00000	.00000
	iPSC5	55.1033	3	5.03530	2.90713
Pair 2	Parental	1.0000	3	.00000	.00000
	iPSC10	77.1133	3	14.70894	8.49221
Pair 3	iPSC5	55.1033	3	5.03530	2.90713
	iPSC10	77.1133	3	14.70894	8.49221

Paired Samples Correlations

		N	Correlation	Sig.
Pair 1	Parental & iPSC5	3	.	.
Pair 2	Parental & iPSC10	3	.	.
Pair 3	iPSC5 & iPSC10	3	-.018	.989

Paired Samples Test

		Paired Differences					t	df	Sig. (2-tailed)
					95% Confidence Interval of the Difference				
		Mean	Std. Deviation	Std. Error Mean	Lower	Upper			
Pair 1	Parental - iPSC5	-54.10333	5.03530	2.90713	-66.61171	-41.59496	-18.611	2	.003
Pair 2	Parental - iPSC10	-76.11333	14.70894	8.49221	-112.65238	-39.57429	-8.963	2	.012
Pair 3	iPSC5 - iPSC10	-22.01000	15.63090	9.02451	-60.83931	16.81931	-2.439	2	.135

PAIRED t-TEST ((H103-Klf4)

Paired Samples Statistics

		Mean	N	Std. Deviation	Std. Error Mean
Pair 1	Parental	1.0000	3	.00000	.00000
	iPSC5	.1400	3	.05000	.02887
Pair 2	Parental	1.0000	3	.00000	.00000
	iPSC10	.1367	3	.06658	.03844
Pair 3	iPSC5	.1400	3	.05000	.02887
	iPSC10	.1367	3	.06658	.03844

Paired Samples Correlations

		N	Correlation	Sig.
Pair 1	Parental & iPSC5	3	.	.
Pair 2	Parental & iPSC10	3	.	.
Pair 3	iPSC5 & iPSC10	3	-.300	.806

Paired Samples Test

		Paired Differences					t	df	Sig. (2-tailed)
					95% Confidence Interval of the Difference				
		Mean	Std. Deviation	Std. Error Mean	Lower	Upper	t	df	Sig. (2-tailed)
Pair 1	Parental - iPSC5	.86000	.05000	.02887	.73579	.98421	29.791	2	.001
Pair 2	Parental - iPSC10	.86333	.06658	.03844	.69793	1.02874	22.458	2	.002
Pair 3	iPSC5 - iPSC10	.00333	.09452	.05457	-.23146	.23812	.061	2	.957

162

PAIRED t-TEST ((H103-C-Myc)

Paired Samples Statistics

		Mean	N	Std. Deviation	Std. Error Mean
Pair 1	Parental	1.0000	3	.00000	.00000
	iPSC5	.0167	3	.01155	.00667
Pair 2	Parental	1.0000	3	.00000	.00000
	iPSC10	.0200	3	.01732	.01000
Pair 3	iPSC5	.0167	3	.01155	.00667
	iPSC10	.0200	3	.01732	.01000

Paired Samples Correlations

		N	Correlation	Sig.
Pair 1	Parental & iPSC5	3	.	.
Pair 2	Parental & iPSC10	3	.	.
Pair 3	iPSC5 & iPSC10	3	-.500	.667

Paired Samples Test

| | | Paired Differences | | | | | | | |
| | | | | | 95% Confidence Interval of the Difference | | | | |
		Mean	Std. Deviation	Std. Error Mean	Lower	Upper	t	df	Sig. (2-tailed)
Pair 1	Parental - iPSC5	.98333	.01155	.00667	.95465	1.01202	147.500	2	.000
Pair 2	Parental - iPSC10	.98000	.01732	.01000	.93697	1.02303	98.000	2	.000
Pair 3	iPSC5 - iPSC10	-.00333	.02517	.01453	-.06585	.05918	-.229	2	.840

PAIRED t-TEST ((H103-Nanog)

Paired Samples Statistics

		Mean	N	Std. Deviation	Std. Error Mean
Pair 1	Parental	1.0000	3	.00000	.00000
	iPSC5	2.8433	3	.97172	.56102
Pair 2	Parental	1.0000	3	.00000	.00000
	iPSC10	7.0733	3	2.43365	1.40507
Pair 3	iPSC5	2.8433	3	.97172	.56102
	iPSC10	7.0733	3	2.43365	1.40507

Paired Samples Correlations

		N	Correlation	Sig.
Pair 1	Parental & iPSC5	3	.	.
Pair 2	Parental & iPSC10	3	.	.
Pair 3	iPSC5 & iPSC10	3	1.000	.016

Paired Samples Test

		Paired Differences			95% Confidence Interval of the Difference				
		Mean	Std. Deviation	Std. Error Mean	Lower	Upper	t	df	Sig. (2-tailed)
Pair 1	Parental - iPSC5	-1.84333	.97172	.56102	-4.25721	.57054	-3.286	2	.081
Pair 2	Parental - iPSC10	-6.07333	2.43365	1.40507	-12.11885	-.02782	-4.322	2	.050
Pair 3	iPSC5 - iPSC10	-4.23000	1.46243	.84433	-7.86288	-.59712	-5.010	2	.038

Appendix M

REPLICATE 1

Fold Change of Pluripotent Genes Expression in Reprogrammed H376 Relative to Parental by ΔΔCT Method

	GENE	AVERAGE C_T (TARGET GENE)	AVERAGE C_T T (ACTB)	ΔC_T = TARGET GENE - ACTB	$\Delta\Delta C_T = \Delta C_T$ TARGET GENE - ΔCT CONTROL	$2^{-\Delta\Delta CT}$
Parental H103	Oct4	30.21 ± 0.28	19.56 ± 0.63	10.65 ± 0.69	0 ± 0.69	1
	Sox2	33.45 ± 1.12	19.56 ± 0.63	13.89 ± 1.29	0 ± 1.29	1
	Klf4	27.94 ± 1.94	19.56 ± 0.63	8.38 ± 2.04	0 ± 2.04	1
	C-Mvc	27.56 ± 1.15	19.56 ± 0.63	8.00 ± 1.63	0 ± 1.63	1
	Nanog	35.97 ± 0.65	19.56 ± 0.63	16.41 ± 0.91	0 ± 0.91	1
IPSC H103 (P5)	Oct4	35.19 ± 0.66	21.93 ± 0.83	13.26 ± 1.06	2.61 ± 1.06	0.16
	Sox2	32.36 ± 0.42	21.93 ± 0.83	10.43 ± 0.93	-3.46 0.93	11.00
	Klf4	32.40 ± 1.05	21.93 ± 0.83	10.47 ± 1.34	2.09 ± 1.34	0.23
	C-Mvc	33.50 ± 1.22	21.93 ± 0.83	11.57 ± 1.48	3.57 ± 1.48	0.08
	Nanog	38.55 ± 0.45	21.93 ± 0.83	16.62 ± 0.94	0.21 ± 0.94	0.86
IPSC H103 (P10)	Oct4	29.10 ± 0.36	17.17 ± 0.36	13.93 ± 0.51	1.28 ± 0.51	0.41
	Sox2	25.11 ± 0.50	17.17 ± 0.36	7.94 ± 0.62	-5.95 ± 0.62	61.82
	Klf4	26.57 ± 0.93	17.17 ± 0.36	9.40 ± 1.0	1.02 ± 1.0	0.49
	C-Mvc	33.12 ± 2.11	17.17 ± 0.36	15.95 ± 2.14	7.95 2.14	0.00
	Nanog	33.28 ± 0.45	17.17 ± 0.36	16.11 ± 0.58	-0.30 ± 0.58	1.23

REPLICATE 2

**Fold Change of Pluripotent Genes Expression in Reprogrammed H376
Relative to Parental by ΔΔCT Method**

	GENE	AVERAGE C_T (TARGET GENE)	AVERAGE C_T T (ACTB)	ΔC_T = TARGET GENE - ACTB	$\Delta\Delta C_T$ = Δ C_T TARGET GENE - ΔCT CONTROL	$2^{-\Delta\Delta CT}$
Parental H103	Oct4	30.14 ± 2.66	19.01 ± 0.10	11.13 ± 2.66	0 ± 2.66	1
	Sox2	33.90 ± 1.70	19.01 ± 0.10	14.89 ± 1.70	0 ± 1.70	1
	Klf4	28.03 ± 0.08	19.01 ± 0.10	9.02 ± 0.13	0 ± 0.13	1
	C-Myc	27.34 ± 0.48	19.01 ± 0.10	8.33 ± 0.49	0 ± 0.49	1
	Nanog	34.31 ± 0.29	19.01 ± 0.10	15.30 ± 0.31	0	1
IPSC H103 (P5)	Oct4	34.82 ± 0.51	22.07 ± 0.86	12.75 ± 0.10	1.62 ± 0.10	0.33
	Sox2	33.67 ± 0.23	22.07 ± 0.86	11.60 ± 0.89	-3.29 ± 0.89	9.78
	Klf4	32.31 ± 1.43	22.07 ± 0.86	10.24 ± 1.67	1.22 ± 1.67	0.43
	C-Myc	35.80 ± 1.54	22.07 ± 0.86	13.73 ± 1.76	5.44 ± 1.76	0.03
	Nanog	38.88 ± 0.24	22.07 ± 0.86	16.81 ± 0.89	1.51 ± 0.89	0.35
IPSC H103 (P10)	Oct4	28.34 ± 0.61	17.00 ± 0.22	11.34 ± 0.65	0.21 ± 0.65	0.86
	Sox2	26.12 ± 0.92	17.00 ± 0.22	9.12 ± 0.89	-5.77 ± 0.89	54.57
	Klf4	26.44 ± 0.69	17.00 ± 0.22	9.44 ± 0.72	0.42 ± 0.72	0.75
	C-Myc	32.77 ± 1.38	17.00 ± 0.22	15.77 ± 1.40	7.44 ± 1.40	0.01
	Nanog	31.21 ± 0.48	17.00 ± 0.22	14.21 ± 0.28	-1.09 ± 0.28	2.13

Fold Change of Pluripotent Genes Expression in Reprogrammed H376 Relative to Parental by ΔΔCT Method

	GENE	AVERAGE C_T (TARGET GENE)	AVERAGE C_T T (ACTB)	$\Delta C_T =$ TARGET GENE - ACTB	$\Delta\Delta C_T = \Delta C_T$ TARGET GENE - ΔCT CONTROL	$2^{-\Delta\Delta CT}$
Parental H103	Oct4	30.21 ± 0.45	19.78 ± 0.38	10.43 ± 0.59	0 ± 0.59	1
	Sox2	33.69 ± 0.56	19.78 ± 0.38	13.91 ± 0.68	0 ± 0.68	1
	Klf4	27.92 ± 2.07	19.78 ± 0.38	8.14 ± 2.10	0 ± 2.10	1
	C-Myc	27.24 ± 0.40	19.78 ± 0.38	7.46 ± 0.30	0 ± 0.30	1
	Nanog	34.11 ± 0.63	19.78 ± 0.38	14.33 ± 0.74	0 ± 0.74	1
IPSC H103 (P5)	Oct4	35.57 ± 0.70	22.72 ± 0.19	12.85 ± 0.73	2.42 ± 0.73	0.19
	Sox2	32.51 ± 0.84	22.72 ± 0.19	9.79 ± 0.86	-4.12 ± 0.86	17.39
	Klf4	32.58 ± 1.43	22.72 ± 0.19	9.86 ± 1.44	1.72 ± 1.44	0.30
	C-Myc	33.33 ± 0.71	22.72 ± 0.19	10.61 ± 0.73	3.15 ± 0.73	0.11
	Nanog	38.11 ± 0.50	22.72 ± 0.19	15.39 ± 0.53	1.06 ± 0.53	0.48
IPSC H103 (P10)	Oct4	30.21 ± 0.42	18.82 ± 0.09	11.39 ± 0.43	0.96 ± 0.43	1.95
	Sox2	26.97 ± 0.85	18.82 ± 0.09	8.15 ± 0.85	-5.76 ± 0.85	54.19
	Klf4	28.45 ± 0.58	18.82 ± 0.09	9.63 ± 0.59	1.49 ± 0.59	0.36
	C-Myc	33.47 ± 0.50	18.82 ± 0.09	14.65 ± 0.51	7.19 ± 0.51	0.01
	Nanog	31.99 ± 2.60	18.82 ± 0.09	13.17 ± 2.60	-1.16 ± 2.60	2.23

In Vitro mRNA Expression of Pluroipotent Genes in Reprogrammed H376 Relative to Parental (n-3)

Sample	Gene	Fold Change				
		Replicate 1	Replicate 2	Replicate 3	Mean	SEM
Parental H103	Oct4	1	1	1	1	0
	Sox2	1	1	1	1	0
	Klf4	1	1	1	1	0
	C-Myc	1	1	1	1	0
	Nanog	1	1	1	1	0
IPSC H103 (P5)	Oct4	0.16	0.33	0.19	0.23	0.06
	Sox2	11.00	9.78	17.39	12.72	2.89
	Klf4	0.23	0.43	0.30	0.32	0.07
	C-Myc	0.08	0.03	0.11	0.07	0.03
	Nanog	0.86	0.35	0.48	0.56	0.19
IPSC H103 (P10)	Oct4	0.41	0.86	1.95	1.07	0.56
	Sox2	61.82	54.57	54.19	56.86	3.04
	Klf4	0.49	0.75	0.36	0.53	0.14
	C-Myc	0.00	0.01	0.01	0.01	0.00
	Nanog	1.23	2.13	2.23	1.86	0.39

PAIRED t-TEST (H376-Oct 4)

Paired Samples Statistics

		Mean	N	Std. Deviation	Std. Error Mean
Pair 1	Parental	1.0000	3	.00000	.00000
	iPSC5	.2267	3	.09074	.05239
Pair 2	Parental	1.0000	3	.00000	.00000
	iPSC10	1.0733	3	.79185	.45718
Pair 3	iPSC5	.2267	3	.09074	.05239
	iPSC10	1.0733	3	.79185	.45718

Paired Samples Correlations

		N	Correlation	Sig.
Pair 1	Parental & iPSC5	3	.	.
Pair 2	Parental & iPSC10	3	.	.
Pair 3	iPSC5 & iPSC10	3	-.069	.956

Paired Samples Test

		Paired Differences							
				Std. Error	95% Confidence Interval of the Difference				
		Mean	Std. Deviation	Mean	Lower	Upper	t	df	Sig. (2-tailed)
Pair 1	Parental - iPSC5	.77333	.09074	.05239	.54793	.99874	14.762	2	.005
Pair 2	Parental - iPSC10	-.07333	.79185	.45718	-2.04041	1.89374	-.160	2	.887
Pair 3	iPSC5 - iPSC10	-.84667	.80326	.46376	-2.84209	1.14875	-1.826	2	.209

PAIRED t-TEST (H376-Sox 2)

Paired Samples Statistics

		Mean	N	Std. Deviation	Std. Error Mean
Pair 1	Parental	1.0000	3	.00000	.00000
	iPSC5	12.7233	3	4.08723	2.35976
Pair 2	Parental	1.0000	3	.00000	.00000
	iPSC10	56.8600	3	4.29969	2.48242
Pair 3	iPSC5	12.7233	3	4.08723	2.35976
	iPSC10	56.8600	3	4.29969	2.48242

Paired Samples Correlations

		N	Correlation	Sig.
Pair 1	Parental & iPSC5	3	.	.
Pair 2	Parental & iPSC10	3	.	.
Pair 3	iPSC5 & iPSC10	3	-.406	.734

Paired Samples Test

		Paired Differences							
					95% Confidence Interval of the Difference				
		Mean	Std. Deviation	Std. Error Mean	Lower	Upper	t	df	Sig. (2-tailed)
Pair 1	Parental - iPSC5	-11.72333	4.08723	2.35976	-21.87657	-1.57010	-4.968	2	.038
Pair 2	Parental - iPSC10	-55.86000	4.29969	2.48242	-66.54101	-45.17899	-22.502	2	.002
Pair 3	iPSC5 - iPSC10	-44.13667	7.03280	4.06039	-61.60710	-26.66623	-10.870	2	.008

PAIRED t-TEST (H376-Klf4)

Paired Samples Statistics

		Mean	N	Std. Deviation	Std. Error Mean
Pair 1	Parental	1.0000	3	.00000	.00000
	iPSC5	.3200	3	.10149	.05859
Pair 2	Parental	1.0000	3	.00000	.00000
	iPSC10	.5333	3	.19858	.11465
Pair 3	iPSC5	.3200	3	.10149	.05859
	iPSC10	.5333	3	.19858	.11465

Paired Samples Correlations

		N	Correlation	Sig.
Pair 1	Parental & iPSC5	3	.	.
Pair 2	Parental & iPSC10	3	.	.
Pair 3	iPSC5 & iPSC10	3	.774	.436

Paired Samples Test

		Paired Differences							
					95% Confidence Interval of the Difference				
		Mean	Std. Deviation	Std. Error Mean	Lower	Upper	t	df	Sig. (2-tailed)
Pair 1	Parental - iPSC5	.68000	.10149	.05859	.42789	.93211	11.605	2	.007
Pair 2	Parental - iPSC10	.46667	.19858	.11465	-.02663	.95996	4.070	2	.055
Pair 3	iPSC5 - iPSC10	-.21333	.13614	.07860	-.55152	.12485	-2.714	2	.113

171

PAIRED t-TEST (H376-c-Myc)

Paired Samples Statistics

		Mean	N	Std. Deviation	Std. Error Mean
Pair 1	Parental	1.0000	3	.00000	.00000
	iPSC5	.0733	3	.04041	.02333
Pair 2	Parental	1.0000	3	.00000	.00000
	iPSC10	.0067	3	.00577	.00333
Pair 3	iPSC5	.0733	3	.04041	.02333
	iPSC10	.0067	3	.00577	.00333

Paired Samples Correlations

		N	Correlation	Sig.
Pair 1	Parental & iPSC5	3	.	.
Pair 2	Parental & iPSC10	3	.	.
Pair 3	iPSC5 & iPSC10	3	-.143	.909

Paired Samples Test

		Paired Differences							
					95% Confidence Interval of the Difference				
		Mean	Std. Deviation	Std. Error Mean	Lower	Upper	t	df	Sig. (2-tailed)
Pair 1	Parental - iPSC5	.92667	.04041	.02333	.82627	1.02706	39.714	2	.001
Pair 2	Parental - iPSC10	.99333	.00577	.00333	.97899	1.00768	298.000	2	.000
Pair 3	iPSC5 - iPSC10	.06667	.04163	.02404	-.03676	.17009	2.774	2	.109

PAIRED t-TEST (H376-Nanog)

Paired Samples Statistics

		Mean	N	Std. Deviation	Std. Error Mean
Pair 1	Parental	1.0000	3	.00000	.00000
	iPSC5	.5633	3	.26502	.15301
Pair 2	Parental	1.0000	3	.00000	.00000
	iPSC10	1.8633	3	.55076	.31798
Pair 3	iPSC5	.5633	3	.26502	.15301
	iPSC10	1.8633	3	.55076	.31798

Paired Samples Correlations

		N	Correlation	Sig.
Pair 1	Parental & iPSC5	3	.	.
Pair 2	Parental & iPSC10	3	.	.
Pair 3	iPSC5 & iPSC10	3	-.943	.216

Paired Samples Test

| | | Paired Differences | | | | | | | |
| | | | | | 95% Confidence Interval of the Difference | | | | |
		Mean	Std. Deviation	Std. Error Mean	Lower	Upper	t	df	Sig. (2-tailed)
Pair 1	Parental - iPSC5	.43667	.26502	.15301	-.22167	1.09500	2.854	2	.104
Pair 2	Parental - iPSC10	-.86333	.55076	.31798	-2.23149	.50482	-2.715	2	.113
Pair 3	iPSC5 - iPSC10	-1.30000	.80554	.46508	-3.30108	.70108	-2.795	2	.108

Appendix N

Microsatellite Analysis (D3S122)
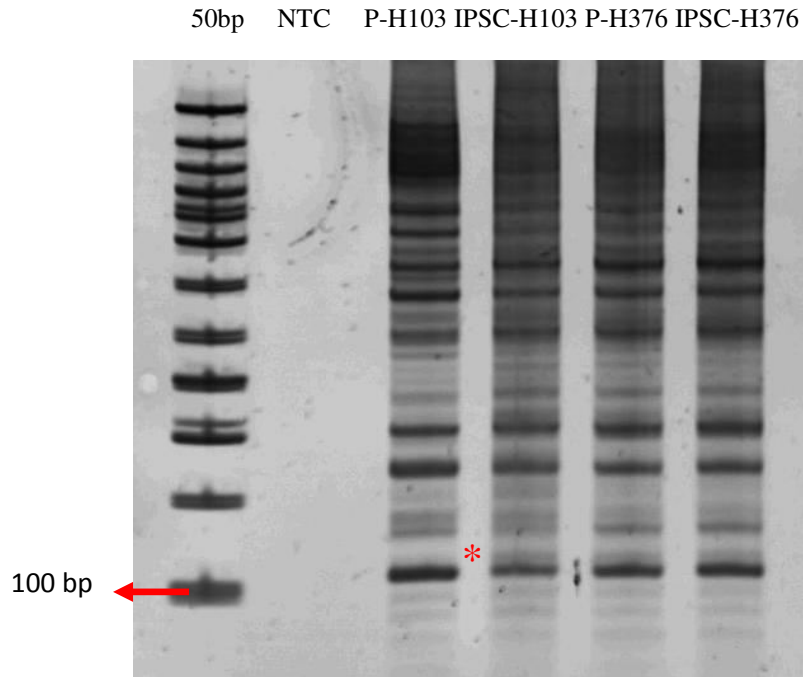
*Remark: LOH is observed at 112-120bp between

Parental - H103 and IPSC H103